NASA-CR-192344

DEVELOPMENT OF HIGH Tc (>110K) Bi, Tl and Y-BASED MATERIALS AS SUPERCONDUCTING CIRCUIT ELEMENTS

GRANT

ANNUAL REPORT

to

National Aeronautics and Space Administration
Langley Research Center
Hampton, VA 23665-5225

Period: February, 1992 - February, 1993

Principal Investigator:
Gene Haertling

Supporting Investigators:
Gregory Grabert
Phillip Gilmour

Contract No. NAG-1-1108

March 31,1993

N93-25219
Unclas
G3/76 0153690
(NASA-CR-192344) DEVELOPMENT OF HIGH TC (GREATER THAN 100 K) Bi, Tl AND Y-BASED MATERIALS AS SUPERCONDUCTING CIRCUIT ELEMENTS Annual Report, Feb. 1992-1993 (Clemson Univ.) 107 p

CLEMSON UNIVERSITY

Department of Ceramic Engineering
College of Engineering

Summary

Results on this project over the past three years have shown that the Bi and Tl-based superconducting materials in bulk form are noticeably different from the Y-based 123 material in that superconductivity is considerably harder to achieve, maintain and reproduce. This is due primarily to the difficulty in obtaining the higher Tc phase in pure form since it commonly co-exists with other undesirable, lower Tc phases. In particular, it has been found that long processing times for calcining and firing (20 - 200 hrs.) and close control of temperatures which are very near the melting point are required in order to obtain higher proportions of the desirable, high Tc (2223) phase.

Thus far, the BSCCO bulk materials has been prepared in uniaxially pressed, hot pressed and tapecast form. The uniaxially pressed material has been synthesized by the mixed oxide, coprecipitation and melt quenching processes. The tapecast and hot pressed materials have been prepared via the mixed oxide process. In addition, thick films of BSCCO (2223 phase) have been prepared by screen printing on to yttria and magnesia stabilized zirconia with only moderate success; i.e., superconductivity was achieved in these thick films, but the highest Tc obtained in these films was 89.0K. The Tc's of the bulk hot pressed, tapecast and screen printed thick film materials were found to be 108.2, 102.4 and 89.0K, respectively.

When synthesizing both the mixed oxide and coprecipitated thin film materials, which includes tapecasting, the best results occurred when the materials were sintered under low oxygen atmosphere because the films could be sintered longer and became more dense. This allowed a larger percentage of the 2223 phase to form. The BSCCO thick films printed on MgO substrates and fired at 845°C for 1 hour had the highest Tc of 89.0K. The Jc's for all films were very low. This could be increased by making denser, single phase films. A MgO buffer layer improved the electrical properties of the BSCCO thick films, and the MSZ substrate was found to be the best material for this work. The coprecipitated powder was preferred over the mixed oxide powder because a larger percentage of the 2223 phase could be formed in a much smaller amount of time.

Research on the Tl-containing superconductors included preliminary investigations into thick films produced via the acetate dip coat process and dielectrophoretic deposition of bismuth containing superconducting films on silver substrates. Of these two coating techniques, it appears dielectrophoretic deposition is a novel technique that has the potential of developing superconductor coatings with preferred orientation.

Acetate dip coating produced 2223 TBCCO superconductor thick films when fired at 600°C for 30 minutes. Using this low temperature firing method, encapsulation is not needed to contain the volatile thallium. It appears thick films produce a greater proportion of the 2223 phase.

Dielectrophoretic depositions were produced on silver wires. In this technique, high voltage is applied between two electrodes which are immersed in a suspension of superconducting powders and an insulating fluid. A non-uniform field is set up when a voltage is applied to a wire electrode that is surrounded by a cylindrical counter electrode. If the particle possesses a relatively high permittivity compared to the suspending fluid, a dipole is created in the particle. The particle is then drawn to the wire electrode due to the attraction of the dipole to the greater field intensity. Results of dielectrophoresis depositions suggest that superconductor films may be produced with particle orientation.

I. Introduction

This report details work that was carried out over the period from February, 1992 thru February, 1993, in the Ceramic Engineering Department of Clemson University under NASA contract No. NAG-1-1108. The work described in this report covers the third year of a program involving the development of high Tc superconducting circuit elements in the Bi-Sr-Ca-Cu-O and Tl-Ba-Ca-Cu-O compositional systems. This effort is intended to build on the results of the previous contract (NAG-1-820) which involved the development of the $YBa_2Cu_3O_{7-x}$ (123) material in circuit elements; and more specifically, a superconducting grounding link for the SAFIRE (Spectroscopy of the Atmosphere using Far Infra-Red Emission) program.

The technology developed for the SAFIRE grounding link involves a rigid-structure approach to superconducting elements rather than the flexible-wire idea promoted by most other institutions. In principle, the rigid-structure concept is quite simple and is tailor-made to take advantage of the inherent desirable properties of the superconducting ceramics while at the same time recognizing the low strength and basic brittleness of these materials. This is accomplished by pre-forming, sintering and testing the ceramic superconductor prior to bonding it to a rigid supporting substrate which is then totally encapsulated for further support and environmental protection. This approach has the advantages of (1) pre-testing of the superconducting material separate from the substrate, (2) optimization of the development of superconductivity in the ceramic without temperature limitations imposed by the substrate, (3) wider selection of substrate materials since the high temperature processing step precedes mounting of the superconductor to the printed circuit board, (4) freedom from firing shrinkage and other material compatibility problems and (5) high anticipated reliability because of its simplicity, rigid design and total encapsulation from the environment.

The report is presented in two parts; i.e., Part I dealing with the Bi-based materials and Part II covering work on the Tl-based materials.

Development of High T_c (>110 K) Bi, Tl and Y-Based Materials as Superconducting Circuit Elements

Annual Report
Part I: Bi-Based Materials

Submitted to

National Aeronautics and Space Administration
Langley Research Center

Submitted by
Gregory Grabert

Principal Investigator
Gene H. Haertling

Department of Ceramic Engineering
Clemson University
Contract No. NAG-1-1108
March, 1993

I. Introduction

Since the discovery of a High T_c superconducting phase in the Bi-Sr-Ca-Cu-O (BSCCO) system by Maeda and his coworkers in January 1988[1], extensive research has gone into the areas of processing, characterization, phase equilibria, physical property measurement, and device fabrication of these materials. Ceramic superconducting devices in the Y-Ba-Cu-O, Bi-Pb-Sr-Ca-Cu-O and Tl-Ba-Ca-Cu-O systems have been fabricated at Clemson University using the rigid conductor process (RCP)[2,3] for the SAFIRE (Spectroscopy of the Atmosphere using Far Infra-Red Emission) program. Of the three material systems (yttrium, bismuth and thallium) that superconduct above liquid nitrogen temperature (77.3 K), the bismuth-based system seems to be the most attractive because of the following reasons:

1) The high critical temperature (T_c) BSCCO 2223 phase has a T_c 17 °K higher than that of the YBCO system.

2) The bismuth-based materials are less oxygen stoichiometry sensitive than the yttrium-based materials.

3) The bismuth-based materials are much more resistant to moisture degradation than the yttrium or thallium-based materials because the bismuth-based materials do not contain barium, which in a moist environment results in the rapid formation of alkaline conditions on the sample surface and accelerated degradation. This is basically due to the formation of $BaCO_3$.

4) The bismuth-based material has a higher intrinsic critical current density (J_c) than the yttrium-based material and with better grain alignment could possibly have higher extrinsic J_c.

5) The bismuth-based materials are easier to prepare than the thallium-based materials due to the extreme volatility of the Tl^{+3} which makes the results nonreproducible and unreliable.

6) The bismuth-based materials are less dangerous than the thallium-based materials due to the poisonous nature of the Tl vapors.

The BSCCO compound consists of an oxygen deficient perovskite layer containing copper oxide planes sandwiched between bismuth oxide layers. The number of copper oxide planes corresponds to the n in the chemical formula $Bi_2Sr_2Ca_{n-1}Cu_nO_x$ where n = 1, 2, or 3. As the number of copper oxide planes increases, so does the critical temperature. The compounds we are most concerned with are the $Bi_2Sr_2Ca_1Cu_2O_x$ (2212 phase), which has a T_c ~ 80 K and primarily the $Bi_2Sr_2Ca_2Cu_3O_x$ (2223 phase), which has a T_c ~ 110 K. The highest T_c material is very difficult to synthesize in phase-pure form because separation of the 2223 phase from the 2212 phase is near impossible in bulk form. The 2223 phase has a very small sintering temperature range and long sintering times are required to obtain bulk material which is almost phase-pure. Many investigators found it necessary to dope the BSCCO material with lead to achieve significant quantities of the 2223 phase. They showed that the lead, although it is not known why, increased the percentage of the 2223 phase formed and acted as a flux by decreasing the sintering temperature and time required to form the 2223 phase[4-10]. The lead was also shown to promote crystallization. Another reason for doping the BSCCO material with lead is to increase the apparent valence of copper. As with the lanthanum-based system, the copper valence should be greater than 2+. By replacing some of the Bi^{3+} with Pb^{2+}, the apparent valence of copper is increased. Other phases that were present in other investigators' work were the 2201 and 2212 phases, Ca_2PbO_4, $(Ca, Sr)_2CuO_3$, a semiconducting phase, $(Sr, Ca)_xCu_yO_z$, Cu_2O, $(Ca, Sr)_{14}Cu_{21}O_{41}$ and excess CuO. Some of these investigators believe that the Ca_2PbO_4 phase, the CuO and the 2212 phase interact with one another by liquid phase sintering, precipitation, dissolution or in some other way to form the 2223 phase[10-21]. Besides lead, a number of other dopants have been studied to determine if the superconducting properties could be improved. Of the many dopants investigated, antimony was one of the

additives which actually improved the electrical properties. Several investigators showed that the critical temperature of the BSCCO superconductor was increased with the addition of small amounts of antimony[22-25]. Again, as with the lead, the antimony appears to enhance the conversion of mixed phases and impurities to the 2223 phase, but the mechanism behind this is not yet understood.

The amount of strontium in these superconductors has also been investigated. It was shown that as the amount of strontium in the superconductor was increased, the 2212 phase tends to form instead of the 2223 phase[26-29]. The reason for this is that the 2212 phase is strontium-rich and leaves the leftover calcium in the Ca_2PbO_4 form. The optimum amount of strontium was found to be somewhere between 1.6 and 1.95 moles. As a result of these ideas the composition decided upon for this investigation was $Bi_{1.6}Pb_{0.4}Sr_{1.9}Ca_{2.05}Cu_{3.05}O_x$ or $Bi_{1.6}Pb_{0.4}Sb_{0.1}Sr_{1.9}Ca_{2.05}Cu_{3.05}O_x$ when the effect of antimony additions was investigated.

In trying to understand the 2223 phase formation of the bismuth-based material, there are many variables which must be considered. First, the lead doped BSCCO system is a five component system and understanding the bulk system requires an understanding of the binary and tertiary systems which make up the bulk system. Some of the phases formed from the smaller systems become impurity phases of the bulk system or the phases actually intergrow within each other. In either case, they are difficult to get rid of. Secondly, the literature is contradictory and more over, confusing. Many investigators have published data on the optimum composition for formation of phase-pure 2223 based on powder X-ray diffraction studies (XRD) and electrical property data. The investigators all had different starting compositions, firing schedules and atmospheric controls. Such disagreement implies that (1) cationic substitutions can occur readily or (2) impurity phases are present and either dissolved to form a glassy phase or their XRD peaks overlap with those of the 2223 phase[28]. The same happens with temperatures, ranging from 827 °C to 890 °C, and atmospheres, which go from reducing to air to oxidizing. In all cases, it appears that no one is really sure exactly what is going on. One

thing is certain, there is still a lot of work to be done on the BSCCO system to fully understand the mechanisms of formation for the different phases. The most important parameters which influence the formation of the 2223 phase are chemical composition, atmosphere, powder preparation, sintering time and sintering temperature. Also important, but rarely mentioned in literature, is the particle size and distribution of the processed powders. These affect the reactivity and density of the bulk superconductor, which has been shown to not only be related to the phase formation but to the final physical properties as well.

The bismuth-based material has been synthesized by several techniques, including glass preparation, melt quenching, mixed oxides and chemical coprecipitation routes[30-39]. Chemical coprecipitation via an oxalate route was chosen for this investigation because of the ability to make very homogeneous and uniform powders. Powder prepared by the mixed oxide process must be ground and calcined several times in order to obtain a powder which gives reliable and reproducible results. However, each time the material is ground or ball milled, impurities are introduced, thus lowering the quality of the powder produced. Coprecipitated powder, on the other hand, because of fine particle size, less than 1 μm, and high purity, is more reactive and may not need to be calcined at all[38]. Although, some investigators have obtain good results using melt quenched or glass prepared powders, we believe that the coprecipitation route is the most reliable technique for this study. The BSCCO material had been coprecipitated at Clemson University using the oxalate route with both the acetates and nitrates. The nitrates were chosen over the acetates for the bismuth-based material because copper acetate is soluble only in a basic solution and bismuth acetate only in an acidic solution. The only problem with the nitrates is the solubility of bismuth nitrate[38-40]. Actually, the bismuth nitrate powder was found to dissolve in a dilute nitric acid solution quite easily.

Among all of the possible applications of high T_c superconductors, electric wiring, high density data transmission lines, magnetic shielding and hybrid technology are the areas in which the first high T_c components could be used. At this time, thick film technology appears to be the best

avenue for making these components. Table 1 shows different phases of BSCCO thick films on a variety of substrate materials. The key substrate materials shown are SrTiO3, MgO, Ag and the zirconia based substrates. The major phases researched are 1112, 2212, 2223 and 4334. The properties range from non-superconducting, due to film-substrate reaction or a yellow-green insulating phase, to transition temperatures in excess of 100 K on MgO. Cold rolling of the BSCCO thick film on silver also produced T_c's greater than 100 K. The highest T_c obtained on a YSZ substrate was 72 K. Al_2O_3 and quartz were shown to be poor substrate materials. Overall, the best superconducting properties were obtained on the MgO substrates. However, the stabilized zirconia substrates are preferred because of their lower thermal conductivity. Some of the problems with thick film technology are low density films and reactions between the substrate and the film. To obtain BSCCO thick films with good properties, very dense, single phase films are required. Long sintering times are necessary to obtain these dense, single phase films. Reactions occurring between the films and the substrate materials are intensified as the sintering times increase. These reactions have been reported by other investigators and are not altogether understood. What is known is that the reactions occurring at the interface between the film and the substrate are the main barrier inhibiting practical device design and understanding them could be the key to avoiding them. Screen printing appears to be the easiest and most economical way of depositing films onto the substrate. Other methods which have been used are tapecasting, spray pyrolysis, molten oxide and rapid quench methods. Due to the different phase transformations occurring in the BSCCO system, fabrication of thick films is much more complex than for other systems. Thick films in both the yttrium and bismuth-based systems have been successfully fabricated at Clemson University by tapecasting and screen printing.

To date, the results in the BSCCO system include synthesis of the BSCCO material by mixed oxide, melt quenching and chemical coprecipitation techniques in bulk, thick film and hot pressed forms. Studies have been performed on the effect antimony additions, the number of calcinations, pressing pressure and atmosphere have on the final superconducting properties as well as the influence of resistance changes

during sintering on phase formation. Table 2 summarizes these results.

This report contains the sample preparation procedure for the bismuth-based materials synthesized in bulk, thick film and hot pressed form by the nitrate and acetate based chemical coprecipitation, mixed oxide and melt quench processes. It also contains data on the bismuth-based superconducting grounding link and material results obtained since May, 1992.

II. Experimental Procedure

As previously stated, the composition decided upon for this investigation was $Bi_{1.6}Pb_{0.4}Sr_{1.9}Ca_{2.05}Cu_{3.05}O_x$ or $Bi_{1.6}Pb_{0.4}Sb_{0.1}Sr_{1.9}Ca_{2.05}Cu_{3.05}O_x$ when the effect of antimony additions was investigated.. All of the materials were first tested for the Meissner effect. The critical temperature and critical current density for both the bulk and the tapecast materials were evaluated using a standard four point method. The resistance was measured by a Keithley, Model 580, micro-ohmmeter with a sensitivity of $10^{-6}\,\Omega$. The critical currents were measured using a 1 μV per mm standard by a Keithley, Model 197, Autoranging MicroVolt DMM. In addition, the structures of the samples were examined by powder X-ray diffraction (XRD) using Cu K_α radiation. Scanning electron microscopy (SEM) and Optical microscopy (OM) were used to observe the homogeneity and surface morphology of the materials. Energy Dispersive X-ray Analysis (EDAX) was used to confirm the composition of all materials. BET Surface Area Analyzer and Micromeritics Sedigraph was used to determine the particle size and distribution of the BSCCO materials. Differential Thermal Analysis (DTA) was used to determine the thermal effects of the BSCCO materials. The electrodes for all materials were applied using a commercial silver paste, C8710 from Heraeus Inc., Cermalloy Division, and fired at 845 °C for eighteen minutes.

1. Coprecipitation Process - Nitrate

Figure 1 shows the preparation process for the coprecipitated bulk

bismuth-based material and Figure 2 shows the process for the tapecast bismuth-based material. In both cases the starting materials were $Bi(NO_3)_3$, in a dilute nitric acid solution, $Pb(NO_3)_2$, $Sr(NO_3)_2$, $Ca(NO_3)_2 \cdot 4H_2O$ and $Cu(NO_3)_2 \cdot 2.5H_2O$. The materials were weighed out according to the batch information sheet shown in Table 3. In the case where small additions of antimony were added, Sb_2O_3 (As = 0.035%) from Metal and Thermit Corporation was used since a nitrate form of antimony was not available. The bismuth nitrate solution was poured into a beaker and the other constituents were added one at a time, until each dissolved in the dilute nitric acid solution. Distilled water was added periodically to aid in this process. The solution was constantly stirred by a magnetic stirrer. Once all the constituents were dissolved, a twenty percent excess aqueous solution of oxalic acid was added and stirred for twenty minutes. During this time, the pH was adjusted to approximately 3.5 with ammonium hydroxide. The solution was then dried in a vacuum oven for twelve hours. After drying, the powder was heated to 600 °C for two hours in an alumina crucible to burn off all of the organic radicals. This precalcined powder was then ground and pressed into pellets and sintered at 845 °C for thirty hours in air or calcined at 830 °C for twelve hours in air. The calcined powder was then ground with a mortar and pestle for processing into bulk and tapecast material or calcined again at 830 °C for twelve hours in air. For the bulk material, the calcined and precalcined powder was sintered at 845 °C for twenty-four to thirty hours hours in air. These materials were then electroded and tested. For the tapecast material, only calcined material was used to cast tape. The calcined powder was ball milled with trichloroethylene for one hour and dried at 100 °C for eighteen hours. The dried powder was then mixed with a commercial binder, B73305 from Metoramic Sciences, Inc., in the ratio of 100 grams of powder to 45 grams of binder and ball milled for one hour. The mixture was deaired for ten minutes and tapecast by a conventional tapecasting processes[57]. The tape was cut into strips with the dimensions 25.4 mm x 2.0 mm x 0.5 mm. The strips were sintered covered at 845 °C for twenty-four to fifty hours in air and sintered covered at 845 °C for twenty-four to fifty hours in a low oxygen atmosphere. Both process used the furnace schedule seen in Figure 3.

2. Coprecipitation Process - Acetate

Figure 4 shows the preparation process for the coprecipitated bulk bismuth-based materials. The starting materials were $Bi(O_2C_2H_3)_3$, $Sb(O_2C_2H_3)_3$, Pb Subacetate in methanol and acetic acid, $Sr(O_2C_2H_3)_2$ in water, $Ca(O_2C_2H_3)_2 \cdot H_2O$ in water and $Cu(O_2C_2H_3)_2 \cdot H_2O$. The materials were weighed out according to the batch information sheet shown in Table 4. The bismuth acetate and antimony acetate were put in a beaker and dissolved with acetic acid. Then, the solutions of strontium, calcium and lead were poured into the beaker as well as some methanol. When everything had dissolved, the solution was made basic with ammonium hydroxide and the copper acetate was added. The solution was constantly stirred by a magnetic stirrer. Once the copper acetate dissolved, the solution was changed to acidic with acetic acid and the excess solution of oxalic acid and methanol was added and stirred for twenty minutes. The solution was then dried in a vacuum oven for twelve hours. After drying, the powder was heated to 600 °C for two hours in an alumina crucible to burn off all of the organic radicals. This precalcined powder was then ground and pressed into pellets and calcined at 830 °C for twelve hours in air. The calcined powder was then ground with a mortar and pestle for processing. For the bulk material, the calcined and precalcined powder was sintered at 845 °C for twenty-four hours in air using the furnace schedule seen in Figure 3. These materials were then electroded and tested.

3. Melt Quench Process Via Mixed Oxides

Figure 5 shows the preparation process for the bulk bismuth-based materials. The starting materials were Bi_2O_3, PbO, Sb_2O_3, $SrCO_3$, $CaCO_3$ and CuO. The powders were weighed out and ball milled with distilled water for one hour and dried at 100 °C for eighteen hours. The dried powder was then calcined once in an alumina crucible at 820 °C for twelve hours. The calcined powder was then ground with a mortar and pestle for melt processing. The powder was then melted in an alumina crucible at 1200 °C for twenty minutes in air and rapidly cooled to 1100 °C for two hours

in air. The crucible was removed from the furnace and the BSCCO melt was quenched in a stainless steel pan. When the material cooled to room temperature, it was cut and subjected to an additional heat treatment at temperatures ranging from 845 °C to 865 °C for twenty-four hours in air. The samples were then electroded and tested.

4. BSCCO Thick Film

The MgO, YSZ (Yttria Stabilized Zirconia), and MSZ (Magnesia Stabilized Zirconia) substrates for this work were made using standard tapecasting processes[57]. The different substrate tapes were cut into strips with the approximate dimensions 45 mm x 13 mm. The silver substrates were cut from 0.127 mm silver foil with the same dimensions as the tapecast substrates. The yttria content in the YSZ substrates varied from 6% to 12% and the magnesia content in the MSZ substrates varied from 8% to 12%. The tapecast substrates were fired between 1500 °C and 1600 °C for four hours in air. Some of these substrates were coated with different buffer layer materials to determine if the reactions between the films and the substrates could be reduced. An MgO buffer layer was used because of the good superconducting properties observed from the films on the MgO substrates. Several BSCCO compounds were also tried as buffer layer materials. The buffer layers were applied by the dip coating process, which can be seen in Figure 6, at 600 °C for 3 minutes per layer. The number of layers applied to the substrates varied from five to twenty layers. After coating, the substrates were annealed at temperatures ranging from 1400 °C to 1600 °C for one hour. All of the thick films were screen printed onto the various substrates. The screen print dimensions were 1.50 in. x 0.25 in. The paste for screen printing was made from nearly single phase coprecipitated BSCCO powders mixed with alpha terpineol, binder, toluene and ethanol in the ratio of 25:7:1:1:1. A flowchart for this process can be seen in Figure 7. After the films were printed onto the substrates, they were dried at room temperature for twelve hours and sintered at temperatures ranging from 830 °C to 890 °C for times ranging from one to twenty-four hours.

5. In-Situ Resistivity Development

In electronic materials, the resistance of the material has a major effect on its physical properties. In superconductivity, it is used to define the material. The resistance of a material must be zero for that material to be classified as a superconductor. Because of this, an in situ resistivity development study was undertaken to determine if a correlation between the resistance of the material during sintering and the formation of the 2223 phase existed. If so, this could aid in determining the optimum firing conditions for the BSCCO materials.

The powder for this study was made by the coprecipitation process described in section II.1. Precalcined, once and twice calcined powder was used for this study. The electrode materials were silver wires of 0.25 mm and 1 mm diameter. The wires were cleaned using a commercial jewelry cleaner and distilled water prior to use. Each of the test samples consisted of twenty-five grams of powder and the silver wires were pressed into the BSCCO pellets using a pressing force of 20,000 psi. Once the electrodes were embedded into the sample, it was sintered at 845 °C for twenty-four to seventy-two hours or until one of the silver wires broke. A low oxygen (6% O_2 / 94% N_2) atmosphere was used to reduce the oxidation or degradation of the silver wires. The embedded silver wires were connected to the Keithley, Model 580, micro-ohmmeter and data points were taken every fifteen minutes using a 100 mA DC testing current. An IBM 386 SX-20 computer acquired the data from the micro-ohmmeter via HPIB (IEEE-488 Bus) interface.

III. Results and Discussion

1. BSCCO Bulk and Tapecast Materials

Figure 8 shows the resistance versus temperature curve for the hot pressed BSCCO coprecipitated compact which was prepared at 845 °C for six hours in oxygen at 5000 psi. The curve showed that the material had a transition to the superconducting state at 84.0 K. Figure 9 shows the resistance versus temperature curve for the same compact with an

additional twenty-four hour heat treatment at 845 °C in air. The curve showed that the material now has a sharp transition to the superconducting state at 108.1 K. This material is now less dense, the bulk density dropped from 6.21 to 6.08 g/cc, but the additional twenty-four hour heat treatment has increased the T_c by 24 K. This is comparable to the data acquired from the mixed oxide materials. In those materials, the T_c increased from 83.3 K to 108.2 K[58]. This again shows the influence that pressure has on the conversion of the lower T_c phase to the higher T_c phase. The higher pressure causes conversion in a substantially shorter amount of time due to the compact being much more dense and uniform. For a comparison with the nitrate based material, the chemically coprecipitated acetate based material was synthesized. The T_c of the uniaxially low pressure sample was 104.1 K, which was approximately the same as the results obtained from the nitrate powder which was 104.4 K.

Again, as with the mixed oxide materials, the number of calcinations had a major effect on the superconducting properties of the bulk material. In the hot pressed material with no additional heat treatment, shown in Figure 10, the one time calcined material did not superconduct, while the two times calcined material had a T_c of 84.0 K. The same two compacts with an additional heat treatment of twenty-four hours at 845 °C in air, shown in Figure 11, showed that the one time calcined material had a T_c of 106.4 K, and the two times calcined material had a higher T_c of 108.2 K. Three times calcined coprecipitated powder has not yet been used to produce the hot pressed material. Conversely, in the uniaxially pressed materials, the critical temperature decreased as the number of calcinations increased. Figures 12 through 14 show the resistance versus temperature curves for the uniaxially pressed BSCCO coprecipitated compacts which were calcined once, twice and three times at 830 °C for twelve hours. These materials were then sintered at 845 °C for twenty-four hours in air. The pressing pressure used to press these materials was 15000 psi. The decrease in critical temperature was most probably due to the increased amount of the 2212 phase being formed during the calcination period. This, in turn, slowed down the conversion to the 2223 phase during sintering.

Due to the results obtained from other investigators, the mixed oxide and chemically coprecipitated powders, both acetate and nitrate based,

were doped with antimony. Figure 15 shows the resistance versus temperature curve for the BSCCO nitrate based coprecipitated compact doped with lead and antimony. The T_c of 106.5 K was not as high as was seen in literature but it was slightly higher than the Tc of the lead doped BSCCO compact which was 104.8. Similarly, the acetate based coprecipitated compact doped with lead and antimony had a Tc of 105.3 K which was higher than lead doped BSCCO acetate based compact's Tc of 104.1 K. The resistance versus temperature curve for the BSCCO acetate based coprecipitated compact doped with lead and antimony can be seen in Figure 16. These materials were calcined once at 830 °C for twelve hours and sintered at 845 °C for twenty-four hours in air. Low pressing pressures were used to press these materials. The melt quenched mixed oxide powders doped with lead and antimony did not show superconducting behavior at liquid nitrogen temperature. Figure 17 shows the resistance versus temperature curve for the BSCCO melt quenched compact doped with lead and antimony. The sections were sintered at 855 °C for twenty-four hours in air.

All of the powder used to make the mixed oxide tapecast material was calcined three times and the powder used to make the coprecipitated tapecast material was calcined at 830 °C for twelve hours. There was a problem with the mixed oxide tapecast material, in that, after thirty hours sintering a percentage of the tapes started to curl and fracture. As the sintering time increased so did the percentage of unacceptable tapes. Initially, the problem was alleviated by covering the tapes and sintering them at 845 °C. Better results were obtained using this method but these tapes partially reacted with the setter plate. Although, curling was not a problem with the coprecipitated tape, low strength was. Both of these problems were solved by firing the tapes in a low oxygen atmosphere. The Tc's remained virtually the same, 101.5 K versus 101.7 K for the mixed oxide tapecast material and 102.4 K versus 102.1 K for the coprecipitated tapecast material[58]. The mixed oxide tapecast material no longer needed to be covered and all of the tapes appeared to be stronger. A resistance versus temperature curve for the coprecipitated tapecast material, which was sintered for thirty hours in the low oxygen atmosphere, can be seen in Figure 18.

The highest critical temperature achieved for the superconducting grounding links that were made from the coprecipitated tapecast material, to date, is approximately 101 K.

2. BSCCO Thick Films

MgO was the first substrate material chosen for the BSCCO thick film material based on the data in Table 1. Figure 19 shows a resistance versus temperature curve for a coprecipitated screen printed thick film which was sintered for one hour at 845 °C in air and had a T_c of 89.0 K. Figure 20 shows an SEM micrograph of the BSCCO thick film on the MgO substrate. It is evident from the microstructure that the film is not very dense, this is due primarily to the short sintering time. As previously stated, longer sintering times are required for denser films and denser films are required for improved properties. The results obtained from the films on the MgO substrates are not bad considering that the substrates were made in house and not purchased for better quality. Once good results were obtained on the MgO substrates, the focus was directed toward the stabilized zirconia substrates.

Figure 21 shows the progression of the YSZ substrate from the zirconia powder through the annealing of the substrate to the application and annealing of the buffer layer from the Xray diffraction data. Comparing the YSZ substrate to that of the JCPDS (Joint Committee on Powder Diffraction Studies) card # 30-1468 for YSZ in Figure 22, one can see that the substrate without a buffer layer was not pure YSZ. This could have been a major factor contributing to the reactions between the film and the substrate. When the substrate was coated with the an MgO buffer layer and annealed at 1500 °C, the XRD pattern matched that of YSZ with the additional MgO peak due to the buffer layer. Figure 23 shows the resistance versus temperature curves for the BSCCO thick films printed on the 10 % YSZ substrates and sintered for three hours at 845 °C in air, with and without the MgO buffer layer. The curves show that the buffer layer definitely improves the electrical properties of the thick film printed on YSZ, although both films were non-superconducting at liquid nitrogen temperature. The amount of reaction with the substrate was reduced with

the addition of the buffer layer but the reactions still occurred. Since the MgO buffer layer changed the phase of the YSZ substrate, the structural integrity of the buffer layer was in question. However, from the Xray data of the top and bottom of the YSZ substrate, shown in Figure 24, it is clear that the MgO peak only occurs on the top of the substrate indicating that this was, in fact, a buffer layer and not a reaction between the MgO layer and the YSZ substrate. An SEM micrograph, shown in Figure 25, of the MgO buffer layer showed microcracks in the buffer layer which explains why the reactions, although reduced, were still occurring. The next step was to consider the amount of yttria used to stabilized the zirconia substrate. Figure 26 shows the resistance versus temperature curves for the BSCCO thick films printed on the 8 % YSZ substrates and Figure 27 shows the resistance versus temperature curves for the BSCCO thick films printed on the 6 % YSZ substrates. All were sintered for three hours at 845 °C in air, with and without the MgO buffer layer. In each case, the buffer layered substrate provided better electrical properties than the substrate without a buffer layer. In addition, as the amount of yttria used to stabilize the zirconia decreased, the electrical properties improved. However, none of the samples superconducted at liquid nitrogen temperature.

Several BSCCO buffer layers were also tried with the YSZ substrates. Figure 28 shows a resistance versus temperature curve for a BSCCO thick film printed on the BSCCO / YSZ substrate and sintered for one hour at 845 °C in air. The Tc was 88.4 K which was comparable to the results observed on the MgO substrates. The only drawback was that the BSCCO buffer layer itself showed metallic behavior after being sintered at 880 °C in air for 10 minutes. The resistance versus temperature curve for the BSCCO / YSZ substrate can be seen in Figure 29. The other BSCCO buffer layers tried did not adhere to the substrate. Silver was also used as a substrate material for the BSCCO thick films. No reactions were observed from the BSCCO thick film sintered in air at 845 °C for 24 hours but an apparatus sensitive enough to measure the properties was not available.

Due, again, to the results obtained by other investigators on MgO and the fact that the MgO buffer layer would be more compatible with a magnesia based substrate, MSZ was used as a substrate material. Figure 30 shows the Xray diffraction pattern obtained from the MSZ

substrates with and without a buffer layer. These patterns show that this substrate is a pure stabilized zirconia substrate as opposed to the YSZ ones. In addition, the pattern shows the MgO peaks after the buffer layer had been applied. There were some problems applying the buffer layers to the MSZ substrates. After approximately seven layers the substrates started to break apart. When the bottom side of the substrate was Xrayed, shown in Figure 31, the MgO peaks appeared on both sides which confirmed the suspicion that the substrate was breaking apart due to the MgO solution reacting with the MSZ substrate. Figure 32 shows a resistance versus temperature curve for a BSCCO thick film printed on a 12 % MSZ substrate without a buffer layer. Due to the metallic behavior of the sample without the buffer layer, which was the best electrical property observed from the stabilized zirconia substrates, it was believed that the MSZ substrate was the best possible substrate for further study. A differential thermal expansion curve, shown in Figure 33, was performed to see which substrate was better in terms of thermal expansion mismatch. The thermal expansion of the BSCCO material was determined to be approximately 12×10^{-6} in/in °C [58], which is very close to that of the MSZ substrate.

Based on the results obtained from the tapecast materials, the BSCCO thick films were fired on 12 % MSZ substrates at 845 °C for two hours under a low oxygen atmosphere. Figure 34 shows the resistance versus temperature curve for the BSCCO thick films printed on the 12 % MSZ substrate with a five coat buffer layer and without a buffer layer. The buffer layer improved the properties again, this time by 7 K. Both thick films superconducted at transitions of 82 K and 89 K respectively. Figure 35 shows the microstructure of two BSCCO thick films. The dense thick film superconducted at 87 K and the porous thick film did not superconduct at liquid nitrogen temperature. These results reinforce the theory that the film must be dense to have the best superconducting properties.

3. In-Situ Resistivity Development

Figure 36 shows the resistivity data taken using the 0.25 mm silver

wires and one time calcined powder. The top graph is the entire run from the initial dwell at 845 °C until a silver wire broke after sixty-four hours. The bottom graph is a close up view of the specific areas of interest. Area 1 starts at the beginning of the 2223 phase formation and continues on through area 2. The break in between the two areas was due to the degradation of the silver wire. In area 3, the temperature was raised to 855 °C to see the effect on the material through the resistance. As one would expect from a material which shows metallic behavior, an increase in the temperature causes an increase in the resistance. The opposite was the case in area 4. The temperature was reduced to 835 °C and the resistance dropped along with it. Figure 37 shows the same run using new powder and silver wire. This time when the silver wire degraded it broke immediately after forty-two hours. These two curves show the influence of the silver wire on the resistance and the unreproducible nature of this particular setup. Because of the difficulty and problems of using the 0.25mm silver wires, the 1 mm wire was used in the next run and the powder used was calcined twice. Figure 38 shows the 2 cycle graph where each cycle lasted twenty-four hours. The purpose of this was to determine whether or not a single sample's resistance curve would be reproducible. By using the two times calcined powder the curves appeared much more regular and controlled. A very interesting point of this run was that the second cycle had a higher dwell resistance than the first cycle. This seemed exactly opposite of what one would expect. The most interesting aspect of the resistivity data is shown in Figure 39. This was the heating curve shown in Figure 38. If the curve would have been run against temperature instead of time, then a resistance versus temperature curve could have been graphed from 77.3 K to 1118 K (845 °C). Even so, it is easy to see from the time data that the metallic behavior continues all the way to the sintering temperature of 845 °C.

IV. Conclusions

In conclusion, to produce coprecipitated hot pressed material with the

best properties the starting material should be calcined at least two times, but for uniaxially pressed materials the starting material should be calcined only once. Higher pressing pressures have, again, shown to produce powders which have better electrical properties than those produced from the lower pressing pressures. Doping the BSCCO material with antimony increases the critical temperature but not to the extent that other invesigators have seen. The acetate and nitrate based coprecipitated powders have approximately the same electrical properties. When synthesizing both the mixed oxide and coprecipitated thick film materials, which includes tapecasting, the best results occur when the materials are sintered under a low oxygen atmosphere because the films can be sintered longer and become more dense. This allows a larger percentage of the 2223 phase to form. The BSCCO thick films printed on MgO substrates and fired at 845°C for 1 hour had the highest T_c of 89.0 K. The J_c for all films is very low due to the poor interconnections. This could be increased by making denser, single phase films. The MgO buffer layer improved the electrical properties of the BSCCO thick films and the MSZ substrate is considered to be the best substrate for this work. The coprecipitated powder is preferred over the mixed oxide powder because a larger percentage of the 2223 phase can be formed in a much smaller amount of time.

V. References

1. Maeda, H., Y. Tanaka, M. Fukutomi and T. Asano, (1988). "A New high-T_c Oxide Superconductor Without a Rare Earth Element," *Jap. J. Appl. Phys.*, vol. 27, No. 2, February, pp. L209-L210.

2. Haertling, G. H., (1990). "Development and Evaluation of Superconducting Circuit Elements," NASA Final Report, Contract No. NAG-1-820, October.

3. Haertling, G. H., (1991). "Ceramic Superconducting Components," *Ceramic Transaction*, Vol. 18

4. Tripathi, R. B., and D. W. Johnson Jr., (1991). "Influence of Lead in the Processing of High Temperature 2223 Bi-Sr-Ca-Cu-O Superconductor," *J. Am. Ceram. Soc.*, vol. 74, No. 1, January, pp. 247-249.

5. Takano M., J. Takada, K. Oda, H. Kitaguchi, Y. Miura, Y. Ikeda, Y. Tomii and H. Mazaki, (1988). "High-T_c Phase Promoted and Stabilized in the Bi, Pb-Sr-Ca-Cu-O System," *Jap. J. Appl. Phys.*, vol. 27, No. 2, February, pg. L1041.

6. Yamada Y., and S. Murase, (1988). "Pb Introduction to the High-T_c Superconductor Bi-Sr-Ca-Cu-O System," *Jap. J. Appl. Phys.*, vol. 27, No. 6, June, pp. L996-L998.

7. Mizuno, M., H. Endo, J. Tsuchiya, N. Kijima, A. Sumiyama and Y. Oguri, (1988). "Superconductivity of $Bi_2Sr_2Ca_2Cu_3Pb_xO_y$ ($x = 0.2, 0.4, 0.6$)," *Jap. J. Appl. Phys.*, vol. 27, No. 7, July, pp. L1225-L1227.

8. Togano, K., H. Kumakura, H. Maeda, E. Yanagisawa and K. Takahashi, (1988). "Properties of the Pb-doped Bi-Sr-Ca-Cu-O Superconductor," *Appl. Phys. Lett.*, 53 (14), 3 October, pp. 1329-1331.

9. Narumi, S., H. Ohtsu, I. Iguchi and R. Yoshizaki, (1989). "Synthesis of 110 K Bi(Pb)-Sr-Ca-Cu-O Oxide Superconductors," *Jap. J. Appl. Phys.*, vol. 28, No. 1, January, pp. L27-L30.

10. Kim, C. J., C. K. Rhee, H. G. Lee, S. J-L. Kang and D. Y. Won, (1989). "The Formation of the High-T_c Phase in the Pb-Doped Bi-Sr-Ca-Cu-O System," *Jap. J. Appl. Phys.*, vol. 28, No. 1, January, pp. L45-L48.

11. Chen, Y. L., and R. Stevens, (1992). "2223 Phase Formation in Bi(Pb)-Sr-Ca-Cu-O: II, The Role of Temperature - Reaction Mechanism," *J. Am. Ceram. Soc.*, vol. 75, No. 5, May, pp. 1150-1159.

12. Wong-Ng, W., C. K. Chiang, S. W. Freiman, L. P. Cook and M. D. Hill, (1992). "Phase Formation of the High T_c Superconducting Oxides in the Bi-Pb-Sr-Ca-Cu-O Glass," *Am. Ceram. Soc. Bull.*, vol. 78, No. 8, August, pp. 1261-1267.

13. Oota A., K. Ohba, A. Ishida, A. Kirihigashi, K. Iwasaki and H. Kuwajima, (1989). "Growth Process of the (2223) Phase in Pb-Added Bi-Sr-Ca-Cu-O," *Jap. J. Appl. Phys.*, vol. 28, No. 7, July, pp. L1171-L1174.

14. Oka, Y., N. Yamamoto, H. Kitaguchi, K. Oda and J. Takada, (1989). "Crystallization Behavior and Partially Melted States in Bi-Sr-Ca-Cu-O," *Jap. J. Appl. Phys.*, vol. 28, No. 2, February, pp. L213-L216.

15. Sasakura, H., S. Minamigawa, K. Nakahigashi, M. Kogachi, S. Nakanishi, N. Fukuoka, M. Yoshikowa, S. Noguchi, K. Okuda and A. Yanase, (1989). "Single High-T_c Region of the Bi-Pb-Sr-Ca-Cu-O," *Jap. J. Appl. Phys.*, vol. 28, No. 7, July, pp. L1163-L1166.

16. Huang, Y. T., W. N. Wang, S. F. Wu, C. Y. Shei, W. M. Hurng, W. H. Lee and P. T. Wu, (1990). "Formation of the Liquid Phase in the System Bi-Pb-Sr-Ca-Cu-O," *J. Am. Ceram. Soc.*, vol. 73, No. 11, pp. 3507-3510.

17. Chen, F. H., H. S. Koo and T. Y. Tseng, (1991). "Effect of Ca_2PbO_4 Additions on the Formation of the 110 K Phase in Bi-Pb-Sr-Ca-Cu-O Superconducting Ceramics," *Appl. Phys. Lett.*, 58 (6), 11 February, pp. 637-639.

18. Kijima, N., H. Endo, J. Tsuchiya, A. Sumiyama, M. Mizuno and Y. Oguri, (1988). "Reaction Mechanism of Forming the High-T_c Superconductor in the Bi-Pb-Sr-Ca-Cu-O System," *Jap. J. Appl. Phys.*, vol. 27, No. 10, October, pp. L1852-L1855.

19. Huang, Y. T., R. G. Liu, S. W. Lu, P. T. Wu and W. N. Wang, (1990). "Accelerated Formation of 110 K High T_c Phase in the Ca- and Cu-rich Bi-Pb-Sr-Ca-Cu-O System," *Appl. Phys. Lett.*, 56 (8), 19 February, pp. 779-781.

20. Yoon, K. H., and H. B. Lee, (1991). "Formation of the High-T_c Phase in Lead-Doped Bi-Sr-Ca-Cu-O Superconductors," *J. Mat. Sci.*, vol. 26, pp. 5101-5106.

21. Hatano T., K. Aota, S. Ikeda, K. Nakamura and K. Ogawa, (1988). "Growth of the 2223 Phase in Leaded Bi-Sr-Ca-Cu-O System," *Jap. J. Appl. Phys.*, vol. 27, No. 11, November, pp. L2055-L2058.

22. Rojek, A., G. Wasilewska, A. Bohdziewicz, B. Cendlewska and E. Trojnar, (1991). "115 K Superconductivity of Bi(Pb/Sb)-Sr-Ca-Cu-O Thick Films," *Physica C*, vol. 183, pp. 130-134.

23. Spencer, N. D., S. D. Murphy, G. Shaw, A. Gould, E. M. Jackson and S. M. Bhagat, (1989). "Solution-Phase Preparation and Characterization of $Bi_{1.6}Pb_{0.3}Sb_{0.1}Ca_2Sr_2Cu_3O_{10}$," *Jap. J. Appl. Phys.*, vol. 28, No. 9, September, pp. L1564-L1567.

24. Komatsu, T., R. Sato, K. Matusita and T. Yamashita, (1989). "Effect of Sb Addition on the Formation of High-T_c Phase in the Bi-Pb-Sr-Ca-Cu-O Ceramics," *Jap. J. Appl. Phys.*, vol. 28, No. 7, July, pp. L1159-L1162.

25. Maeda, T., K. Sakuyama, H. Yamauchi and S. Tanaka, (1989). "Effects of Sb-Doping on the Formation of Superconducting Phases in Bi-Pb-Sr-Ca-Cu Oxides," *Physica C*, vol. 159, pp. 784-788.

26. Endo, U., S. Koyama and T. Kawai, (1989). "Composition Dependence on the Superconducting Properties of Bi-Sr-Ca-Cu-O," *Jap. J. Appl. Phys.*, vol. 28, No. 2, February, pp. L190-L192.

27. Zorn, G., B. Seebacher, B. Jobst and H. Gobel, (1991). "Investigation of Formation Reactions in the System Bi-Pb-Sr-Ca-Cu-Oxide Starting from Oxides and Carbonates," *Physica C*, vol. 177, pp. 494-508.

28. Chen, Y. L., and R. Stevens, (1992). "2223 Phase Formation in Bi(Pb)-Sr-Ca-Cu-O: I, The Role of Chemical Composition," *J. Am. Ceram. Soc.*, vol. 75, No. 5, May, pp. 1142-1149.

29. Seshu Bai, V., S. Ravi, T. Rajasekharan and R. Gopalan, (1991). "On the Composition of 110 K Superconductor in a (Bi, Pb)-Sr-Ca-Cu-O System," *J. Appl. Phys.*, vol. 70, No. 8, October, pp. 4378-4382.

30. Endo, U., S. Koyama and T. Kawai, (1988). "Preparation of the High-T_c Phase of Bi-Sr-Ca-Cu-O Superconductor," *Jap. J. Appl. Phys.*, vol. 27, No. 8, August, pp. L1476-L1479.

31. Koyama, S., U. Endo and T. Kawai, (1988). "Preparation of Single 110 K Phase Bi-Pb-Sr-Ca-Cu-O Superconductor," *Jap. J. Appl. Phys.*, vol. 27, No. 10, October, pp. L1861-L1863.

32. Garzon, F. H., J. G. Beery and I. D. Raistrick, (1988). "Amorphous-to-Crystalline Transformations in the Bismuth-Oxide-Based High T_c Superconductors," *Appl. Phys. Lett.*, 53 (9), 29 August, pp. 805-807.

33. Komatsu, T., R. Sato, K. Matusita and T. Yamashita, (1989). "Superconducting Glass Ceramics With T_c= 100 K Based on the Bi-Pb-Sr-Ca-Cu-O System," *Appl. Phys. Lett.*, 54 (12), 20 March, pp. 1169-1171.

34. Nakajima, M., S. Kawarabuki, T. Sasaki, N. Nojiri, Y. Watanabe, H. Ikeda and R. Yoshizaki, (1989). "Synthesis of a 107 K Superconducting Phase in the Bi-Sr-Ca-Cu-O System," *Jap. J. Appl. Phys.*, vol. 28, No. 6, June, pp. L943-L945.

35. Tarascon, J. M., W. R. McKinnon, P. Barbour, D. M. Hwang, B. G. Bagley, L.H. Green, G. Hull, Y. LePage, N. Stoffel and M. Groud, (1988). "Preparation, Structure and Properties of the Superconducting Compound Series $Bi_2Sr_2Ca_{n-1}Cu_nO_y$ with n=1, 2 and 3." *Phys. Rev. B*, vol. 38, No. 13, November, pp. 8885-8892

36. Ono, A.,(1988). "Synthesis of the 107 K Superconducting Phase in the Bi-Sr-Ca-Cu-O System," *Jap. J. Appl. Phys.*, vol. 27, No. 7, July, pp. L1213-L1215.

37. Ibara, Y., H. Nasu, T. Imura and Y. Osaka, (1988). "Preparation and Crystallization Process of the High-T_c Superconducting Phase (Tc(end)>100 K) in Bi, Pb-Sr-Ca-Cu-O Glass-Ceramics," *Jap. J. Appl. Phys.*, vol. 28, No. 1, January, pp. L37-L40.

38. Hagberg, J., A. Uusimaki, J. Levoska and S. Leppavuori, (1989). "Preparation of Bi-Pb-Sr-Ca-Cu-O High-T_c Superconducting Material via oxalate route at Various pH Values," *Physica C*, vol. 160, pp. 369-374.

39. Shei, C. Y., R. S. Liu, C. T. Chang and P. T. Wu, (1990). "Preparation and Characterization of Superconducting (Bi, Pb)$_2$Sr$_2$Ca$_2$Cu$_3$ Oxides with T_c above 110 K by Coprecipitation in Triethylamine Media," *Inorg. Chem.*, vol. 29, pp. 3117-3119.

40. Weast, R. C., (1987). *CRC Handbook of Chemistry and Physics*, CRC Press Inc., Boca Raton, Florida

41. Hashimoto, T., T. Kosaka, Y. Yoshida, K. Fueki and H. Koinuma, (1988). "Superconductivity and Substrate Interaction of Screen-Printed Bi-Sr-Ca-Cu-O Films," *Jap. J. Appl. Phys.*, vol. 27, No. 3, March, pp. L384-L386.

42. Przybylski, K., J. Koprowski, J. Oblakowski and M. Wierzbicka, (1990). "Deposition Thick Film Patterns of the High T_c Superconducting Y-Ba-Cu-O and Bi-Sr-Ca-Cu-O Systems on Ceramic Substrate," *J. of Less Common Metals*, I64 & I65, pp. 470-477.

43. Tabuchi, J., Y. Shimakawa, A. Ochi and K. Utsumi, (1989). "Fabrication of Screen-Printed High-T_c Superconducting Thick Films on Several Substrates," *High Tc Superconductor I*, pp. 464-473.

44. Lee, K., and G. Park, (1991). "Patterned Bi-Sr-Ca-Cu-O Films on $Sr_2Ca_2Cu_4O_y$ Substrates by Surface Diffusion of Metallic Bismuth," *Jap. J. Appl. Phys.*, vol. 30, No. 10, October, pp. 2468-2470.

45. Barboux, P., J. M. Tarascon, F. Shokoohi, B. J. Wikens and C. L. Schwartz, (1988). "Thick Films of Bi-Sr-Ca-Cu-O and Tl-Ba-Ca-Cu-O by Solution Process," *J. Appl. Phys.*, 64 (11), 1 December, pp. 6382-6387.

46. Ho, J. C., C. Y. Wu, X. W. Cao and F. J. Schmidt, (1991). "Melt Textured Thick Films of $Bi_{1.7}Pb_{0.3}Sr_2CaCu_2O_y$ Prepared by Electrophoretic deposition," Supercond. Sci. Technol. (UK), Vol. 4, no. 10, October,pg. 507-508.

47. Bohn, C. L., J. R. Delayen, U. Balachandran and M. T. Lanagan, (1989). "Radio Frequency Surface Resistance of large-Area Bi-Sr-Ca-Cu-O Thick Films on Ag Plates," *Appl. Phys. Lett.*, 55 (3), 17 July, pp. 304-306.

48. Kumakura, H., K. Togano, J. Kase, T. Morimoto and H. Maeda, (1990). "Superconducting Properties of Textured Bi-Sr-Ca-Cu-O Tapes Prepared by Applying Doctor Blade Casting," *Cryogenics*, 30, November, pp. 919-923.

49. Hoshino,K., and T.Takahara, (1989). "Fabrication of High-T_c Bi-Pb-Sr-Ca-Cu-O Superconducting Printed Films on Ag Tape," *Jap. J. Appl. Phys.*, vol. 28, No. 7, July, pp. L1214-L1216.

50. Hoshino, K., H. Takahara and M. Fukutomi, (1988). "Preparation of Superconducting Bi-Sr-Ca-Cu-O Printed Thick Films on MgO Substrate and Ag Metal Tape," *Jap. J. Appl. Phys.*, vol. 27, No. 7, July, pp. L1297-L1299.

51. Muthe, K. P., S. K. Sinha, S. C. Gadkari, S. C. Sabharwal and M. K. Gupta, (1990). "Phase Formation abd Crystallization in Bi-Sr-Ca-Cu-O Thick Films," *Appl. Phys. A*, 51, pp. 65-67.

52. Kobayashi, T., K. Nomura, F. Uchikawa, T. Masumi and Y. Uehara, (1988). "Superconducting Bi-Sr-Ca-Cu-O Thick Films by the Sol-Gel Method," *Jap. J. Appl. Phys.*, vol. 27, No. 10, October, pp. L1880-L1882.

53. Tohge, N., Y. Akamatsu, S. Tsuboi, M. Tatsumisago and T. Minami, (1989). "Substitution effects of Pb for Bi on the Formation of High-Tc Superconducting Thick Films in the Bi-Pb-Sr-Ca-Cu-O System by the Melt-Solidification Method," *Jap. J. Appl. Phys.*, vol. 28, No. 8, August, pp. L1408-L1410.

54. Brousse, T., R. Retoux, G. Poulain, J. Provost, H. Murray, D. Bloyet and B. Raveau, (1989). "Superconducting Screen-Printed Thick Films of $YBa_2Cu_3O_7$ and $Bi_{1.6}Pb_{0.4}Sr_{1.6}Ca_{2.4}Cu_{3.6}O_{10}$ on Polycrystalline Substrates," *Appl. Phys. A*, 49, pp. 217-220.

55. Uusimaki, A., I. Kirschner, J. Levoska, J. Hagberg, G. Zsolt, G. Kovacs, T. Porjesz, I. Dodony, S. Leppavuori, E. Lahderanta and R. Laiho, (1990). "Relationship Between Microstructure and Critical Parameters in High-T_c Superconducting Bi-Pb-Sr-Ca-Cu-O Thick Films ," *Cryogenics*, 30, July, pp. 593-598.

56. Kim, D. H., W. S. Um, K. No and H. G. Kim, (1991). "Preparation of Superconducting Bi(Pb)-Sr-Ca-Cu-O Thick Films on Magnesia Substrate," *J. Am. Ceram. Soc.*, vol. 74, No. 9, September, pp. 2102-2106.

57. Reed, J. S., (1988). *Introduction to the Principles of Ceramic Processing*, John Wiley & Sons, New York.

58. Haertling, G. H., (1991). "Development of High Tc (>110 K) Bi, Tl and Y-Based Materials as Superconducting Circuit Elements," NASA Annual Report, Contract No. NAG-1-1108, May.

59. Sax, N. I., and R. J. Lewis Sr., (1988). *Hawley's Condensed Chemical Dictionary*, 11 th ed., Van Nostrand Reinhold Co., New York.

Substrate	Phase	Firing Condition	T_c (K)	Reference
Quartz	1112	830°C - 1hr.	NS	41
Alumina	1112	830°C - 1hr. 850°C - 1hr.	NS NS	41
Alumina	2223	890°C - 10 min.	M	42
Sapphire	1112 2223	890°C - 900°C 890°C - 900°C	I I	43
$Sr_2Ca_2Cu_4O_y$	2212	830°C - 1min.	79	44
SrTiO3	1112	840°C - 1hr. 850°C - 1hr.	11 NS	41
SrTiO3	4334	875°C - 2 min.	76	45
Ag	2212	900°C - 3 min. 860°C - 5-10 min.	75	46
Ag	2212	910°C - 10 min. 825°C - 4 hr.	81 - 83	47
Ag	2212	870°C (slow cooled) 870°C (quenched)	>77 89	48
Ag	2223	830°C - 845°C – 48 hr. - 72 hr. 830°C - 845°C – 12 hr. - 48 hr.	CR 100 - 105	49
Ag	2223	880°C - 10 min.	76	50
YSZ	1112	890°C - 1 hr. 890°C - 4 hr. 890°C - 5 min.	40 I 45	43
YSZ	1112	840°C - 1hr. 850°C - 1hr. 900°C - 1hr. 850°C - 1hr.	22 65 NS 11	41
YSZ	2212	840°C - 1hr. 850°C - 1hr.	35 68	41

NS -- Non Superconducting
CR -- Cold Rolling
D -- Two Phase
S -- Semiconducting
I --- Insulating
M -- Metallic

Table 1 Review of BSCCO Thick Films.

Substrate	Phase	Firing Condition	T_c (K)	Reference
YSZ	2223	890°C - 4 hr.	I	43
		900°C - 5 min.	66	
		900°C - 1 hr.	72	
MgO	1112	890°C - 1 hr.	60	43
		890°C - 4 hr.	S	
		890°C - 5 min.	62	
MgO	2212	890°C (quenched)	84	51
MgO (100)	2112	860°C - 2 hr.	18 S	52
		870°C - 2 hr.	84 D	
		880°C - 2 hr.	76	
		890°C - 2 hr.	77	
		900°C - 2 hr.	78	
MgO	4334	860°C - 10 min.	NS	45
MgO (100)	2223	860°C - 30 min.	40	50
		880°C - 30 min.	80	
		885°C - 1 hr.--	107	
		872°C - 72 hr.		
MgO	$Bi_{1.8}Pb_{0.2}Sr_2Ca_2Cu_3O_{10}$	1000°C - 5 min. --		53
		840°C - 30 min.	82	
		850°C - 30 min.	90	
		850°C - 15 hr.	102	
		850°C - 38 hr.	92	
		860°C - 30 min.	M	
MgO	2223	890°C - 4 hr.	S	43
		900°C - 5 min.	55	
		900°C - 1 hr.	NS	
MgO	$Bi_{1.6}Pb_{0.4}Sr_{1.6}Ca_{2.4}Cu_3O_{10}$	865°C - 1 hr.	92	54
		865°C - 3 hr.	95	
		865°C - 5 hr.	101	
		865°C - 7 hr.	85	
		865°C - 10 hr.	99	
		865°C - 15 hr.	86	
		865°C - 250 hr.	104	
MgO	$Bi_{1.9}Pb_{0.4}Sr_{1.9}Ca_{2.1}Cu_{3.2}O_{10}$	895°C - 3 min.--		55
		852°C - 80 hr.	57	
		865°C - 80 hr.	105	

NS -- Non Superconducting
CR -- Cold Rolling
D -- Two Phase
S -- Semiconducting
I --- Insulating
M -- Metallic

Table 1 Cont.

Substrate	Phase	Firing Condition	T_c (K)	Reference
MgO	2223	890°C - 10 min.	M	42
MgO (100)	2223	500°C - 4 hr. --		56
		840°C - 4 hr.	50	
		+830°C - 30 hr.	80	
		+830°C - 60 hr.	89	
		+830°C - 90 hr.	45	
MgO (100)	$Bi_{1.6}Pb_{0.3}Sr_2Ca_2Cu_3O_{10}$	840°C - 60 hr.	85	22
	$Bi_{1.9}Pb_{0.6}Sr_2Ca_2Cu_3O_{10}$	920°C - 6 min.--		
		840°C - 65 hr.	102	
	$Bi_{1.9}Pb_{0.6}Sb_{0.1}Sr_2Ca_2Cu_3O_{10}$	920°C - 6 min.--		
		845°C - 65 hr.	115	

NS -- Non Superconducting
CR -- Cold Rolling
D -- Two Phase
S -- Semiconducting
I --- Insulating
M -- Metallic

Table 1 Cont.

Table 2 The results of the bismuth base material to date. The table contains information on the material, the process used, the Tc, the Jc, the bulk density and any special procedures used in synthesizing the material.

Material	Process	Special	T_c (K)	J_c (A/cm^2)	Bulk Density (gms/cc)
Mixed oxide	Bulk	200 hr Sintering	108.1	80	4.5
		High pressure (125 hr)	107.3	78	4.8
		Low pressure (125 hr)	106.8	75	4.4
		20 hr Sintering	98.9	50	4.1
		2 Calcines (30 hr)	99.1	50	4.1
		3 Calcines (30 hr)	102.0	50	4.2
		4 Calcines (30 hr)	102.0		
	Hot pressed	2 Calcines NAHT	M	M	M
		3 Calcines NAHT	83.3		6.2
		2 Calcines (24 hr)	104.4	100	5.7
		3 Calcines (24 hr)	108.2	140	6.0
	Tapecast	Single ramp	99.5	20	3.3
		Single ramp (covered)	101.5	81	3.5
		Double ramp (covered)	99.0	47	3.3
		Low O_2 Atmosphere	101.7	48	
Melt Quenched	Bulk	As quenched	T	T	T
		30 hr Sintering	M	M	M
		60 hr Sintering	M	M	M
		90 hr Sintering	102.3	72	4.9
		24 hr (Antimony)	M	M	M
Coprecipitated	Acetate Bulk	1 Calcine	104.1		
		1 Cal (Antimony)	105.3		
	Nitrate bulk	No Calcine	99.1		4.0
		1 Calcine	104.8	100	4.4
		1 Cal (Antimony)	106.5		
		High pressure (860 °C Calcine)	108.8		5.2

NAHT - No Additional Heat Treatment NBL - No Buffer Layer BL - Buffer Layer

IS - Insulating/Semiconducting MS - More Sensitivity M - Metal T - Transition

Table 2 Cont.

Material	Process	Special	T_c (K)	J_c (A/cm^2)	Bulk Density (gms/cc)
Coprecipitated	Bulk (Cont.)	High pressure (830 °C Calcine)	108.4		5.1
		2 Calcine (high)	104.3		
		3 Calcine (high)	102.9		
	Hot pressed	1 Calcines NAHT	M	M	M
		2 Calcines NAHT	84.0		6.2
		1 Calcines (24 hr)	106.4	144	6.0
		2 Calcines (24 hr)	108.2	193	6.1
	Tapecast	Single ramp	102.4	120	3.9
		Low O_2 Atmosphere	102.1		
		Link	100.5		
	Thick Film				
	MgO	NBL	89.0		
	MSZ (12%)	NBL	M	M	M
		MgO 10 BL	M	M	M
		Low O_2, NBL	82.0		
		Low O_2, MgO 5 BL	89.0		
	YSZ	10 %, NBL	IS	IS	IS
		10 %, 10 BL	T	T	T
		8 %, NBL	IS	IS	IS
		8 %, 10 BL	T	T	T
		6 %, NBL	T	T	T
		6 %, 10 BL	M	M	M
		6% BSCCO 10 BL	88.4		
	Ag	NBL	MS	MS	MS

NAHT - No Additional Heat Treatment NBL - No Buffer Layer BL - Buffer Layer
IS - Insulating/Semiconducting MS - More Sensitivity M - Metal T - Transition

Batch Information Sheet

Composition # 1 **Batch #** 31

Formula $Bi_{1.6}Pb_{0.4}Sr_{1.9}Ca_{2.05}Cu_{3.05}O_x$

Batch Size 100 gms. **Date** November 13, 1992

Raw Materials and Source

$Bi(NO_3)_3$ Mallinckrodt $Pb(NO_3)_2$ Fisher $Sr(NO_3)_2$ Mallinckrodt

$Ca(NO_3)_2 \cdot 4H_2O$ Mallinckrodt HNO_3 Mallinckrodt NH_4OH Fisher

$Cu(NO_3)_2 \cdot 2.5H_2O$ Mallinckrodt Sb_2O_3 Metal and Thermit Corp.

Batching

Oxide	Mole Wt	Moles	Formula Wt	Wt %	% Oxide	Batch Wt
Bi2O3	465.96	0.80	372.768	36.672	11.030	332.478
SrO	103.62	1.90	196.878	19.369	48.963	39.558
CaO	56.08	2.05	114.964	11.310	23.748	47.626
CuO	79.54	3.05	242.597	23.866	34.198	69.790
PbO	223.19	0.40	89.276	8.783	67.388	13.033
			1016.483	100		502.484

Table 3 The batch information for the materials in the BSCCO nitrate coprecipitation process, showing the raw materials used, their source, and the amounts of each needed to achieve the required batch size.

Batch Information Sheet

Composition # 5 **Batch #** 12

Formula $Bi_{1.6}Pb_{0.4}Sr_{1.9}Ca_{2.05}Cu_{3.05}O_x$

Batch Size 100 gms. **Date** October 2, 1992

Raw Materials and Source

$Bi(O_2C_2H_3)_3$ Johnson Matthey $Sr(O_2C_2H_3)_2$ Johnson Matthey

$Ca(O_2C_2H_3)_2 \cdot H_2O$ Johnson Matthey $Sb(O_2C_2H_3)_3$ Johnson Matthey

Pb Subacetate Fisher NH_4OH Fisher $Cu(O_2C_2H_3)_2 \cdot H_2O$ Fisher

Acetic Acid Fisher **Methanol** Fisher

Batching

Oxide	Mole Wt	Moles	Formula Wt	Wt %	% Oxide	Batch Wt
Bi2O3	465.96	0.80	372.768	36.672	60.339	60.777
SrO	103.62	1.90	196.878	19.369	15.410	125.688
CaO	56.08	2.05	114.964	11.310	8.440	134.004
CuO	79.54	3.05	242.597	23.866	39.760	60.026
PbO	223.19	0.40	89.276	8.783	44.800	19.605
			1016.483	100		400.100

100

Table 4 The batch information for the materials in the BSCCO acetate coprecipitation process, showing the raw materials used, their source, and the amounts of each needed to achieve the required batch size.

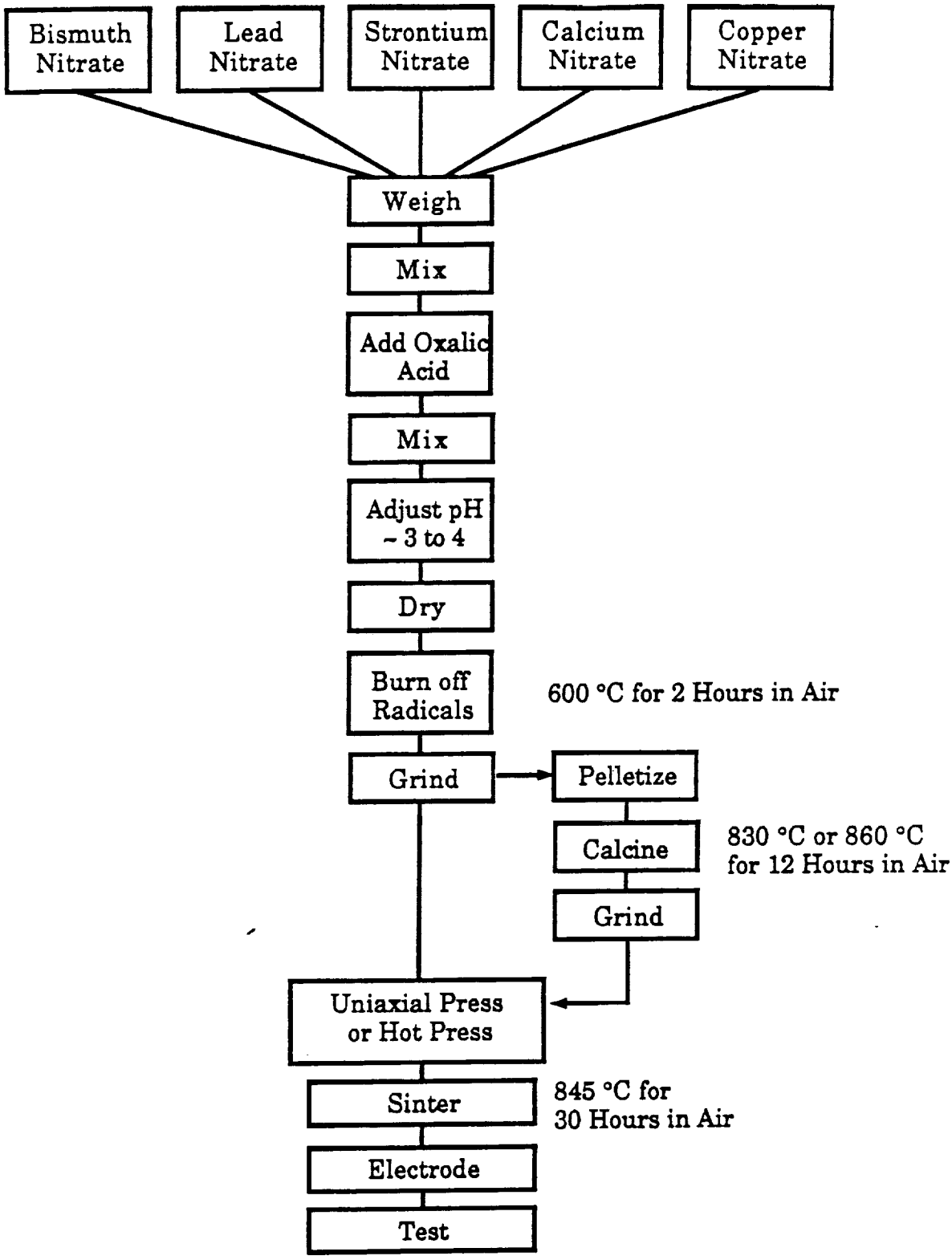

Figure 1 Flow chart for the nitrate coprecipitated bismuth-based materials showing the procedures used to synthesize these materials. These materials were synthesized using both calcined and uncalcined powder.

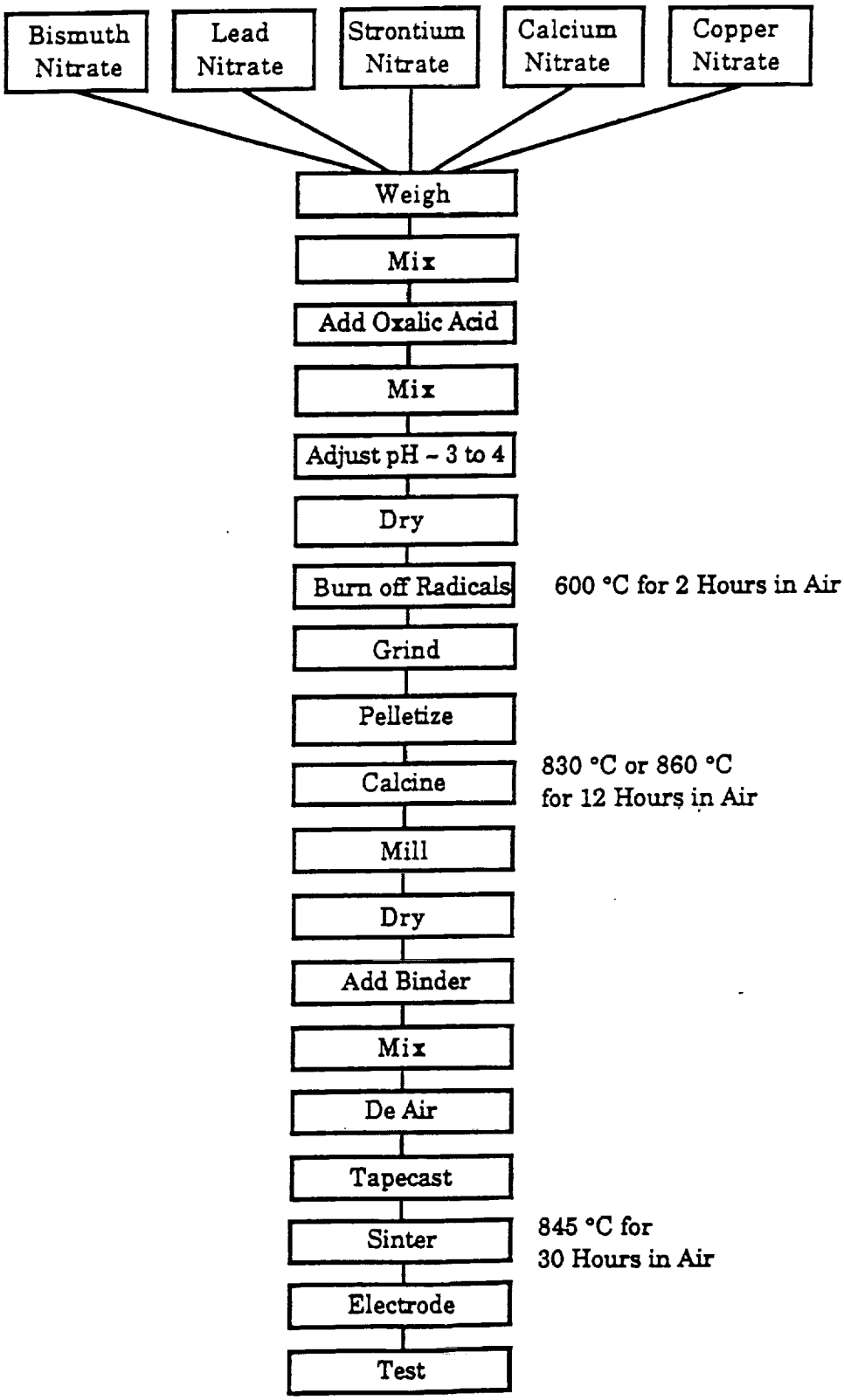

Figure 2 Flow chart for the tapecast bismuth-based materials, made by the nitrate coprecipitation process, showing the procedures used to synthesize these materials. These materials were synthesized using one time calcined powder.

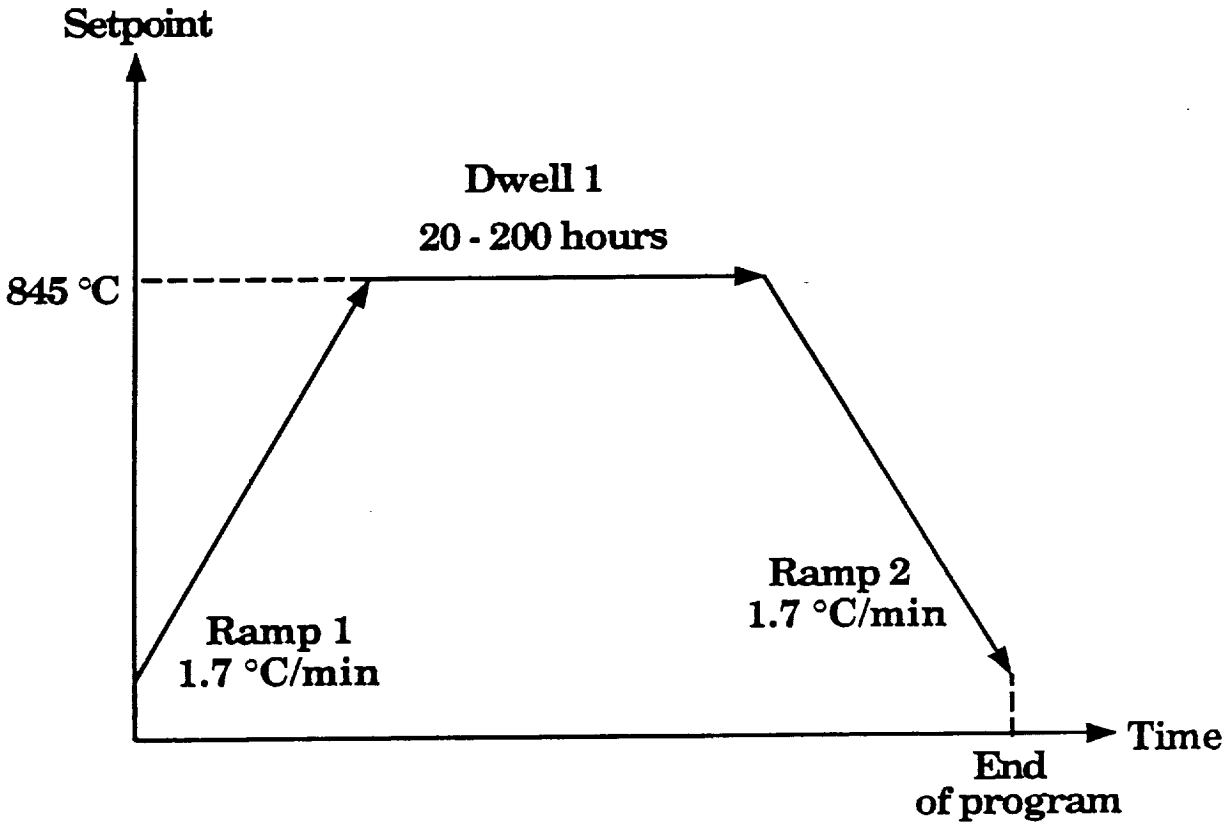

Figure 3 The furnace schedule and operation for the bulk, melt quench, and single ramp tapecast bismuth-based materials.

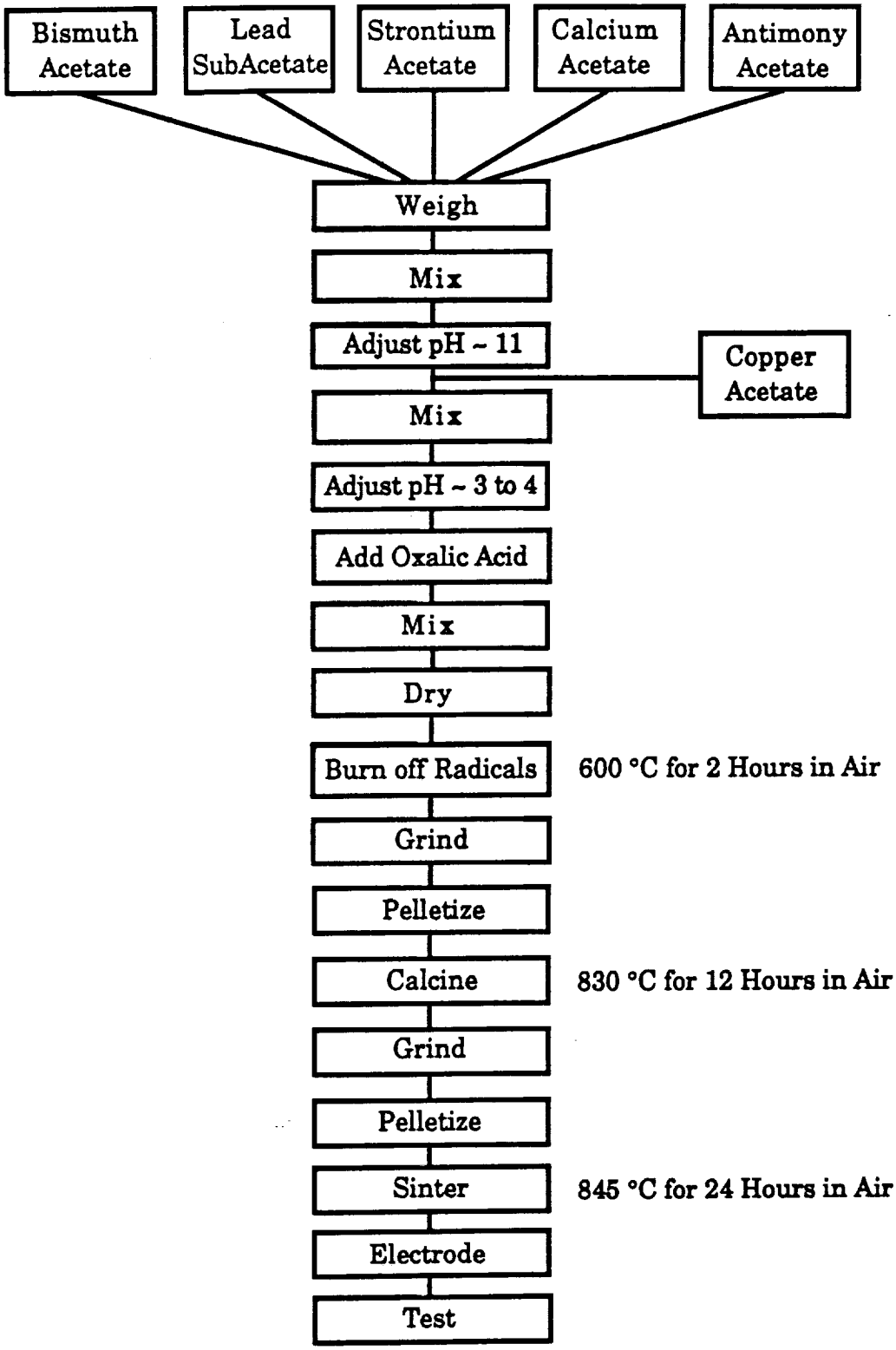

Figure 4 Flow chart for the acetate coprecipitated bismuth-based materials showing the procedures used to synthesize these materials. These materials were synthesized using both calcined and uncalcined powder.

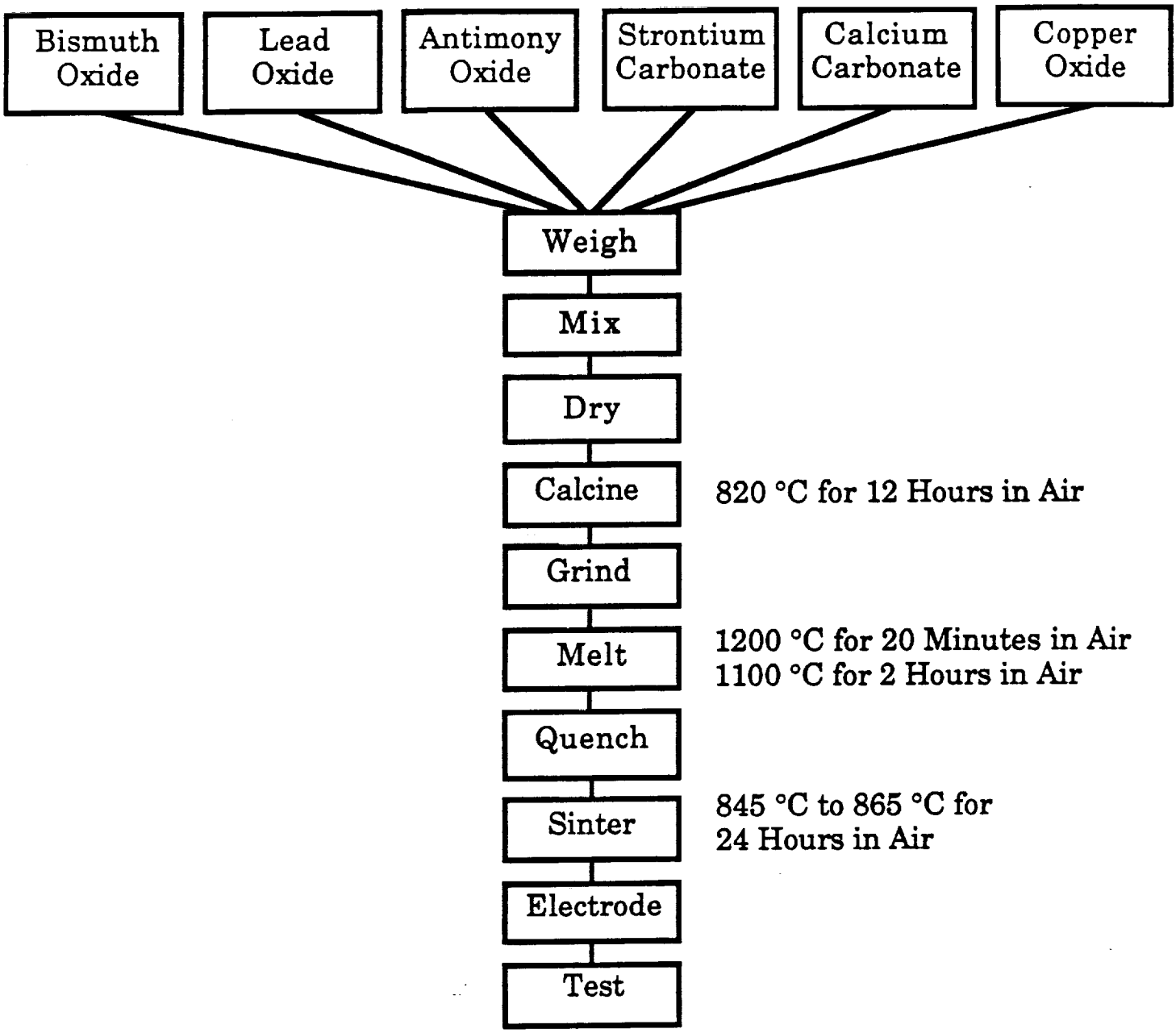

Figure 5 Flow chart for the melt quench process using powder prepared by the mixed oxide process for the bismuth-based materials showing the procedures used to synthesize these materials.

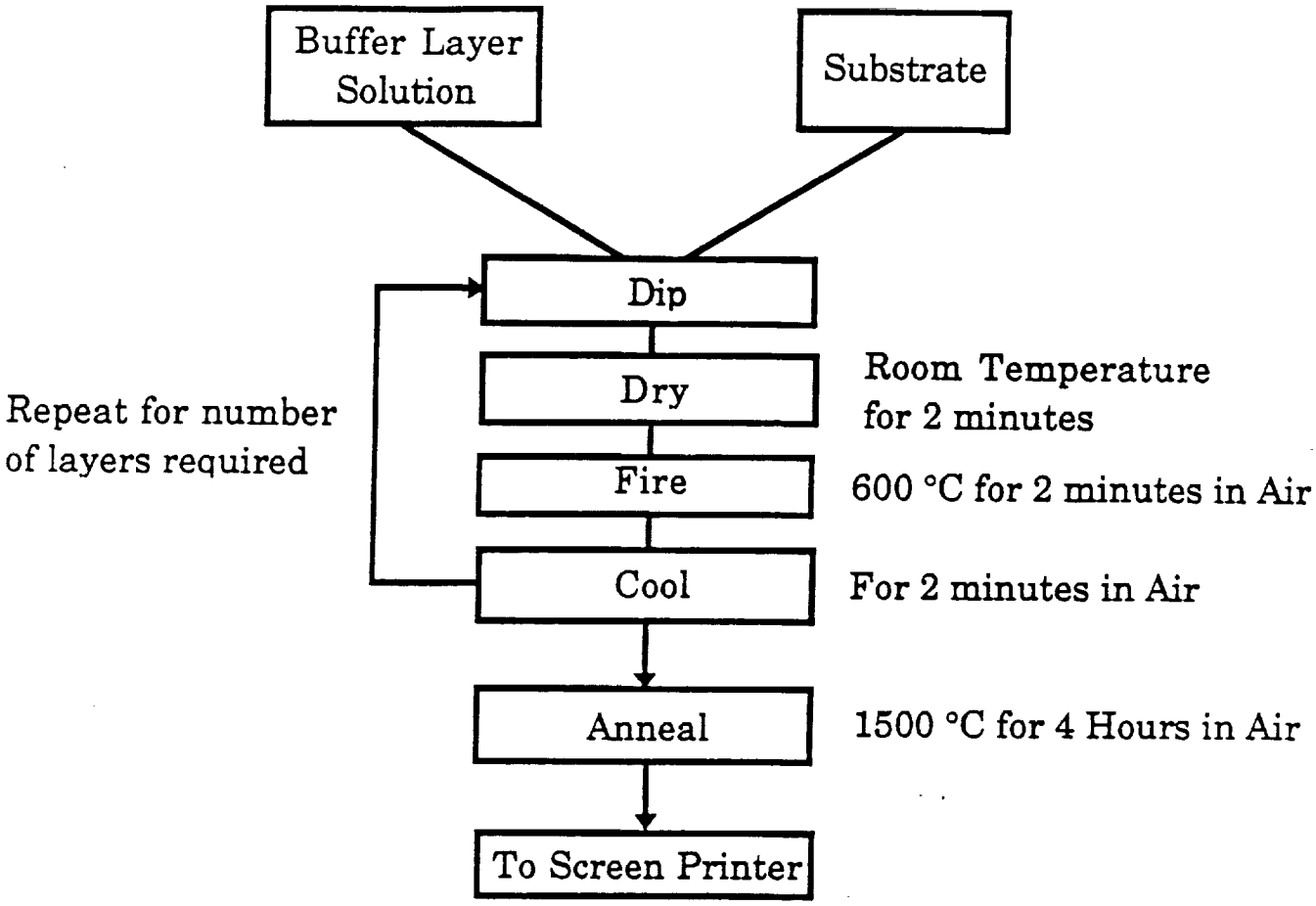

Figure 6 Flowchart of the dip coating process used to apply the buffer layers to the various substrates used for the BSCCO thick films.

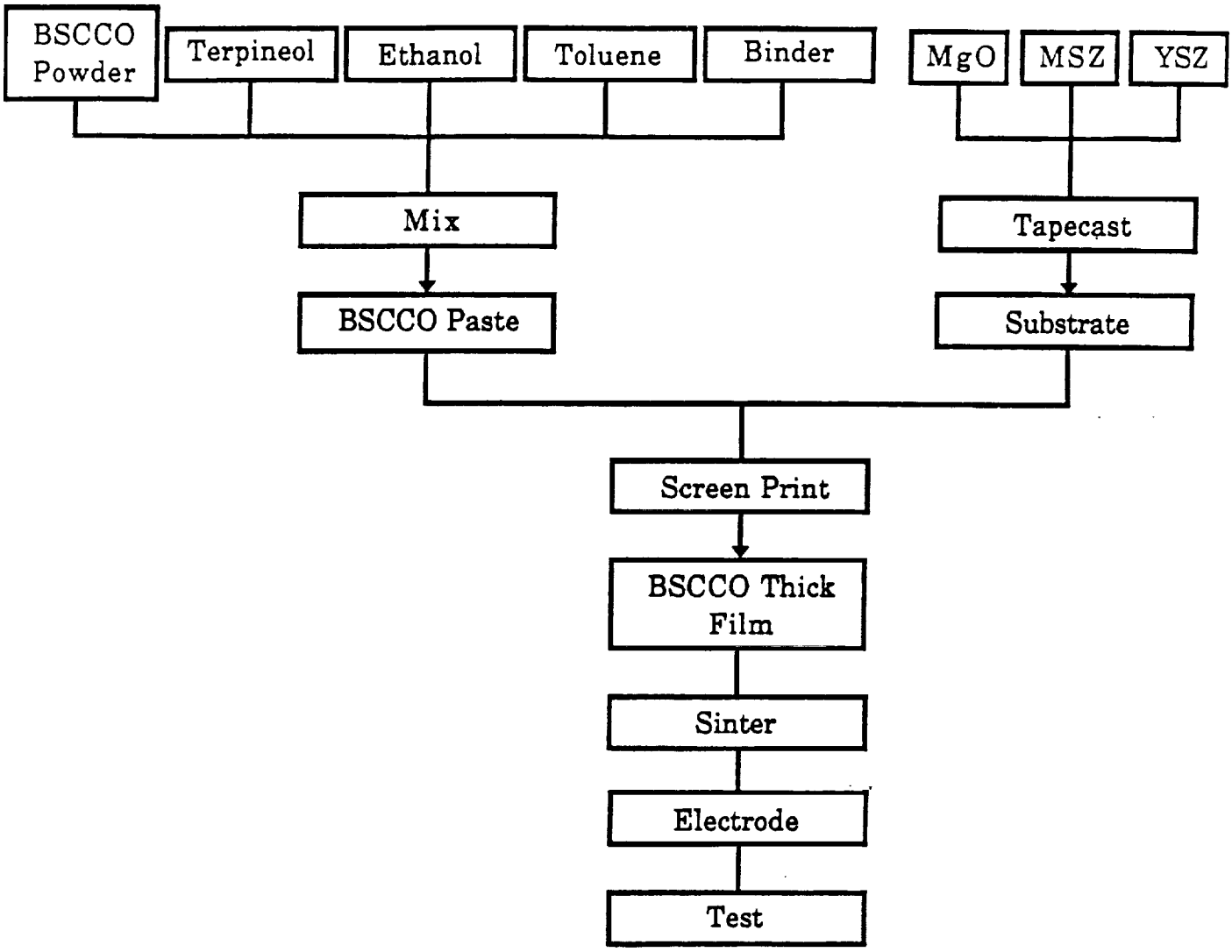

Figure 7 Fabrication process of the BSCCO superconducting thick films.

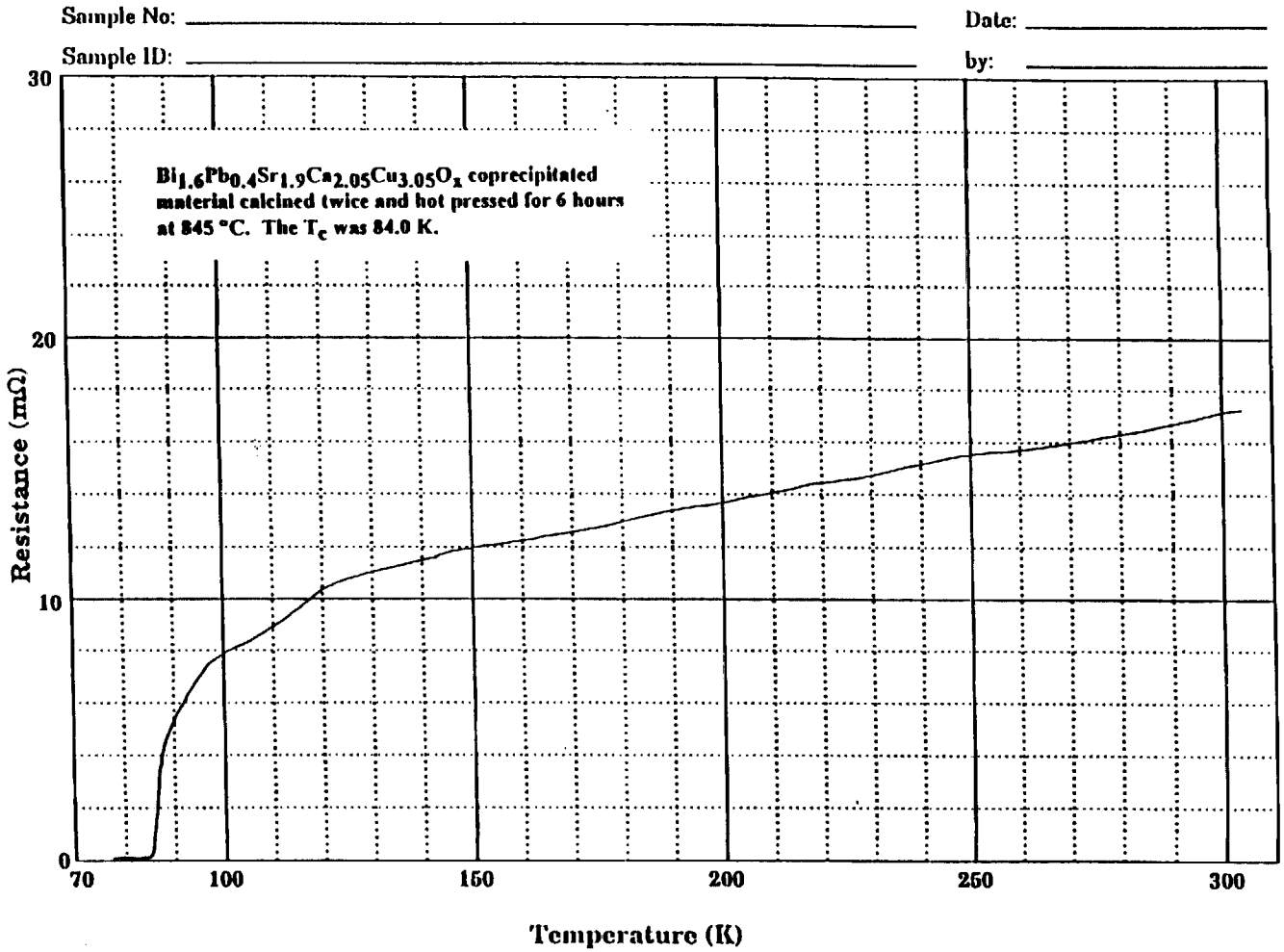

Figure 8 Resistance versus Temperature curve for coprecipitated hot pressed sample with no additional heat treatment.

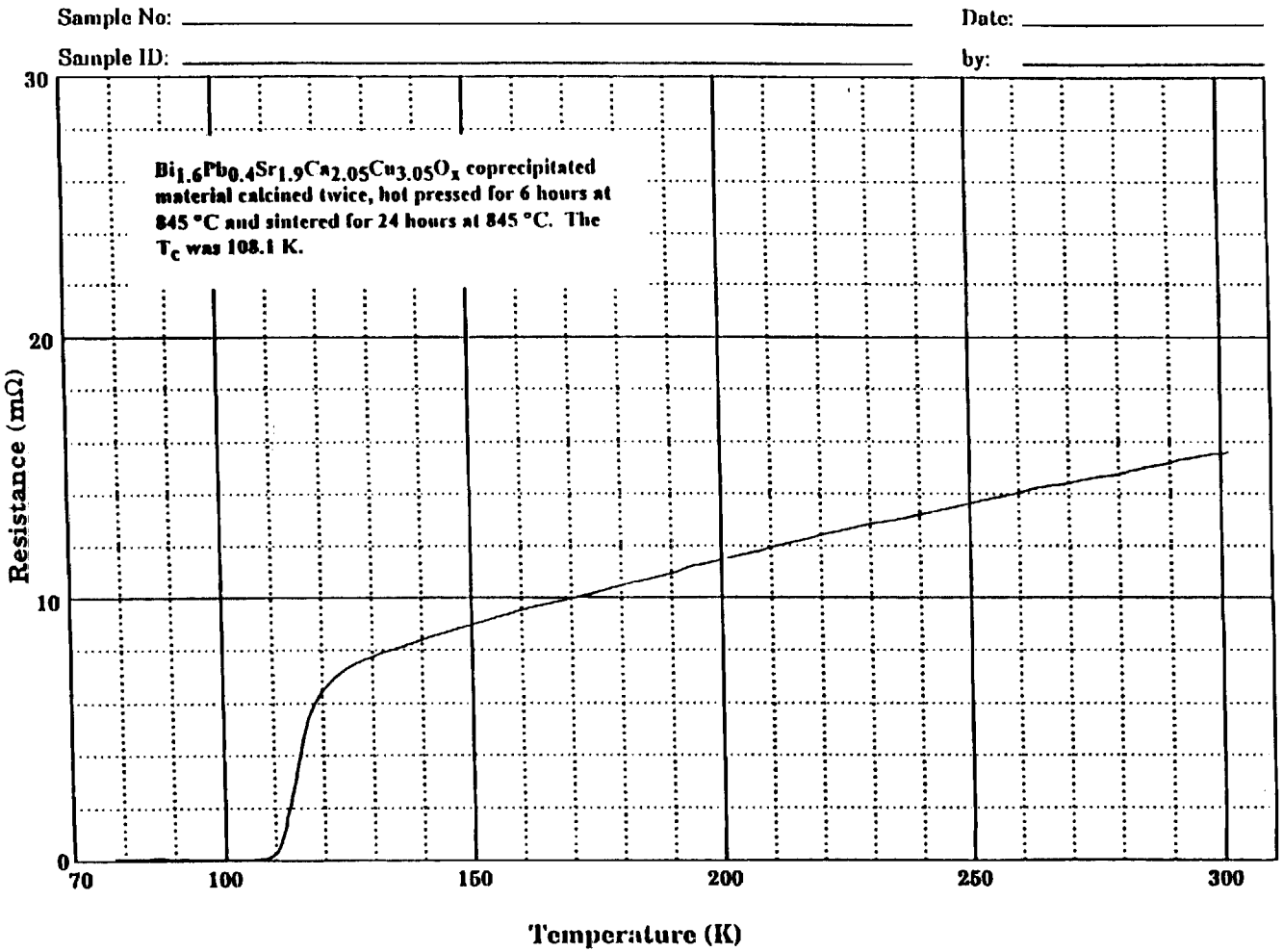

Figure 9 Resistance versus Temperature curve for coprecipitated hot pressed sample with twenty-four hours additional heat treatment at 845 °C.

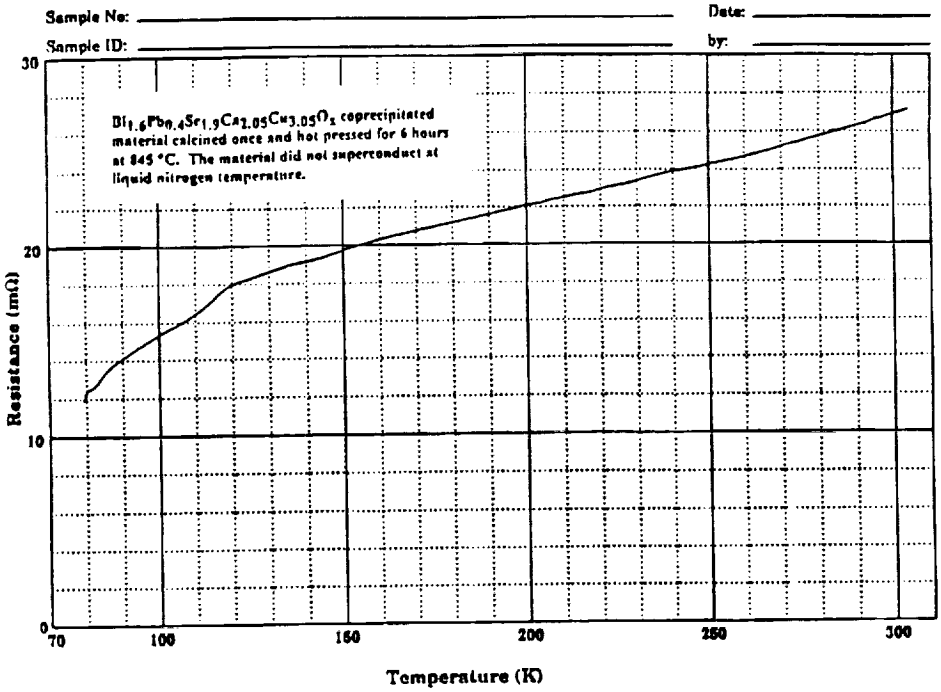

a) Hot pressed pellet with no additional heat treatment, calcined once. The material did not superconduct at liquid nitrogen temperature.

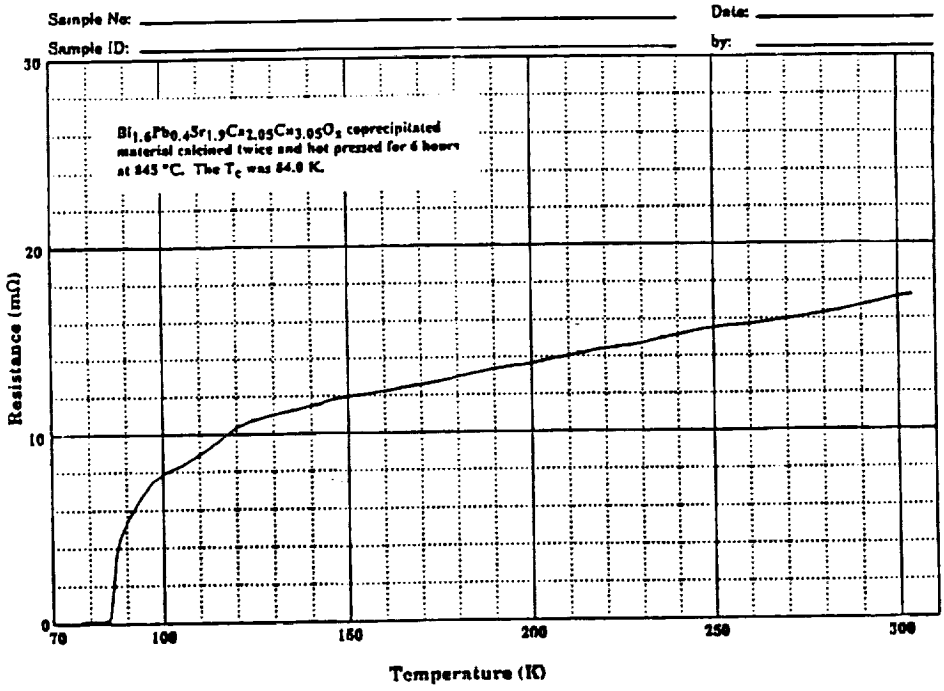

b) Hot pressed pellet with no additional heat treatment, calcined twice. The Tc was 84.0 K.

Figure 10 Resistance versus Temperature curves for coprecipitated hot pressed samples with no additional heat treatment. They varied in number of times the material was calcined.

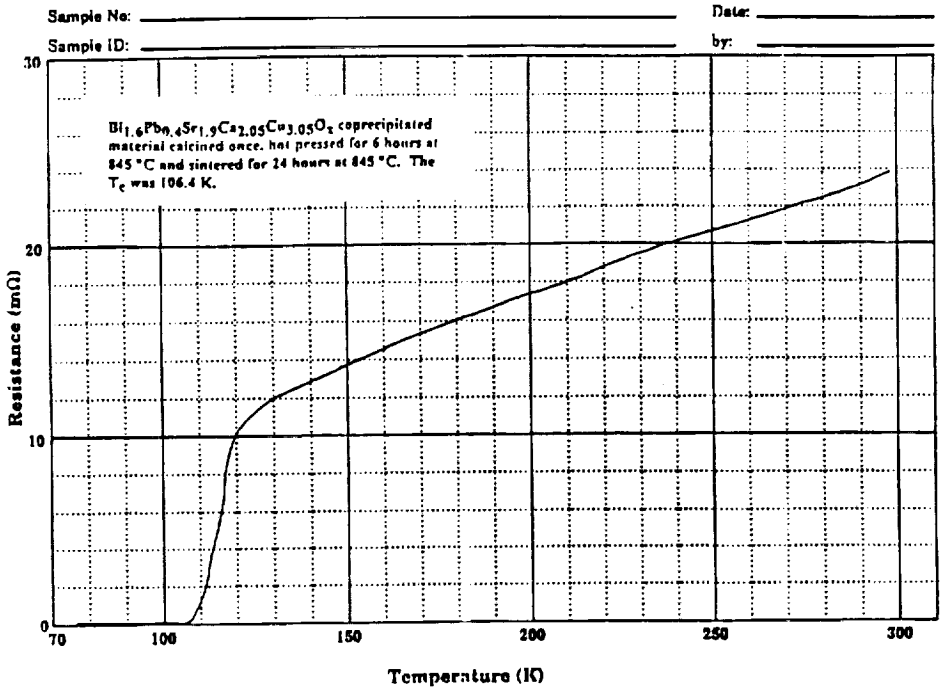

a) Hot pressed pellet with additional heat treatment, calcined once. The Tc was 106.4 K.

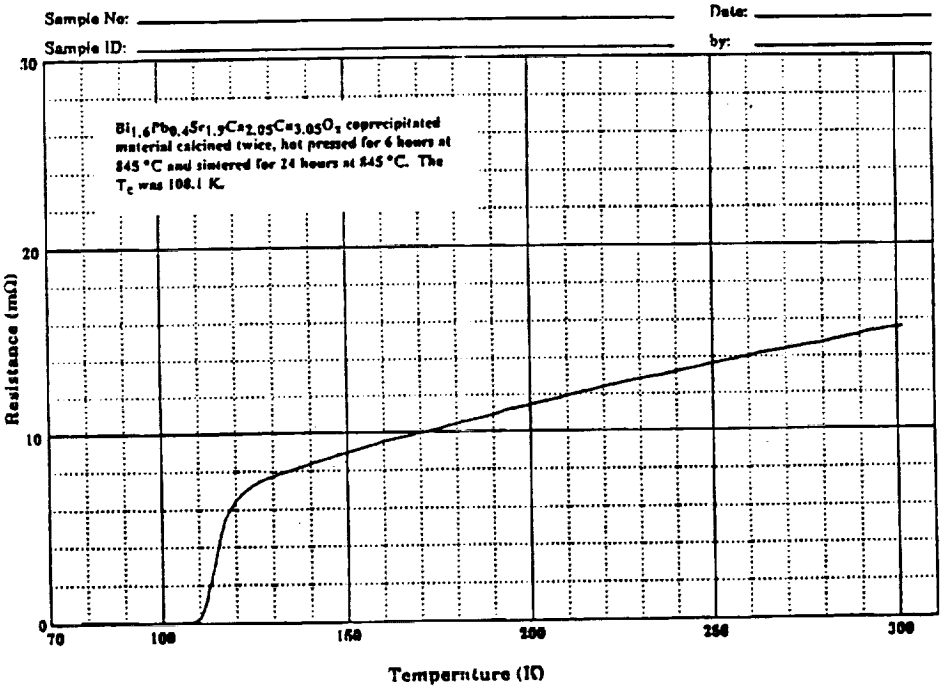

b) Hot pressed pellet with additional heat treatment, calcined twice. The Tc was 108.1 K

Figure 11 Resistance versus Temperature curves for coprecipitated hot pressed samples with twenty-four hours additional heat treatment at 845 °C. They varied in number of times the material was calcined.

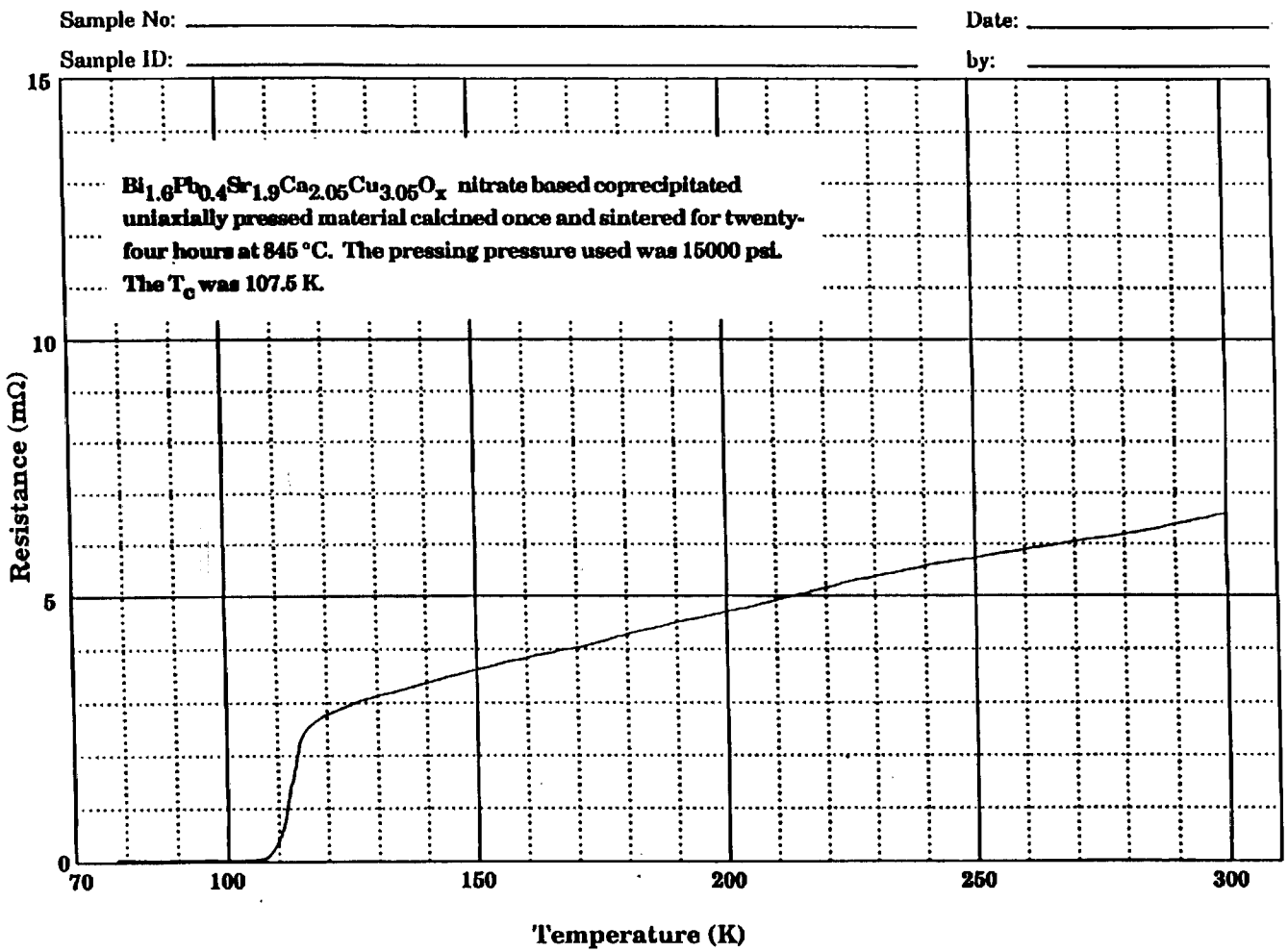

Figure 12 Resistance versus Temperature curve for nitrate based coprecipitated uniaxially pressed sample calcined once and sintered for twenty-four hours at 845 °C. The pressing pressure used was 15000 psi. The T_c was 107.5 K.

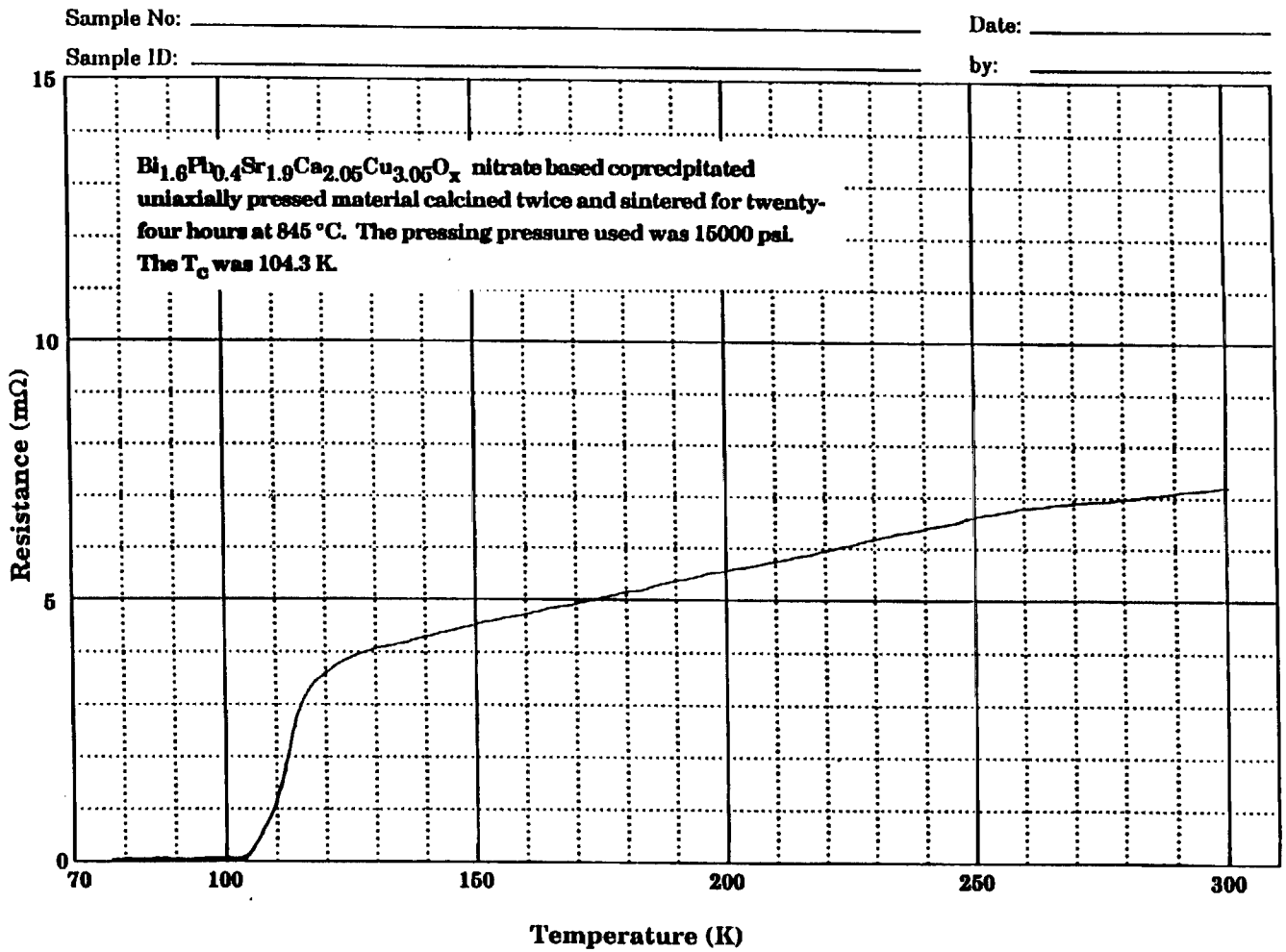

Figure 13 Resistance versus Temperature curve for nitrate based coprecipitated uniaxially pressed sample calcined twice and sintered for twenty-four hours at 845 °C. The pressing pressure used was 15000 psi. The T_c was 104.3 K.

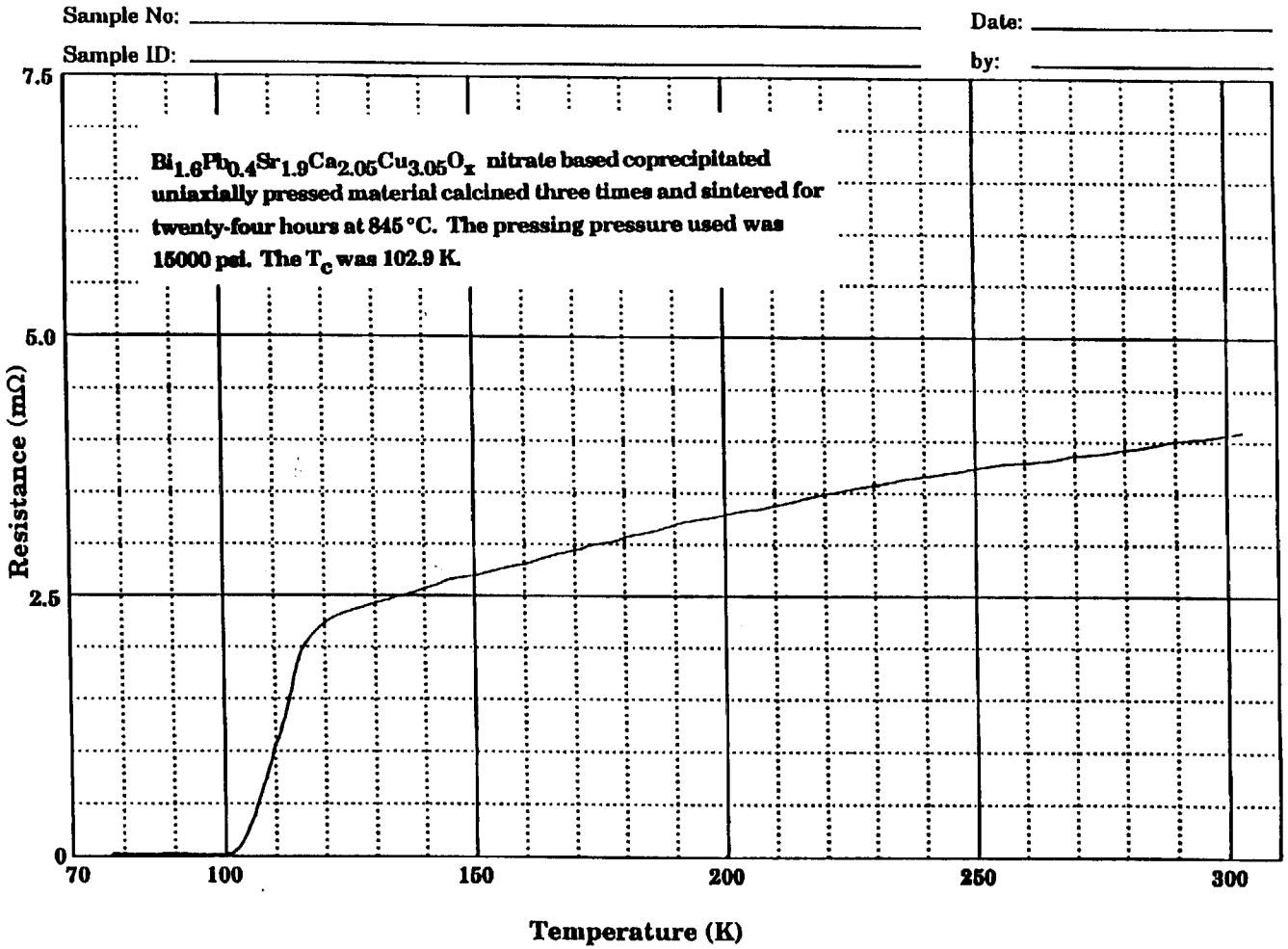

Figure 14 Resistance versus Temperature curve for nitrate based coprecipitated uniaxially pressed sample calcined three times and sintered for twenty-four hours at 845 °C. The pressing pressure used was 15000 psi. The T_c was 102.9 K.

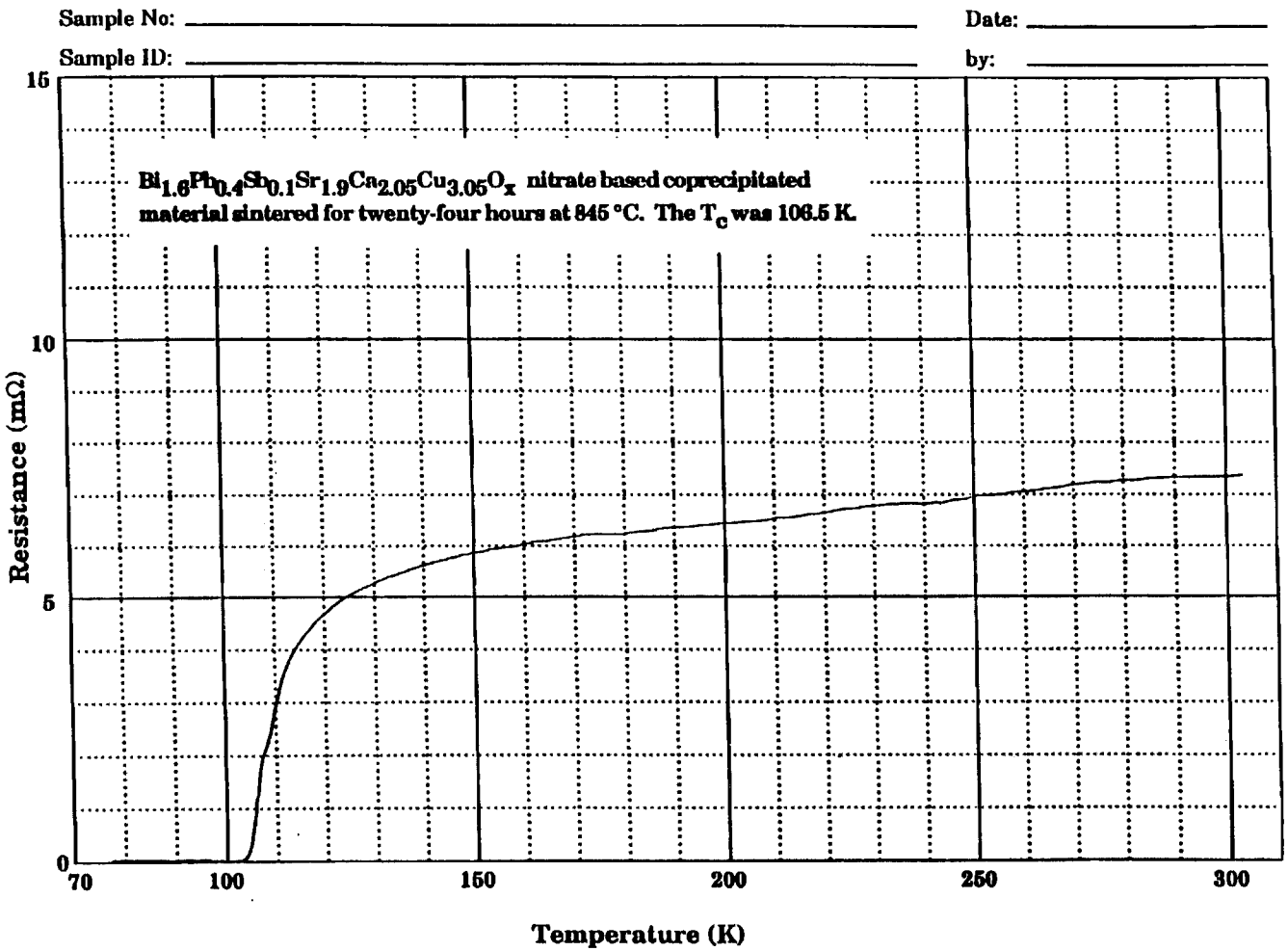

Figure 15 Resistance versus Temperature curve for antimony doped nitrate based coprecipitated material sintered for twenty-four hours at 845 °C. The T_c was 106.5 K.

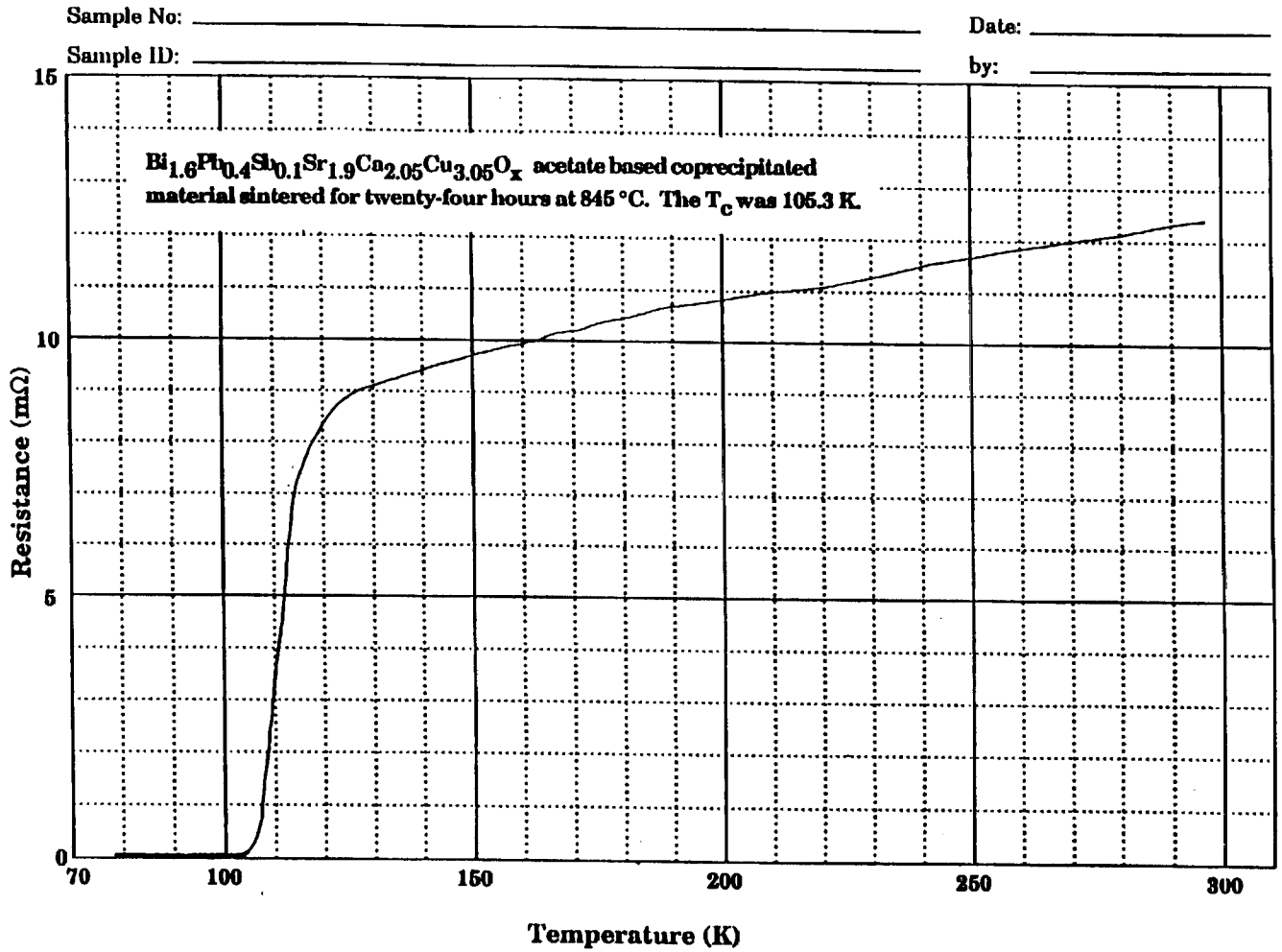

Figure 16 Resistance versus Temperature curve for antimony doped acetate based coprecipitated material sintered for twenty-four hours at 845 °C. The T_c was 105.3 K.

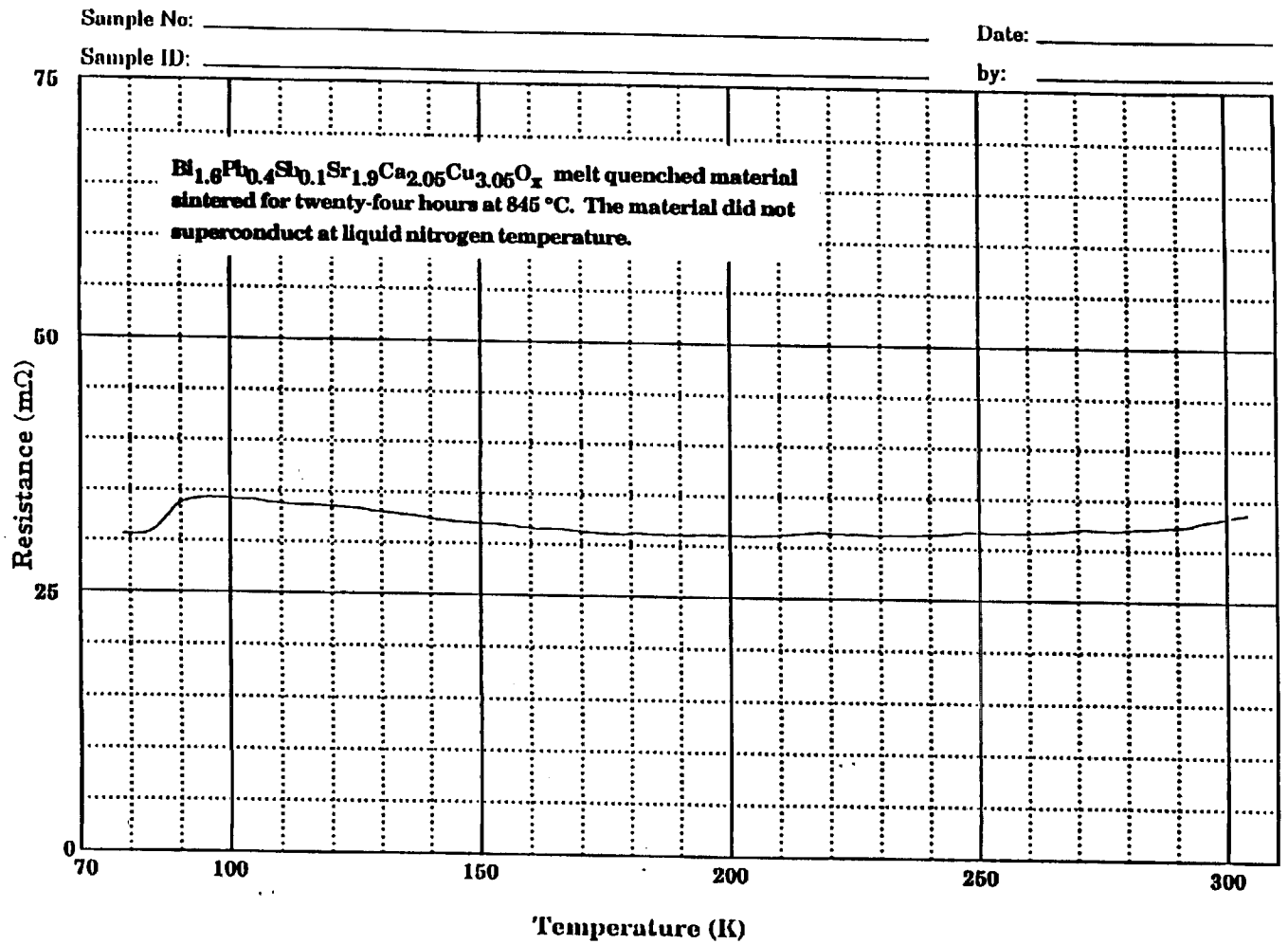

Figure 17 Resistance versus Temperature curve for antimony doped melt quenched material sintered for twenty-four hours at 855 °C. The material did not superconduct at liquid nitrogen temperature.

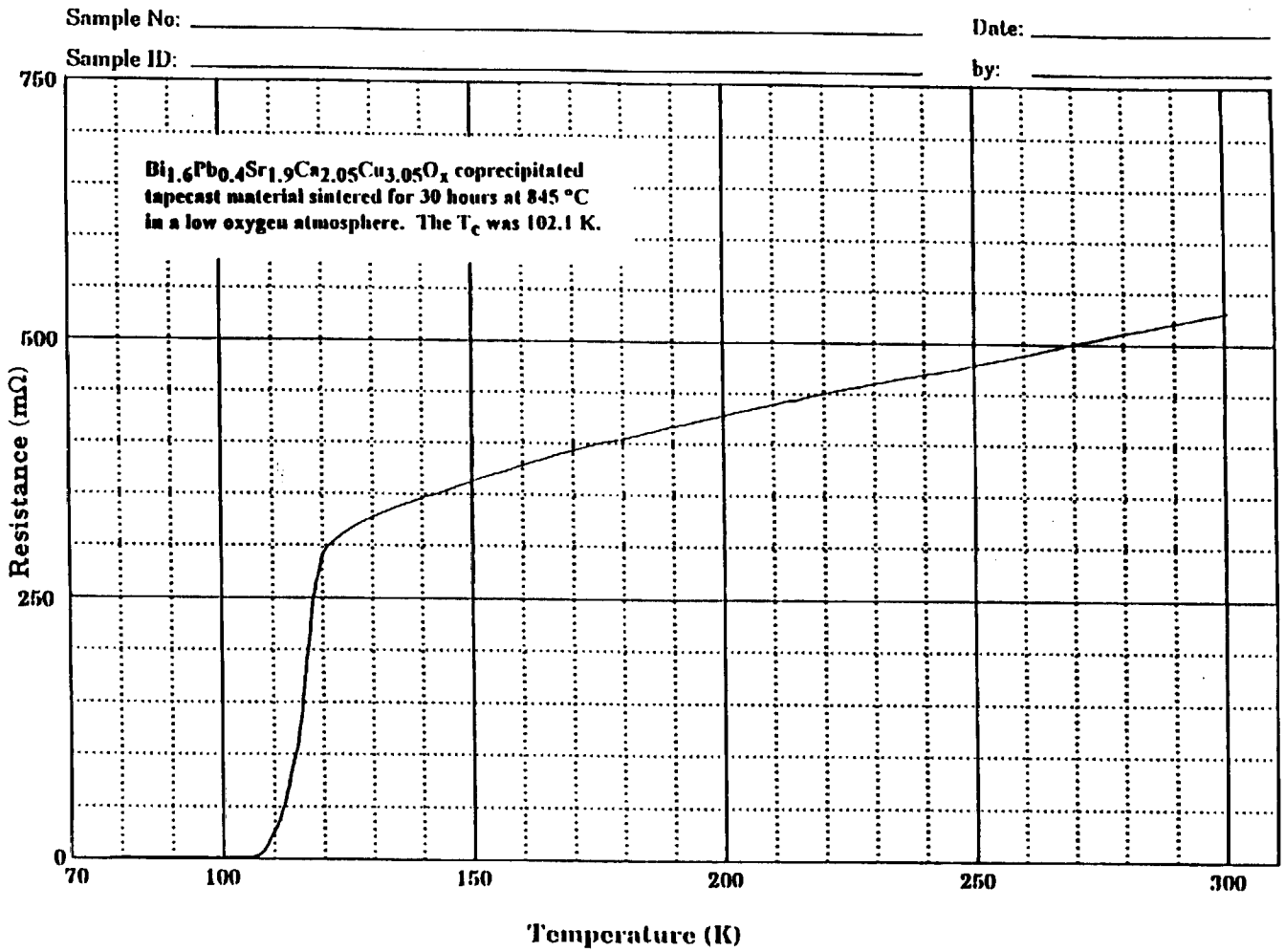

Figure 18 Resistance versus temperature curve for coprecipitated tapecast material which was sintered for thirty hours in the low oxygen atmosphere at 845 °C.

PRECEDING PAGE BLANK NOT FILMED

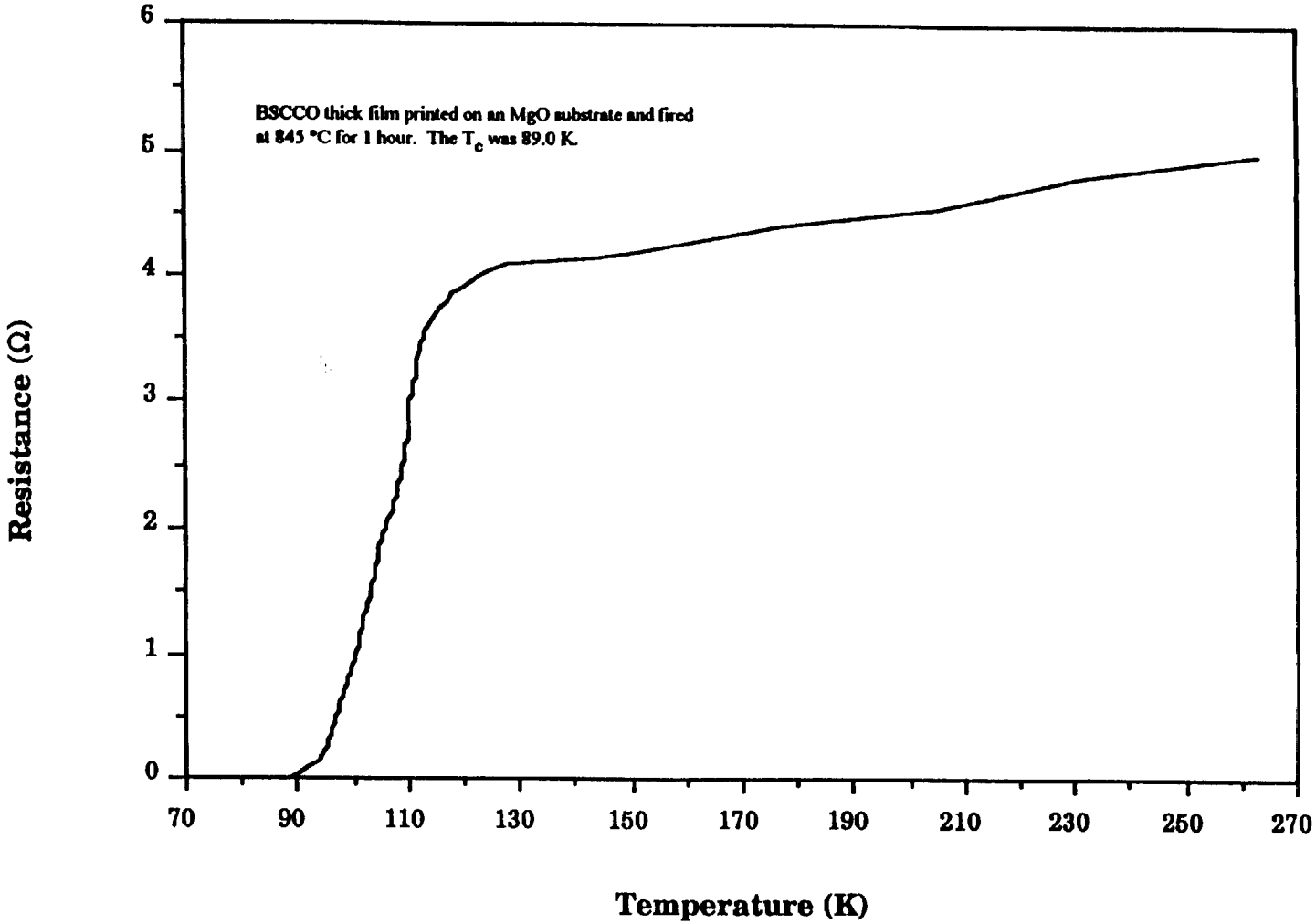

Figure 19 Resistance versus temperature curve for BSCCO coprecipitated screen printed thick film which was sintered for one hour at 845 °C in air. The T_c was 89.0 K.

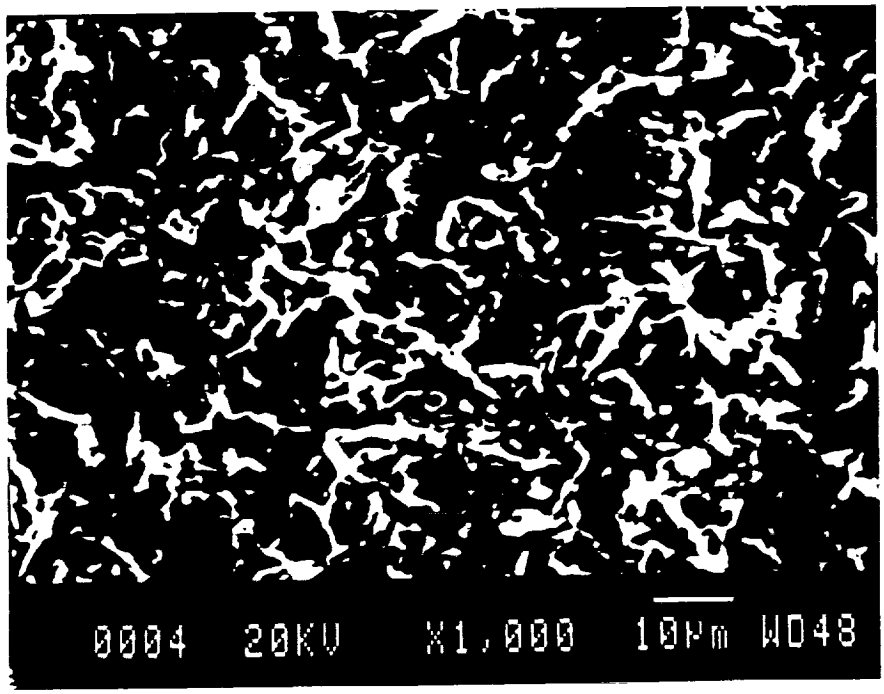

Figure 20 SEM Micrograph for BSCCO coprecipitated thick film printed on an MgO substrate. The film sintered at 845 °C for one hour in air.

PRECEDING PAGE BLANK NOT FILMED

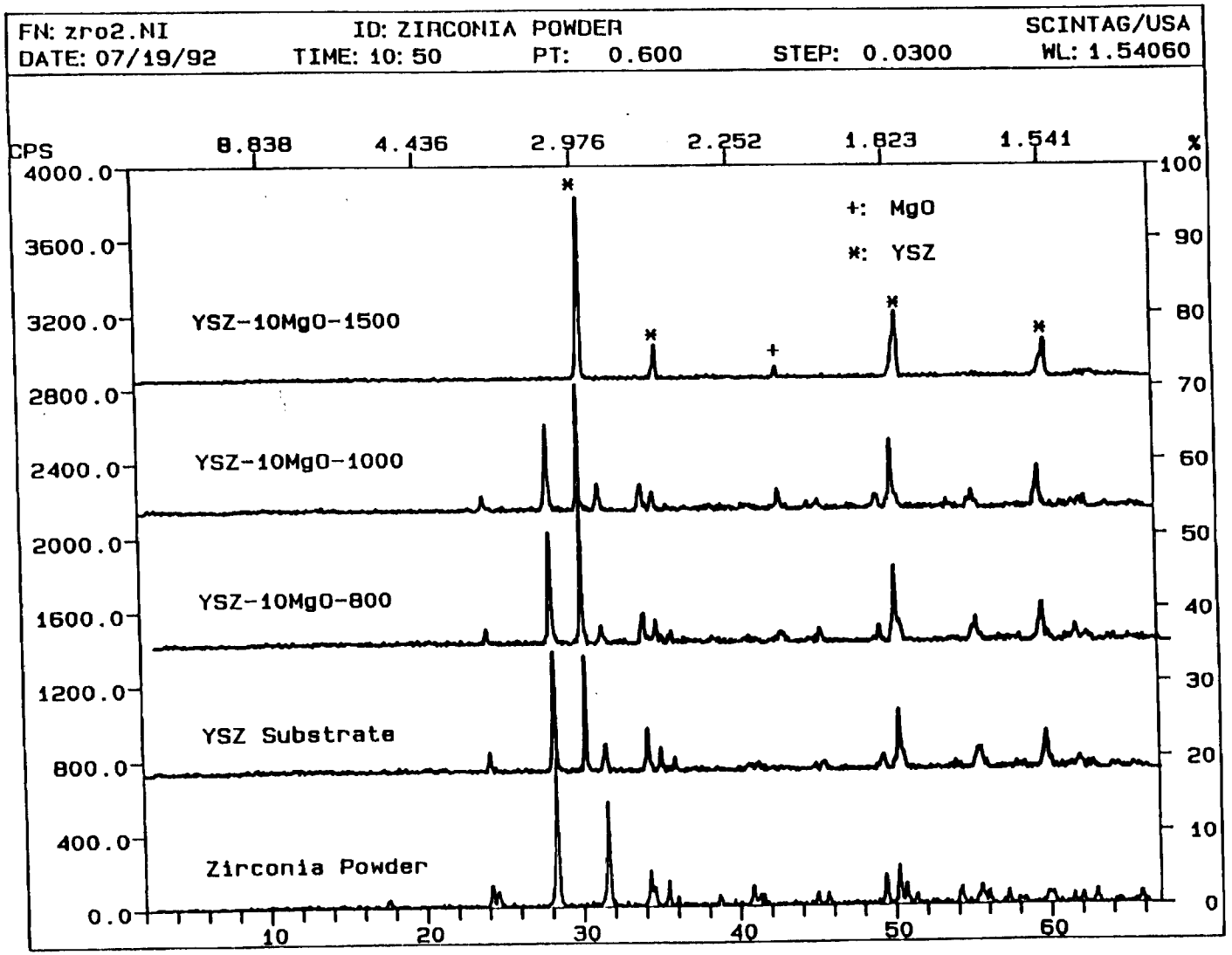

Figure 21 Xray Diffraction data for the YSZ substrate from the zirconia powder through the annealing of the substrate to the application and annealing of the MgO buffer layer.

PRECEDING PAGE BLANK NOT FILMED

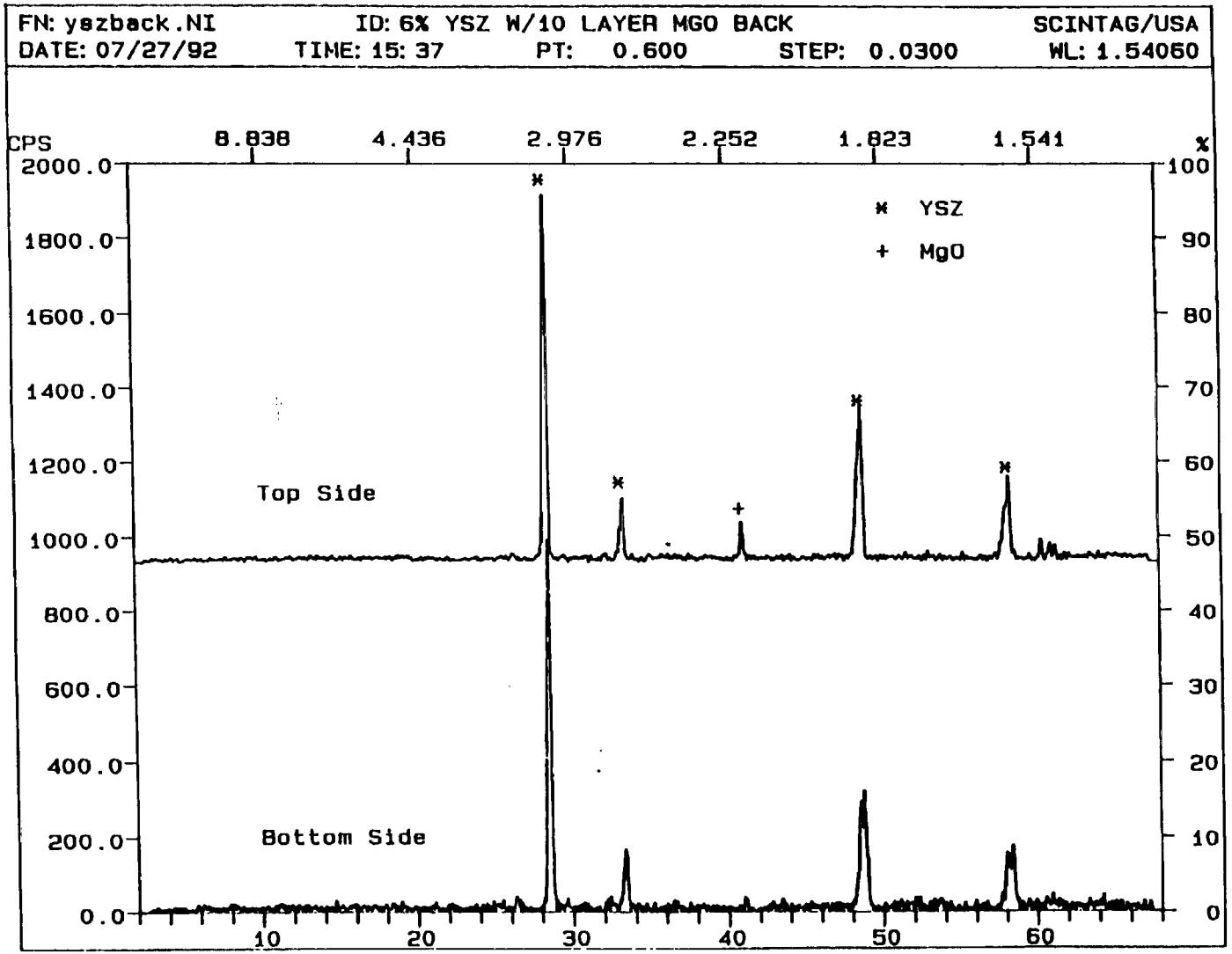

Figure 22 Xray Diffraction data for a YSZ substrate with an MgO buffer layer and the JCPDS standards XRD patterns for YSZ and MgO.

PRECEDING PAGE BLANK NOT FILMED

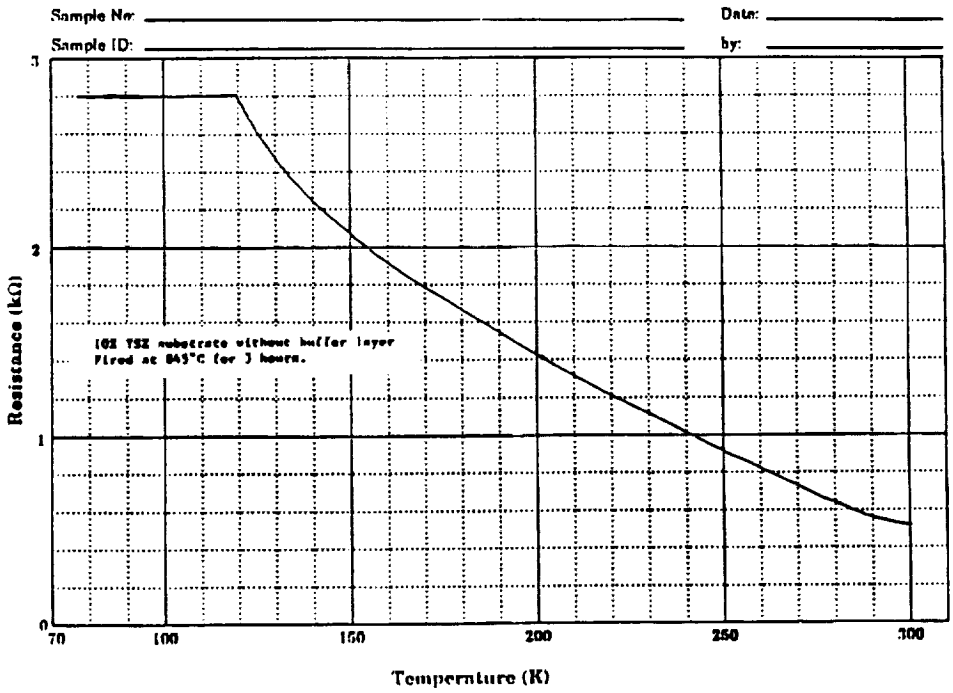

a) BSCCO coprecipitated thick films printed on the 10 % YSZ substrates without the MgO buffer layer.

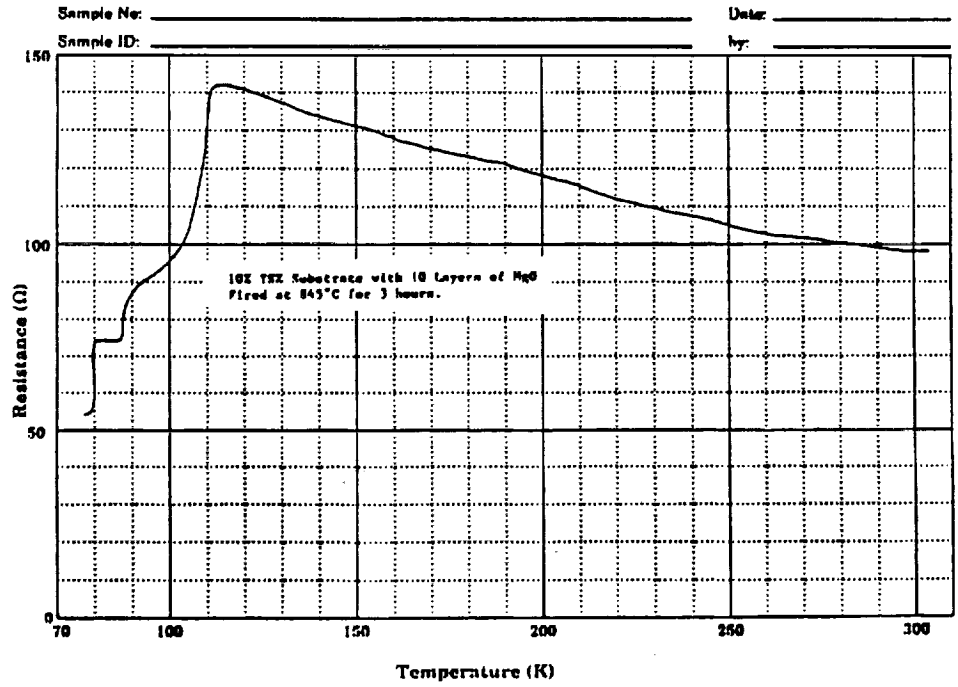

b) BSCCO coprecipitated thick films printed on the 10 % YSZ substrates with the MgO buffer layer.

Figure 23 Resistance versus Temperature curves for the BSCCO coprecipitated thick films printed on the 10 % YSZ substrates and sintered for three hours at 845 °C in air, with and without the MgO buffer layer.

PRECEDING PAGE BLANK NOT FILMED

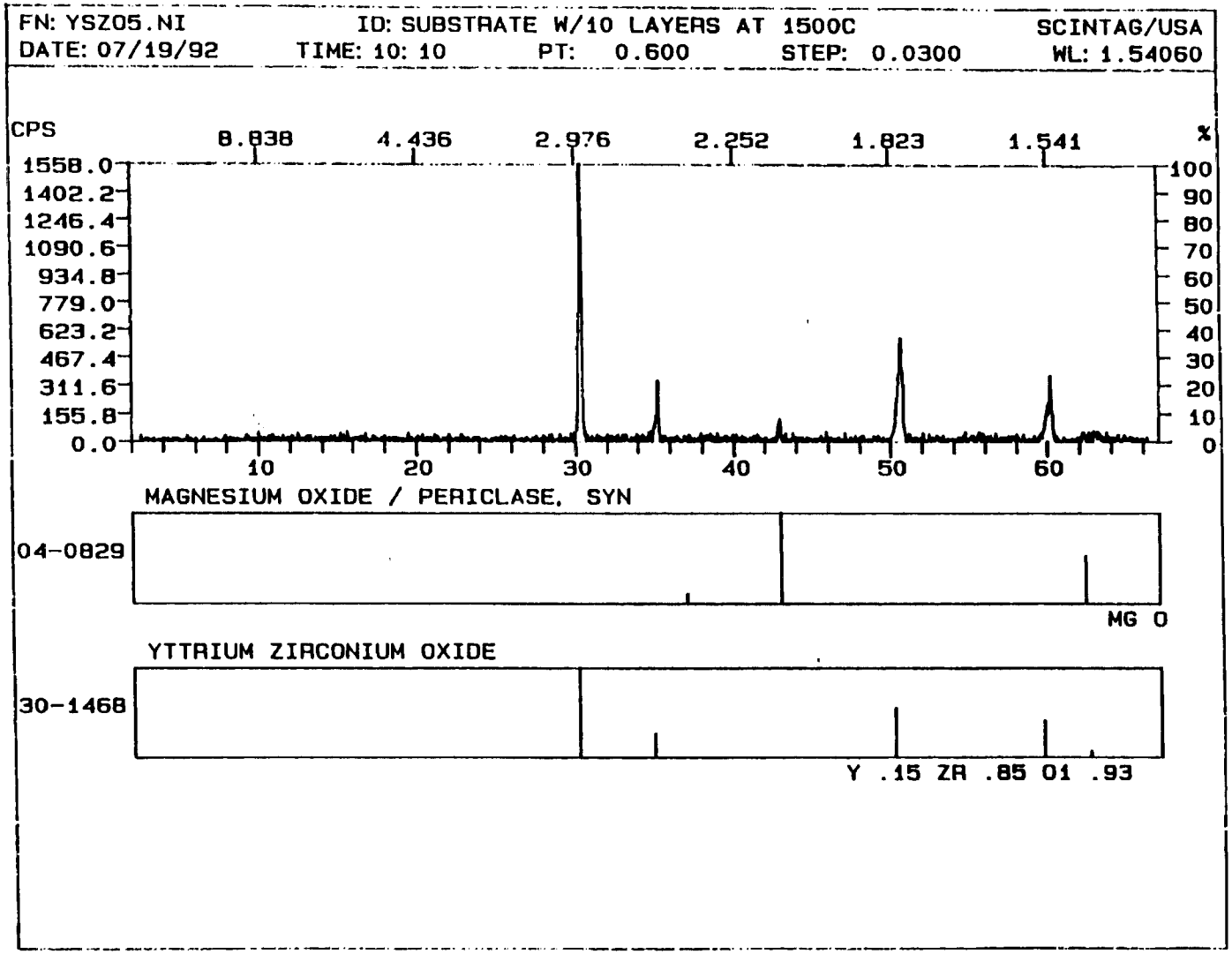

Figure 24 Xray Diffraction data for the top and bottom of the YSZ substrate coated with the MgO buffer layer.

PRECEDING PAGE BLANK NOT FILMED

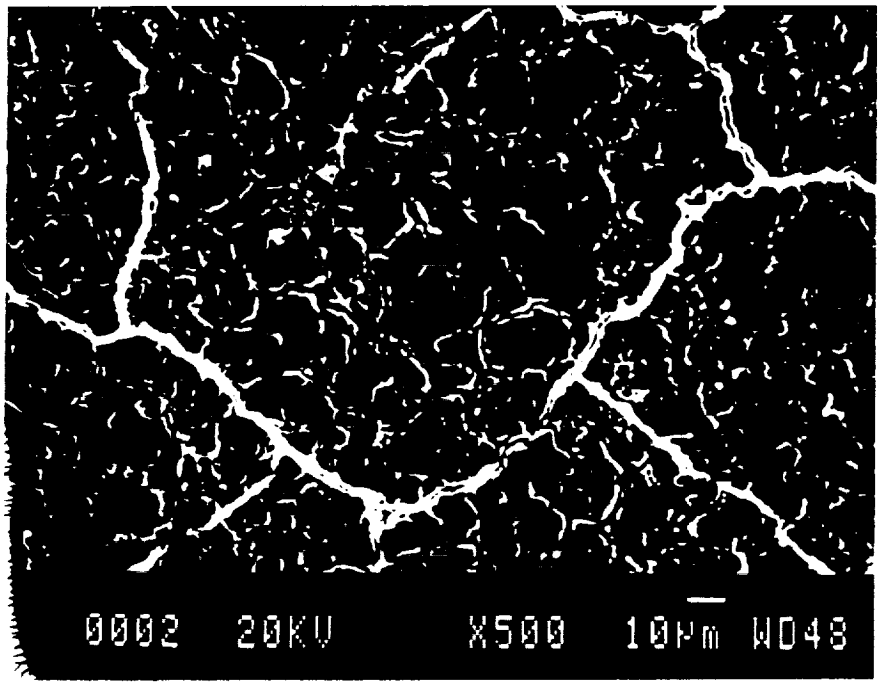

Figure 25 SEM Micrograph of the MgO buffer layer showing the microcracks in the buffer layer.

PRECEDING PAGE BLANK NOT FILMED

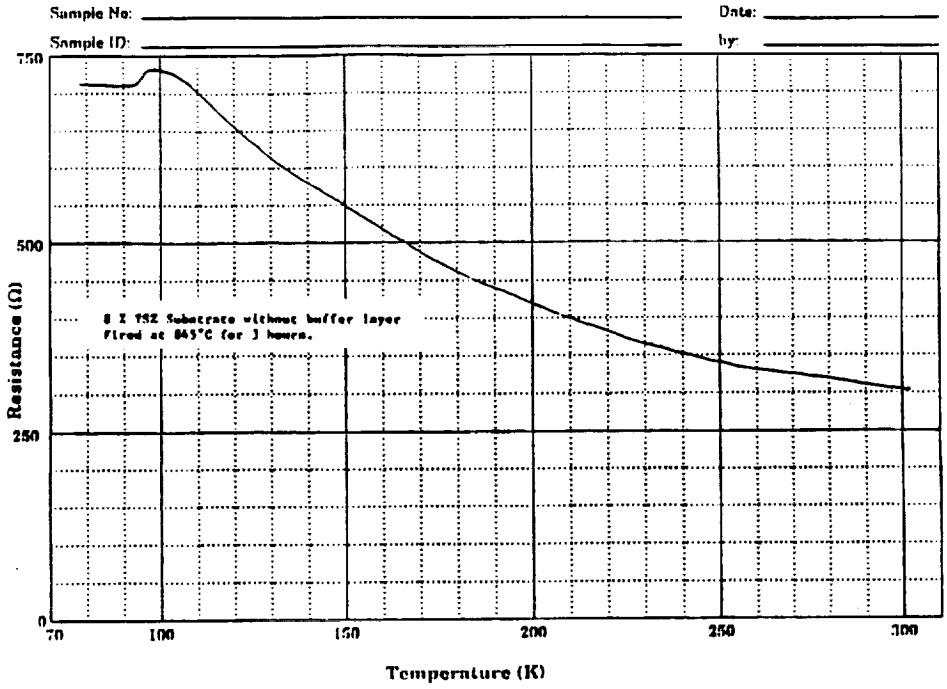

a) BSCCO coprecipitated thick films printed on the 8 % YSZ substrates without the MgO buffer layer.

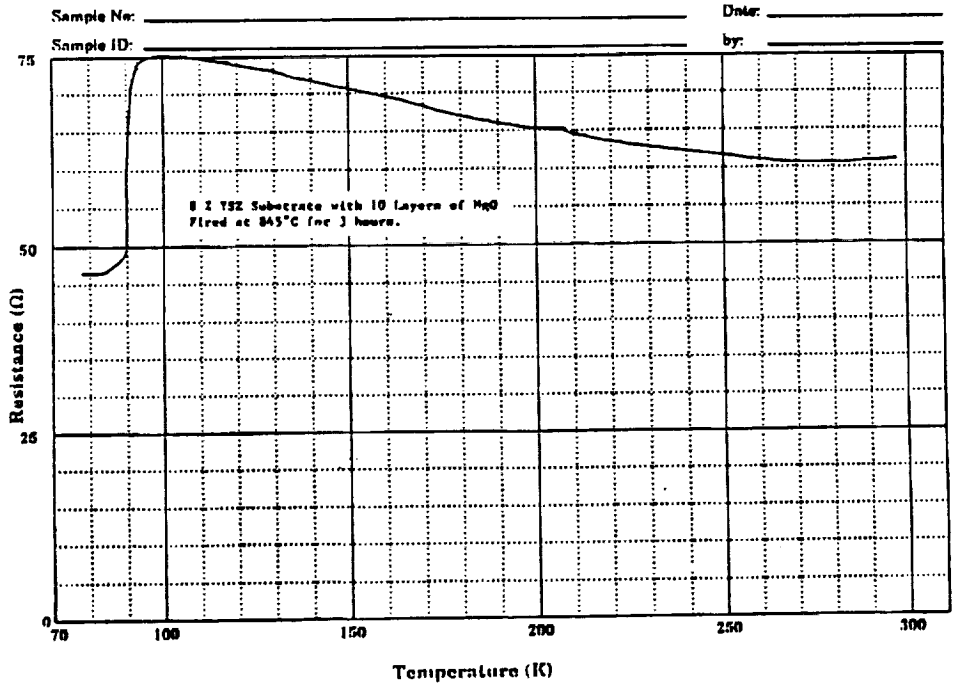

b) BSCCO coprecipitated thick films printed on the 8 % YSZ substrates with the MgO buffer layer.

Figure 26 Resistance versus Temperature curves for the BSCCO coprecipitated thick films printed on the 8 % YSZ substrates and sintered for three hours at 845 °C in air, with and without the MgO buffer layer.

PRECEDING PAGE BLANK NOT FILMED

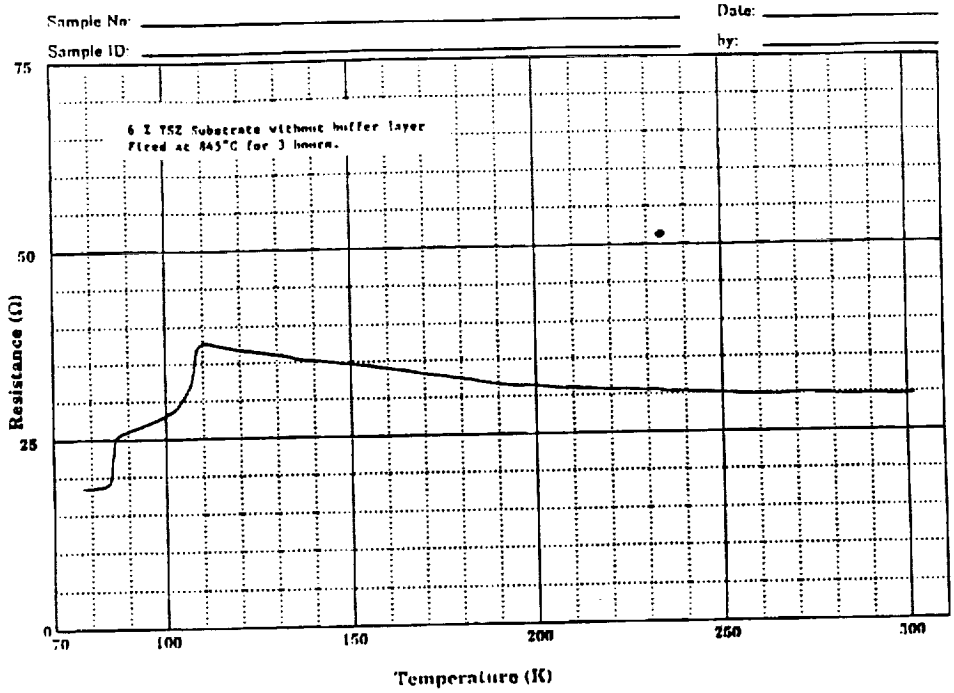

a) BSCCO coprecipitated thick films printed on the 6 % YSZ substrates without the MgO buffer layer.

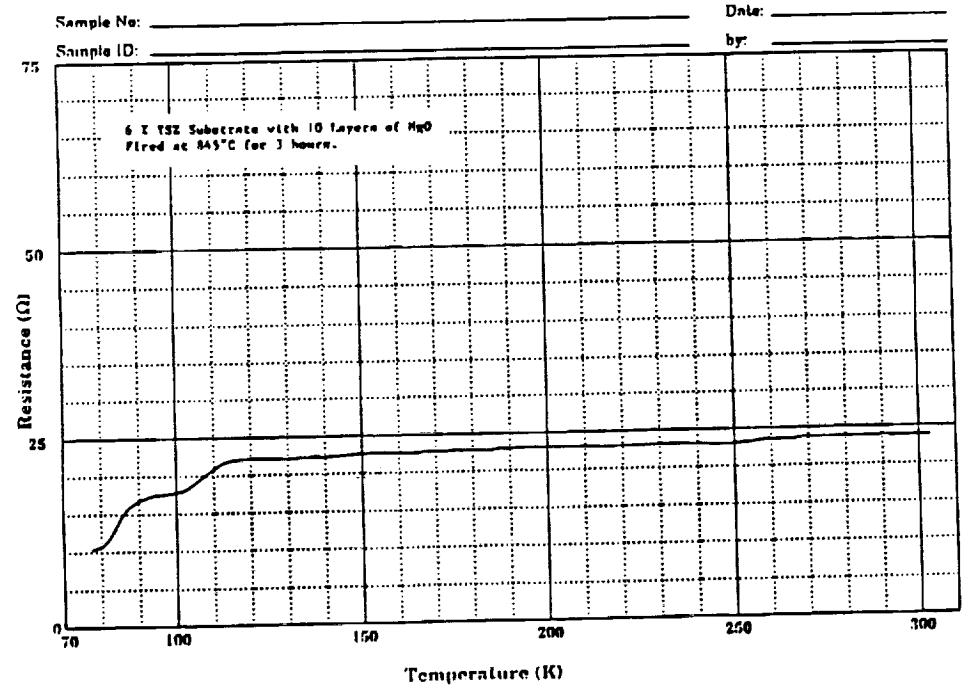

b) BSCCO coprecipitated thick films printed on the 6 % YSZ substrates with the MgO buffer layer.

Figure 27 Resistance versus Temperature curves for the BSCCO coprecipitated thick films printed on the 6 % YSZ substrates and sintered for three hours at 845 °C in air, with and without the MgO buffer layer.

PRECEDING PAGE BLANK NOT FILMED

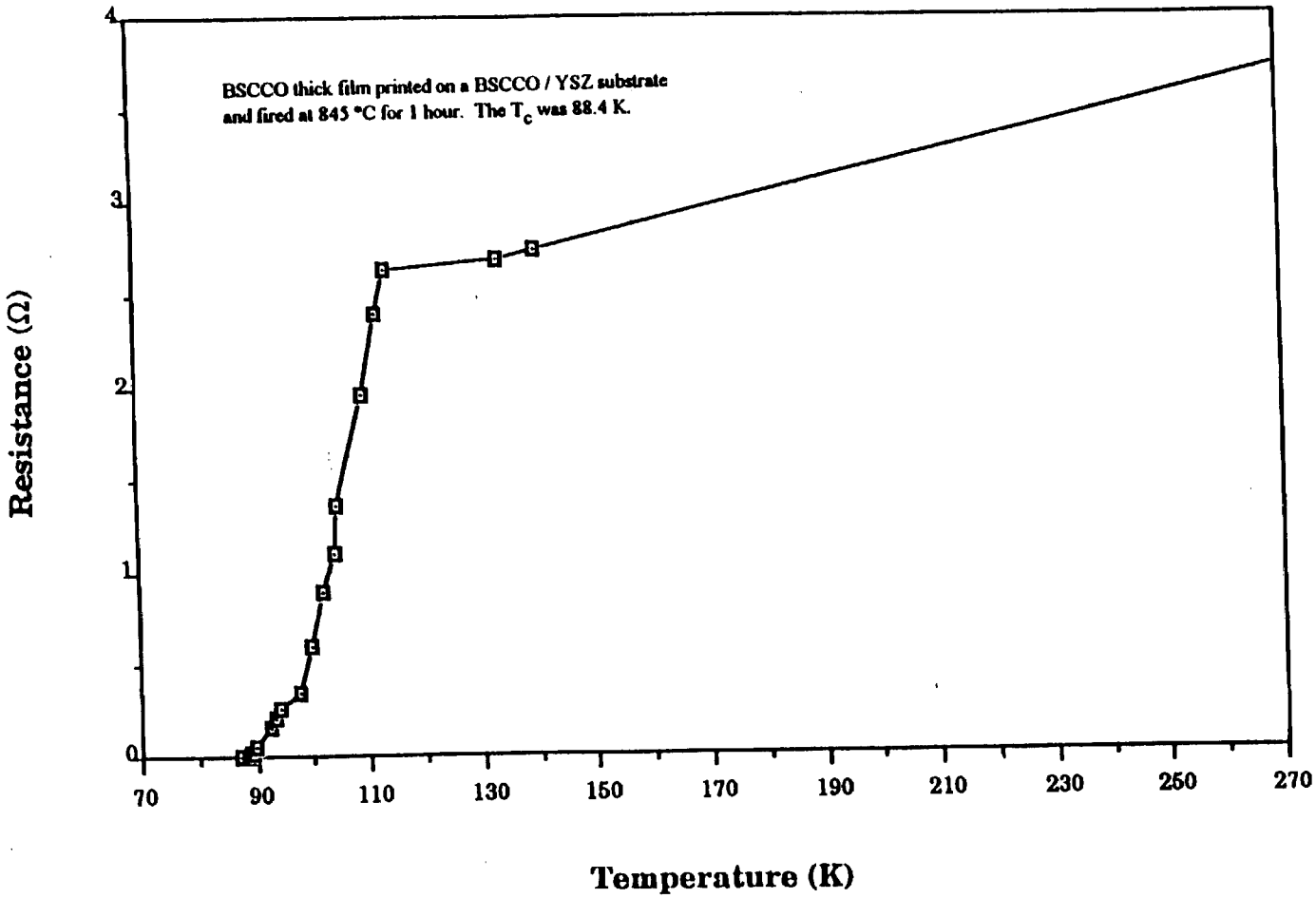

Figure 28 Resistance versus temperature curve for BSCCO thick film printed on the BSCCO / YSZ substrate and sintered for one hour at 845 °C in air. The Tc was 88.4 K.

PRECEDING PAGE BLANK NOT FILMED

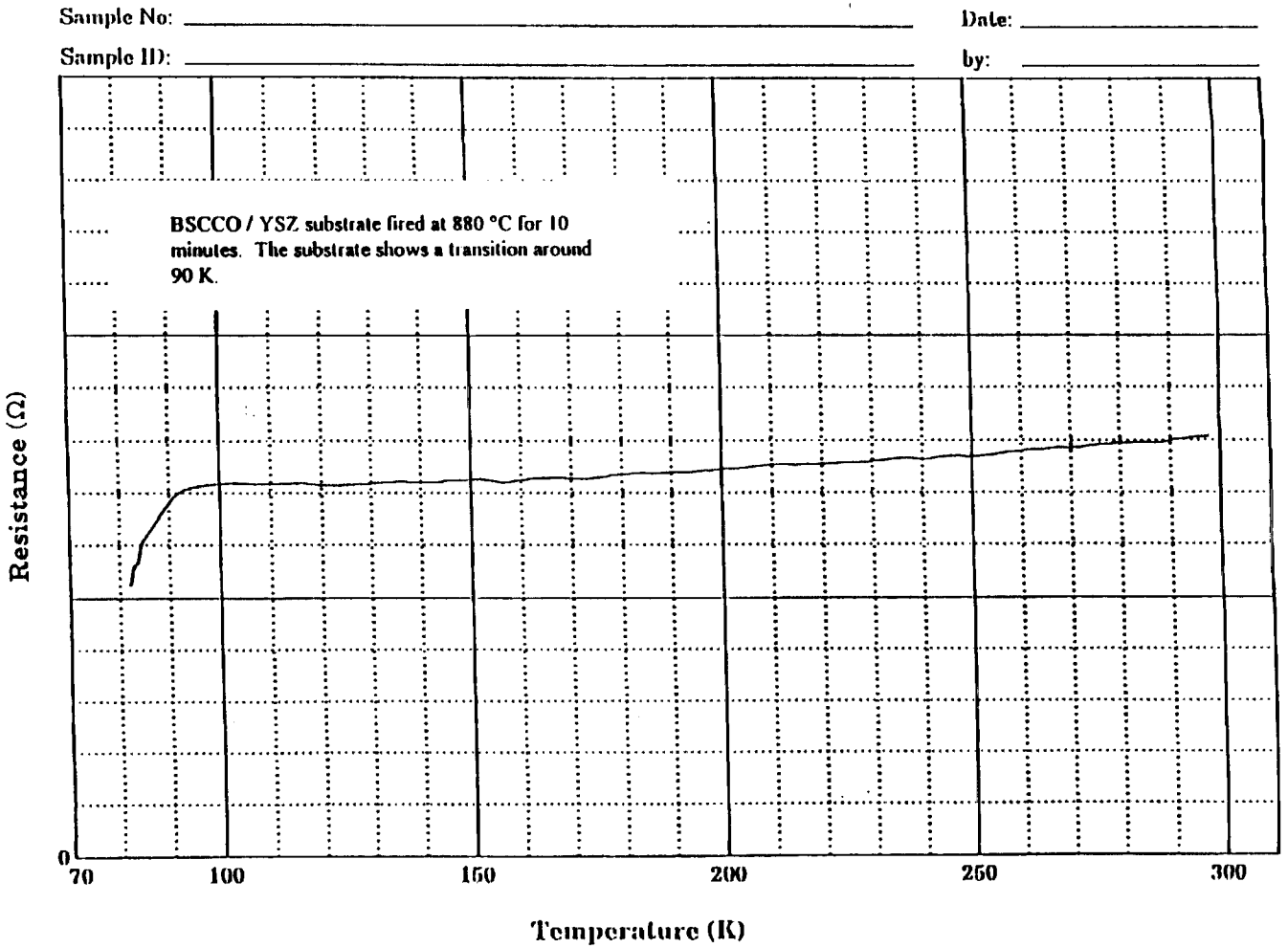

Figure 29 Resistance versus temperature curve for the BSCCO / YSZ substrate sintered at 880 °C in air for 10 minutes.

PRECEDING PAGE BLANK NOT FILMED

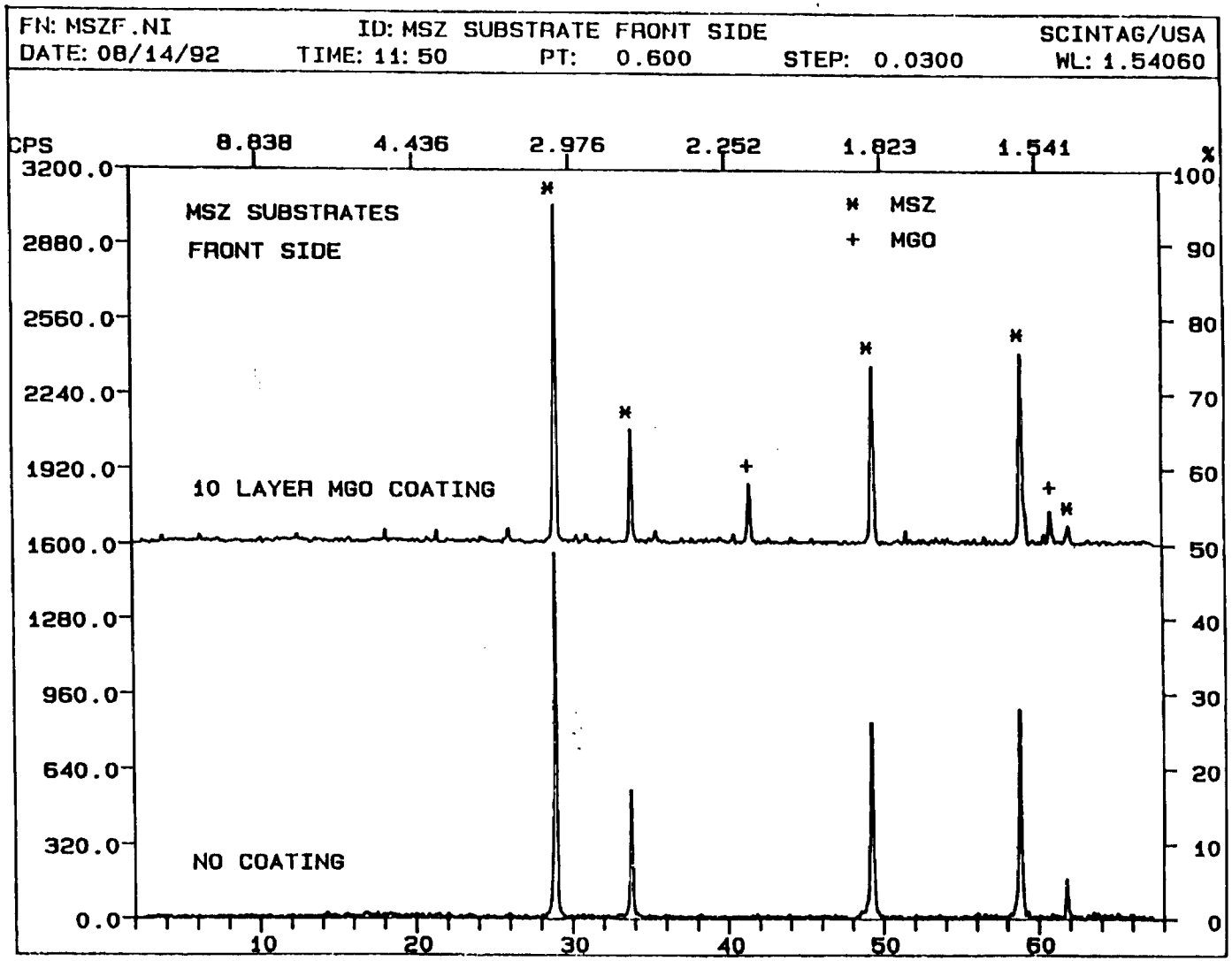

Figure 30 Xray Diffraction data obtained from the MSZ substrates with and without a MgO buffer layer.

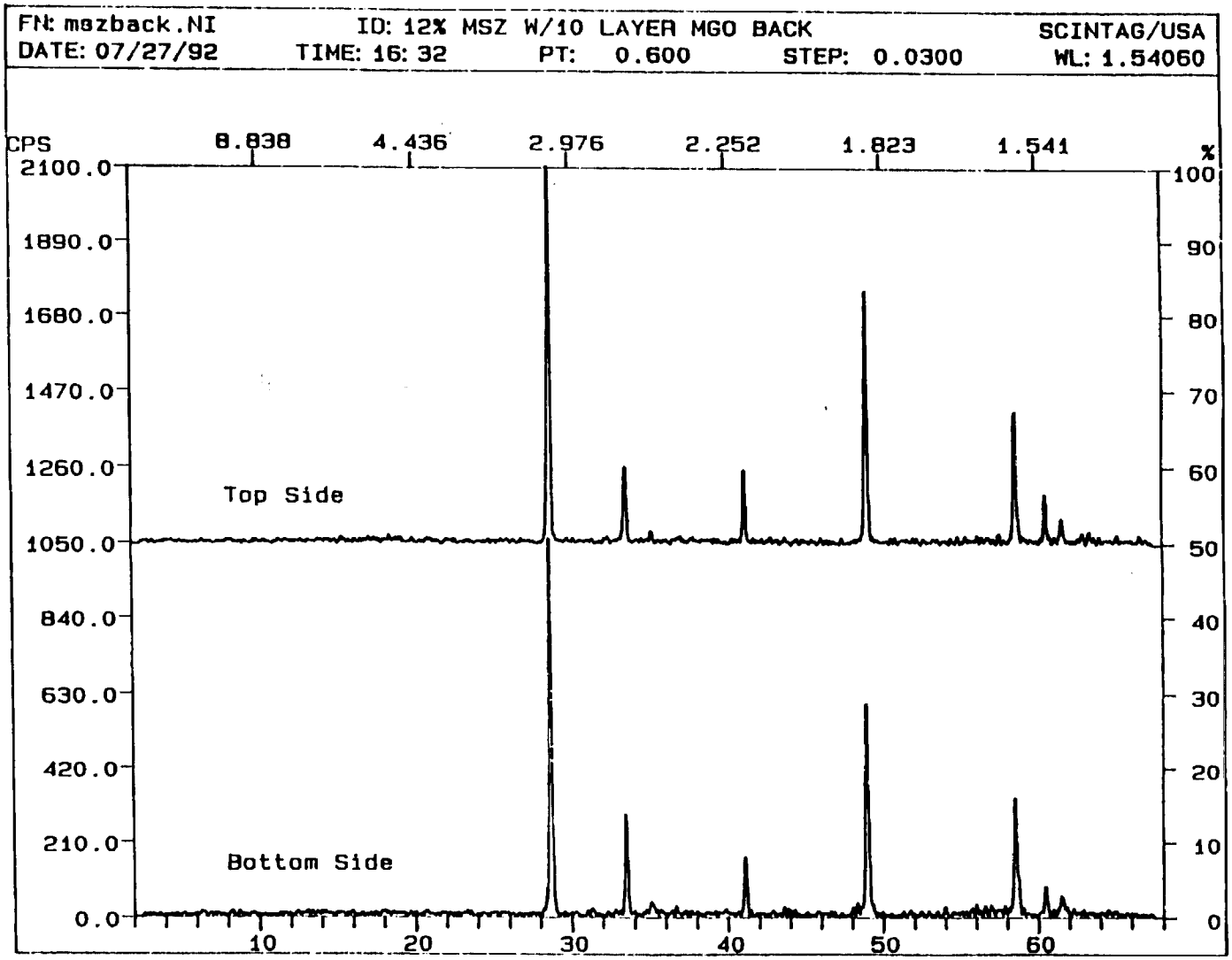

Figure 31 Xray Diffraction data for the top and bottom of the MSZ substrate coated with the MgO buffer layer.

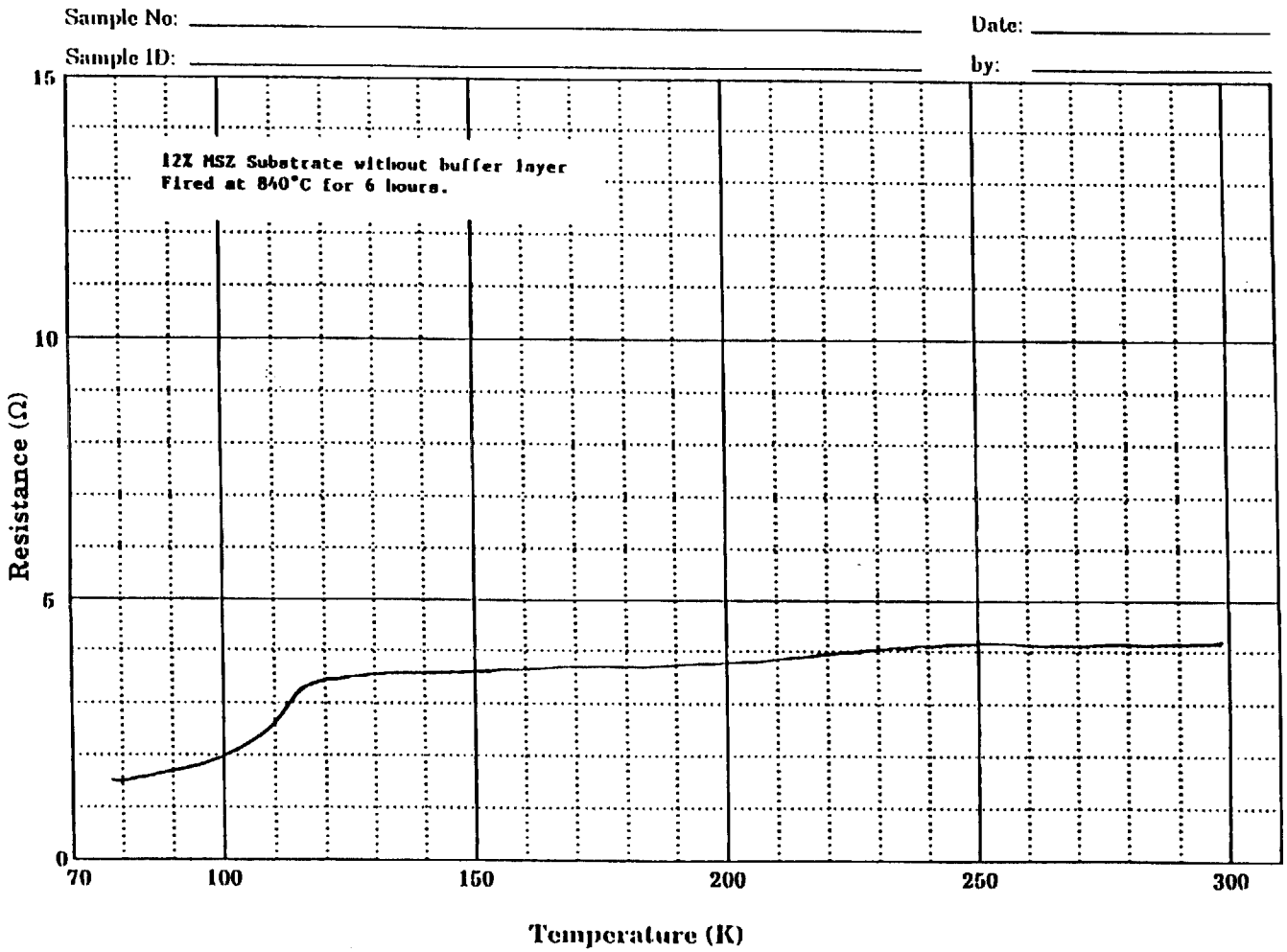

Figure 32 Resistance versus temperature curve for BSCCO thick film printed on a 12 % MSZ substrate without a buffer layer and sintered for six hour at 845 °C in air.

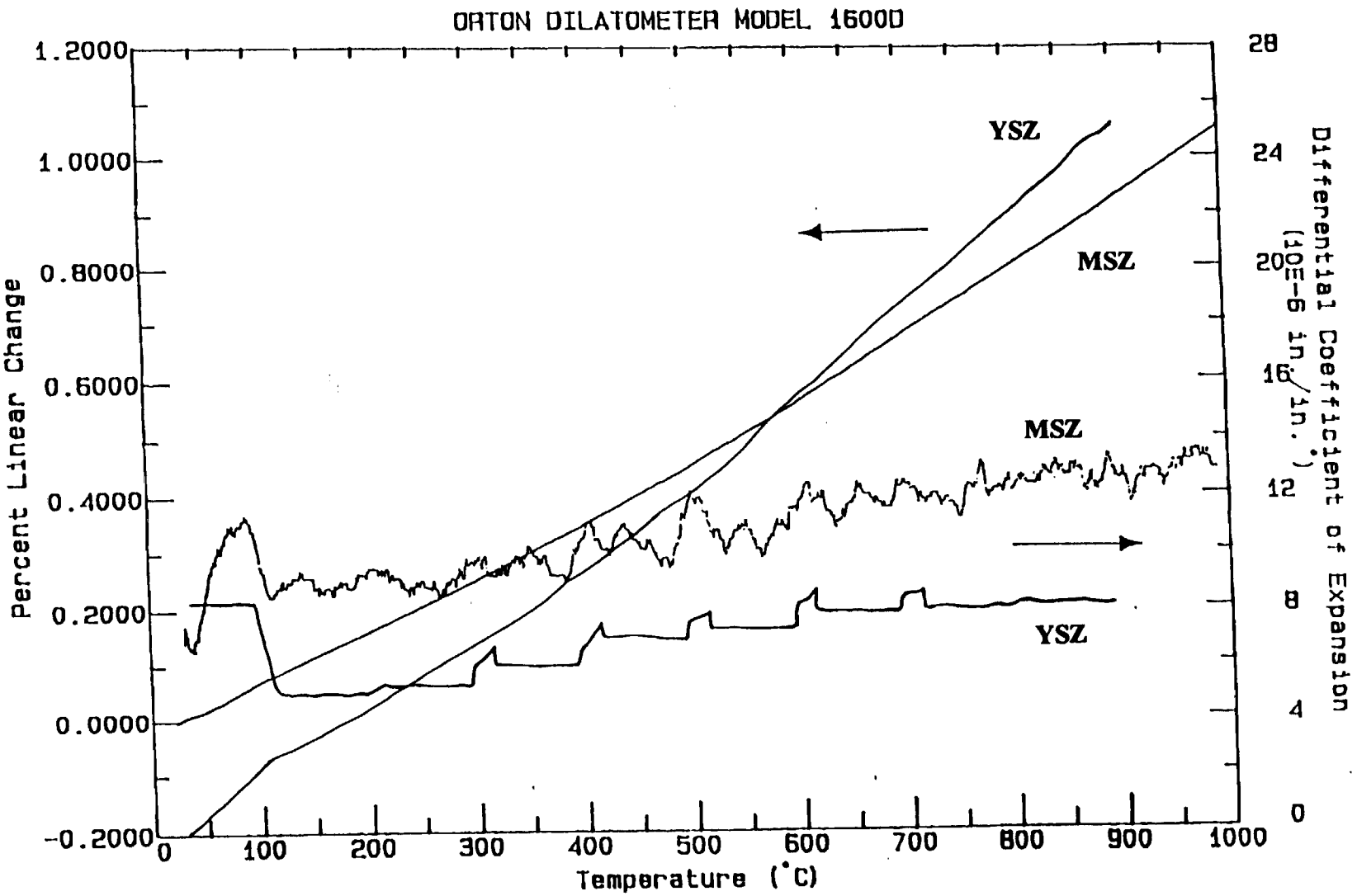

Figure 33 The thermal expansion curve of the MSZ and YSZ substrates. The TE for MSZ is 12 x 10^{-6} in/in °C and the TE for YSZ is 8 x 10^{-6} in/in °C

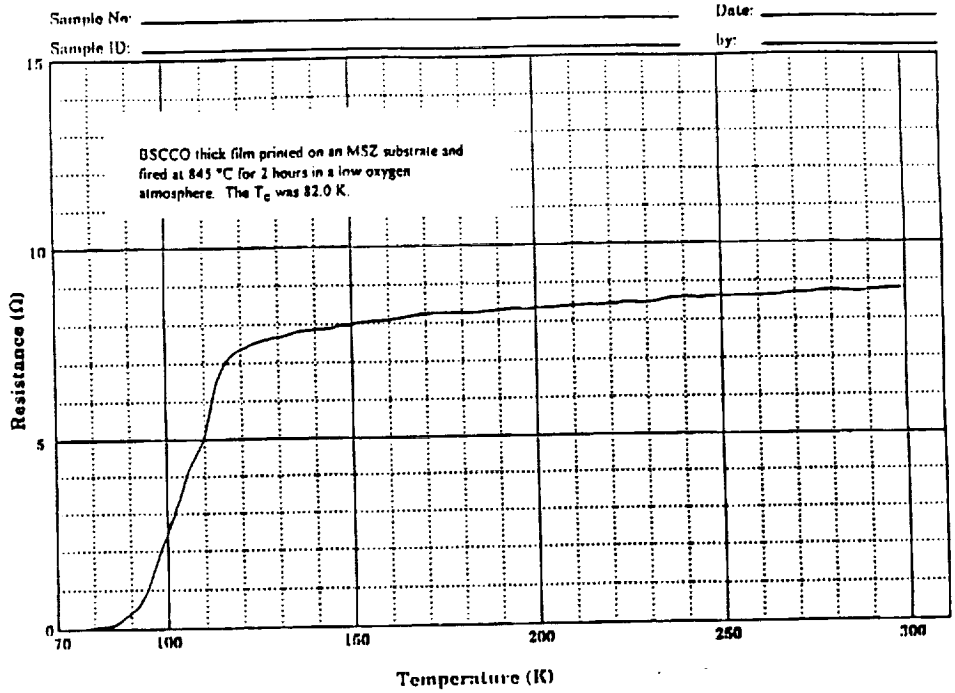

a) BSCCO thick film printed on the 12 % MSZ substrate without the MgO buffer layer.

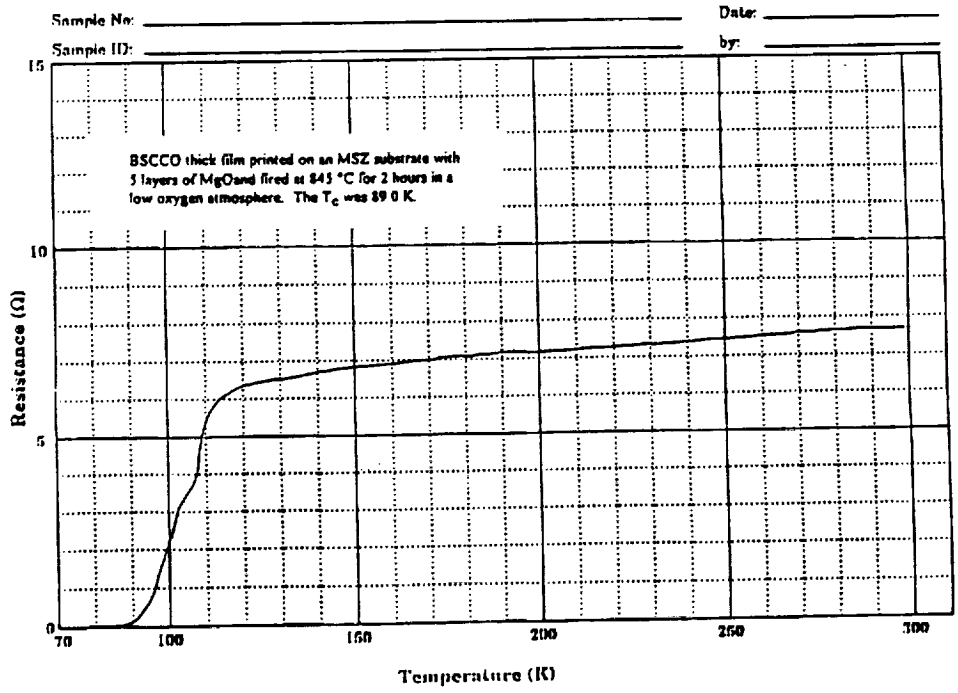

b) BSCCO thick film printed on the 12 % MSZ substrate with a five coat MgO buffer layer.

Figure 34 Resistance versus Temperature curves for the BSCCO coprecipitated thick films printed on the 12 % MSZ substrates and sintered at 845 °C for two hours under a low oxygen atmosphere, with and without the MgO buffer layer.

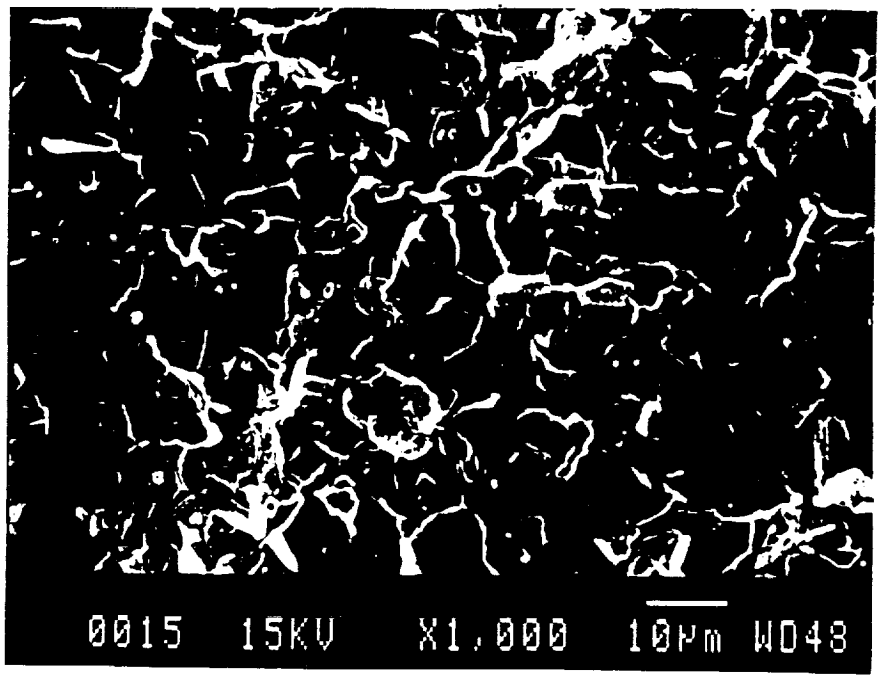

a) An example of a dense BSCCO thick film printed on the 12 % MSZ substrate. The thick film superconducted at 87 K.

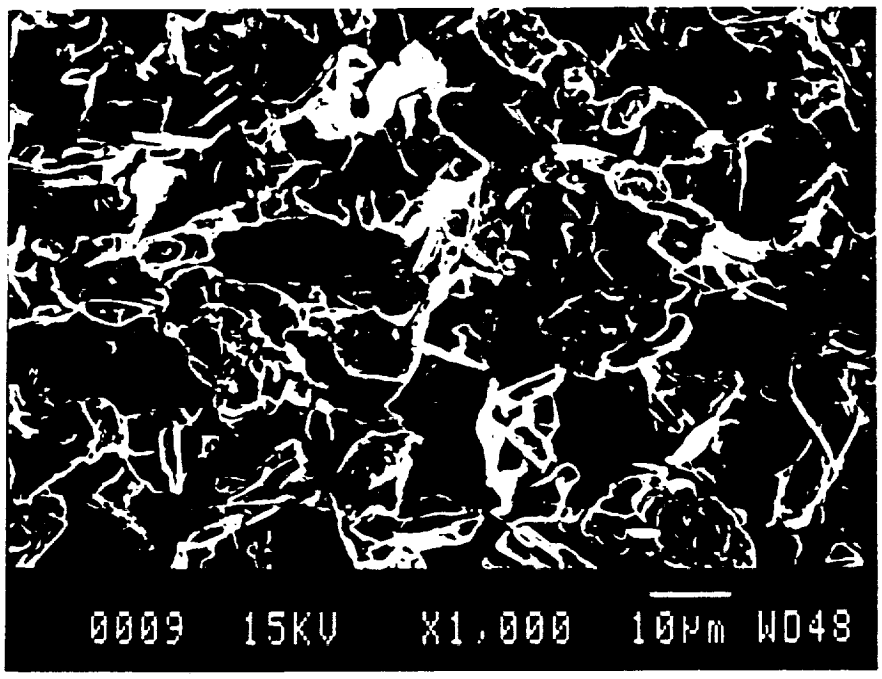

b) An example of a porous BSCCO thick film printed on the 12 % MSZ substrate. The thick film did not superconduct at liquid nitrogen temperature.

Figure 35 SEM Micrographs of two BSCCO thick films on MSZ substrates.

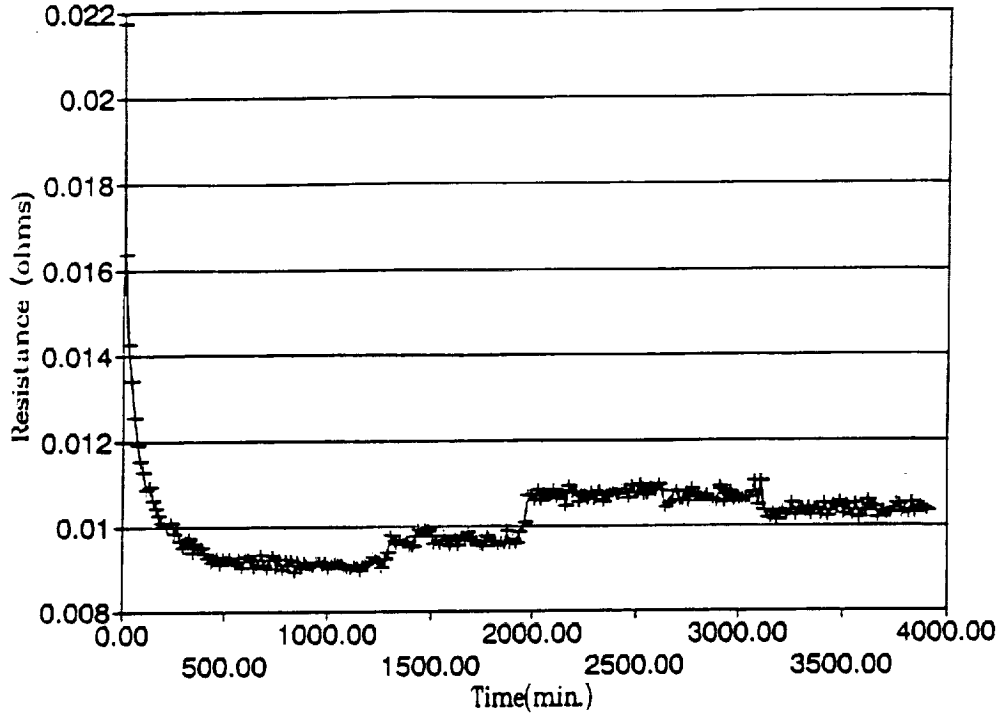

a) The entire resistivity run from the initial dwell at 845 °C until a silver wire broke after sixty-four hours.

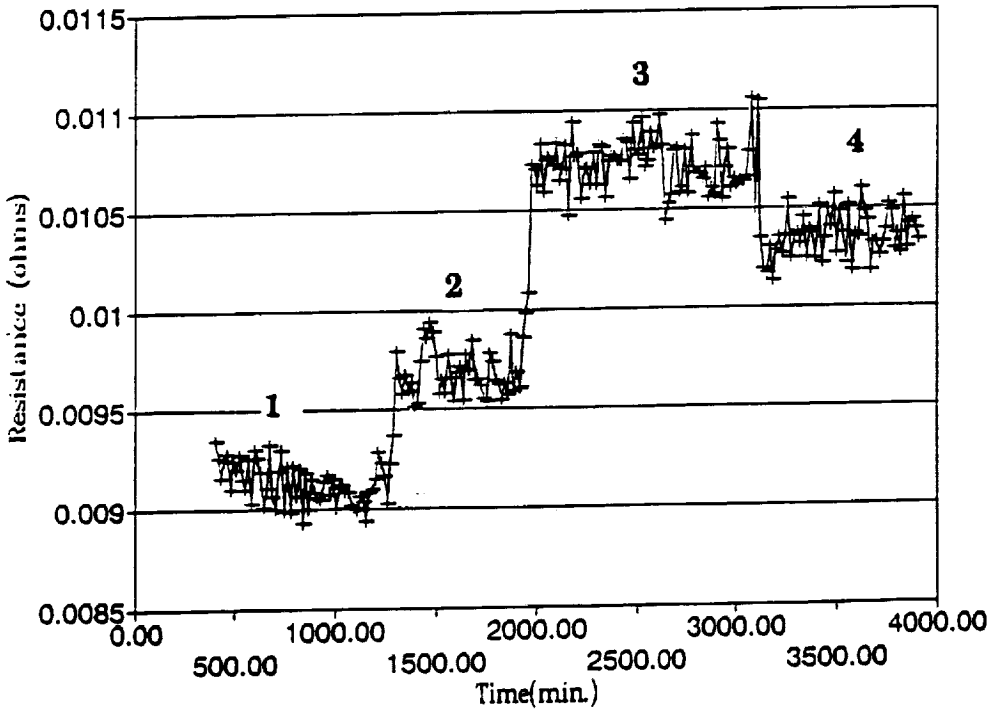

b) A close up view of the specific areas of interest.

Figure 36 In-Situ Resistivity Development showing the resistivity data taken using the 0.25 mm silver wires and one time calcined powder.

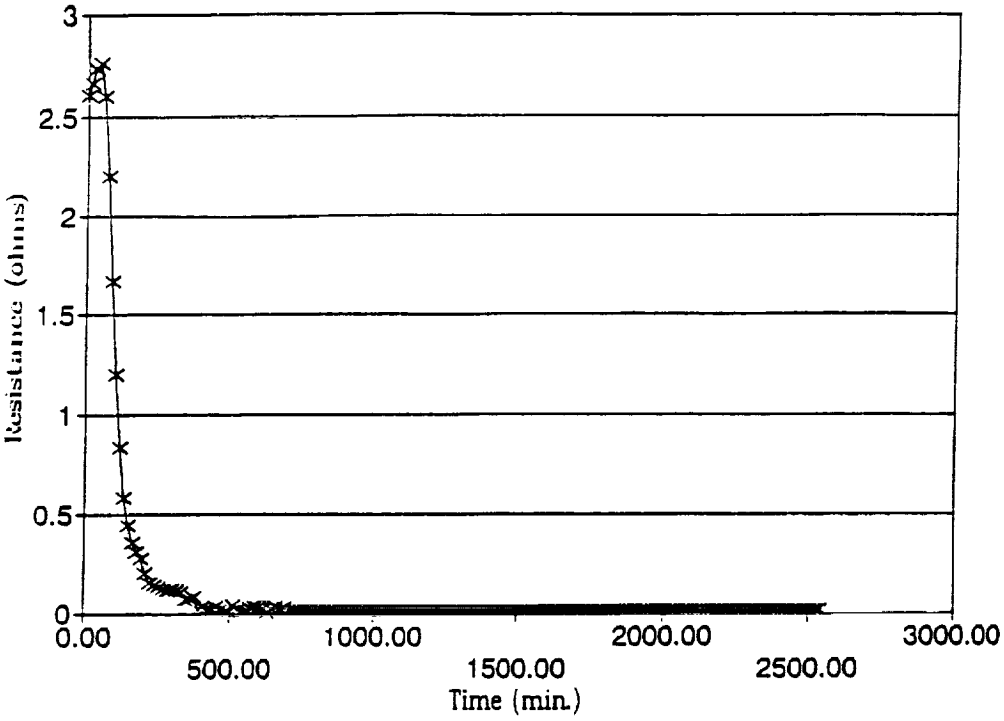

a) The entire resistivity run from the initial dwell at 845 °C until a silver wire broke after forty-two hours.

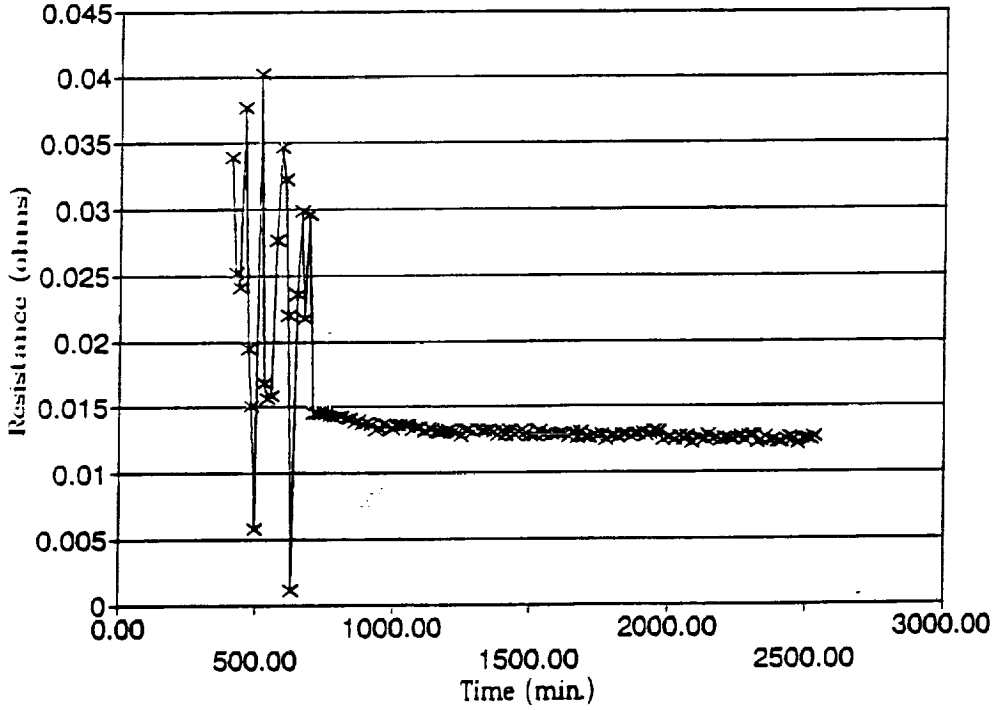

b) A close up view of the specific areas of interest.

Figure 37 In-Situ Resistivity Development showing the resistivity data taken using the 0.25 mm silver wires and one time calcined powder.

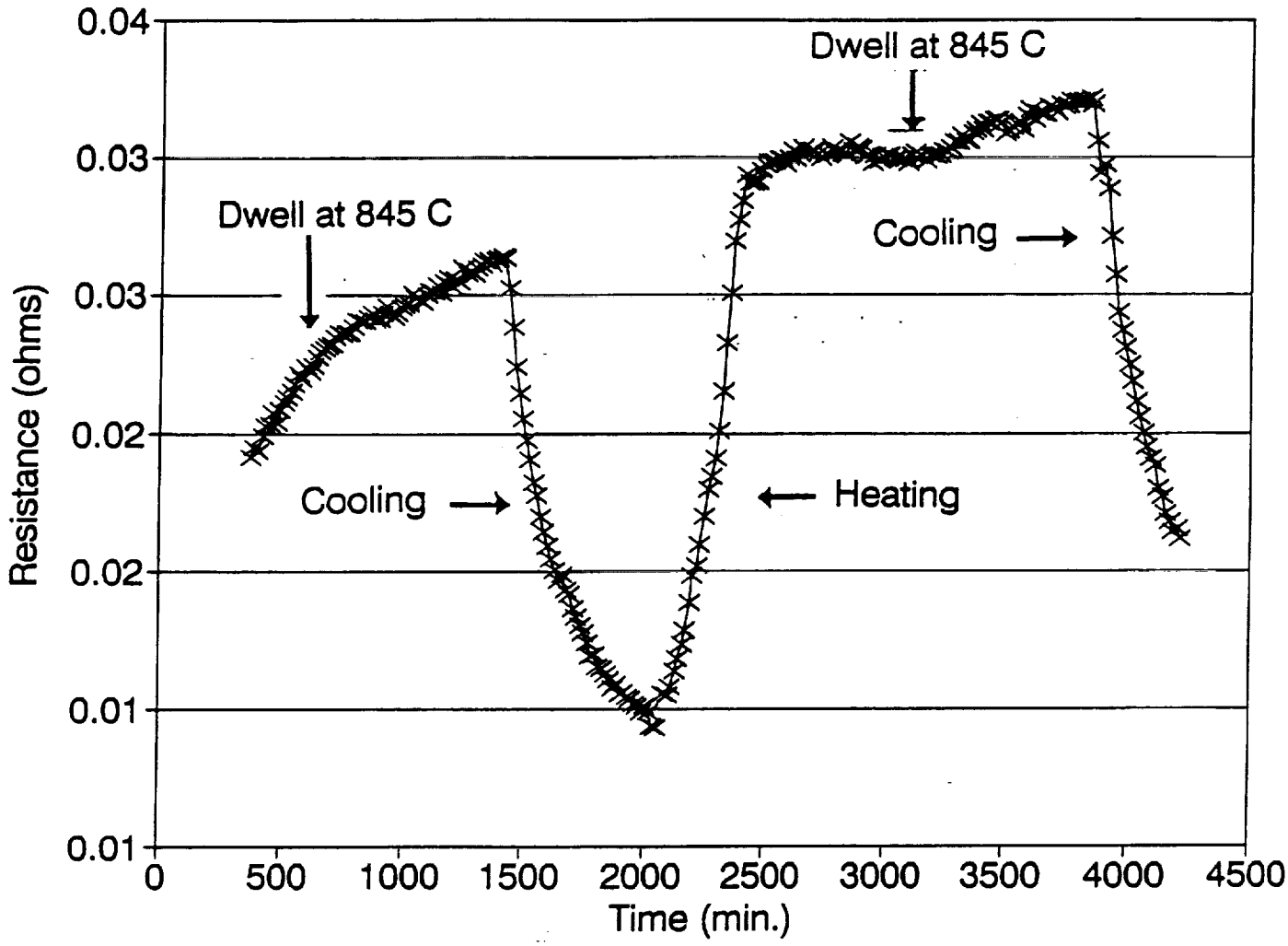

Figure 38 In-Situ Resistivity Development showing the resistivity data taken using 1 mm silver wires and two time calcined powder. The run had two cycles, where each cycle lasted twenty-four hours.

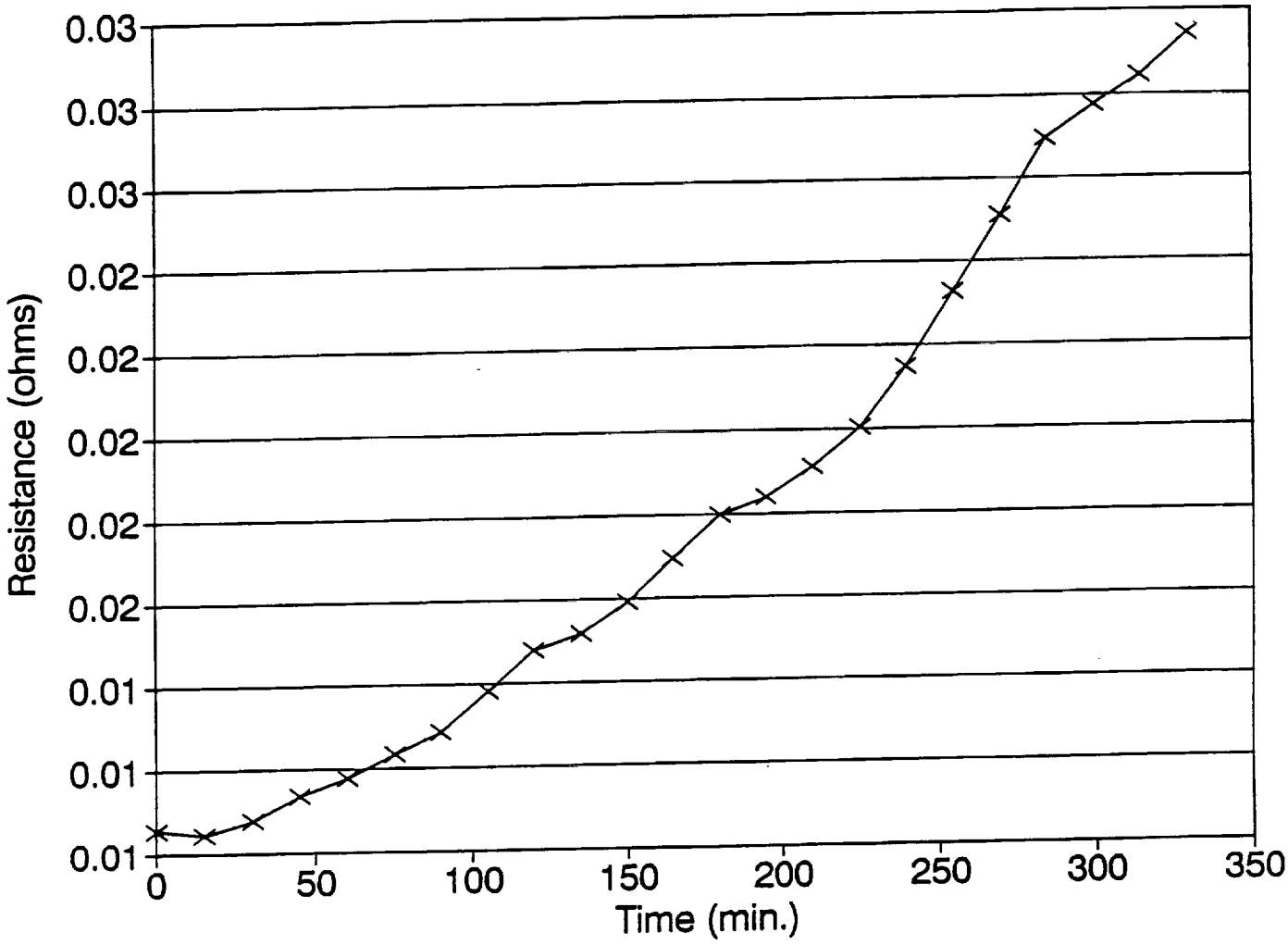

Figure 39 In-Situ Resistivity Development showing the resistivity data taken on the heat up curve between the two cycles. 1 mm silver wires and two time calcined powder was used for this run.

Annual Report
Part II

Development of Tl- and Bi-Based Superconducting Thick Film Coatings and $YBa_2Cu_3O_{7-\delta}$ Aqueous Processing

Submitted to

National Aeronautics and Space Administration
Langley Research Center

Submitted by
Phillip Gilmour

Principal Investigator
Gene H. Haertling

Department of Ceramic Engineering
Clemson University
Contract No. NAG-1-1108
March 1993

Abstract

Research performed during this period included preliminary investigations into thick films produced via the acetate dip coat process and dielectrophoretic deposition of bismuth-superconductor films on silver substrates. Of these two coating techniques, it appears dielectrophoretic deposition is a novel technique that has the potential of developing superconductor coatings with preferred orientation.

Acetate dip-coating produced $Tl_2Ba_2CaCu_2O_8$ superconductor thick films when fired at 600°C for 30 minutes. Using this low temperature firing method, encapsulation is not needed to contain the volatile thallium. It appears thicker films produce a greater proportion of the $Tl_2Ba_2CaCu_2O_8$ phase.

Dielectrophoretic depositions were produced on silver wires. In this technique, high-voltage is applied between two electrodes which are immersed in a suspension of superconducting powders and an insulating fluid. A nonuniform field is set up when a voltage is applied to a wire electrode that is surrounded by a cylindrical counter electrode. If the particle contains a relatively high permittivity compared to the suspending fluid, a dipole is created in the particle. The particle is then drawn to the wire electrode due to the attraction of the dipole to the greater field intensity. Result of dielectrophoretic depositions suggest superconductor films may be produced with slight particle orientation.

Another investigation examined aqueous processing of $YBa_2Cu_3O_{7-\delta}$ ceramics. Silane additions to water while milling seemed to reduce the decomposition of the superconducting phase with water. Silane appeared to coat the superconductor particles with a hydrophobic layer reducing the barium and copper leaching from the superconducting phase. Ceramic pellets which were milled with water and silane exhibited a Meissner effect almost as strong as pellets which were milled in an unreactive, inorganic liquid. However, transition temperature curves of superconductors with silane additions showed nonzero resistance below the superconducting transition.

Introduction

To obtain optimum superconducting properties of superconducting thick films, e.g. critical current densities and high transition temperatures, it is important not only to have a relatively pure superconducting phase but also preferred orientation of films. Due to the highly anisotropic crystal structure of nearly all high-temperature superconductors, c-axis orientation normal to the substrate as well as a-b in plane orientation yields the highest critical current densities. This can be easily understood if one realizes the superconducting electron pairs have high mobility along the a-b plane with little conduction along the c-axis. Most techniques which produce oriented superconducting films are costly and cannot easily fabricate long superconducting wires.

Research in this report concentrates on acetate dip-coating and dielectrophoresis to develop superconductor thick films. These are preliminary studies which assess the potential of further research. Both techniques were studied because they could be relatively inexpensive processes to produce superconducting films. In addition, due to the basic nature of one of the methods studied in this report, i.e. dielectrophoresis, it was believed c-axis oriented superconducting wires (on a silver substrate) could be produced.

An ancillary study examines aqueous milling of superconducting $YBa_2Cu_3O_{7-\delta}$ powders. If quality superconductor powder could be prepared from aqueous processing, the cost and health hazards associated with organic suspensions will be eliminated. The 123 phase readily reacts with water to produce a nonsuperconducting phase. However if a hydrophobic layer could be place on the 123 powder, reaction with water may be limited. The coating should be relatively inert and inexpensive. For these reasons silane additions to water to produce a nonreactive coating on the superconductor particles were investigated.

$Tl_2Ba_2CaCu_2O_8$ Thick Films

Dip Coat Background

As discussed in a previous report,[1] thallium is extremely volatile; loss of thallium will seriously degrade superconducting properties. If a dip coat process was developed for precursor deposition onto a substrate, it may be possible to fire at lower temperatures thereby reducing thallium volatility. Most previous studies of $YBa_2Cu_3O_7$, Bi- and Tl-based superconductors found in the literature sinter dip-coated or sprayed films close to temperatures used to form superconductors derived from oxide precursors. However, one study by Kordas investigated the effect of sintering temperature on the superconducting properties of sol-gel films.[2] It was found that superconducting $YBa_2Cu_3O_7$ thick films were formed when sintered at a 700°C. Lower sintering temperatures were possible apparently because of greater homogeneity and smaller particle size. In the present study, acetate films were developed to produce Tl-superconductors at low sintering temperatures. Such a process could yield some important advantages: 1) less thallium loss from the film, 2) possibility of producing Tl-based superconductors without the need for encapsulation, and 3) reduced Ag-Tl reactions which have a deleterious effect on the superconducting properties.

Thallium-Based Superconductor Acetate Process

An acetate precursor solution was developed for coating silver foil. The schematic diagram for the dip coating process is shown in Figure 1. The solution was batched to the stoichiometric composition $Tl_2Ba_2Ca_2Cu_3O_{10}$--the 125K superconducting phase. A few important points should be mentioned about the solution. Rapid drying and uniform spreading of the films on the silver substrate requires maximizing the methanol to water ratio. However, a large concentration of water is needed to produce a solution with a 20 weight percent oxide content (after acetate burnout). The concentrated solution used in the study allowed fewer coats in order to produce a relatively thick film. Solutions with lower oxide contents will allow a higher methanol/water ratio to be used. Also, since Cu^{2+} is not appreciably soluble in a neutral or acidic solution, ammonium hydroxide was added before the copper oxide addition. Prior to the first dip-coat, zirconium acetate was sprayed on the silver substrate; then, excess

zirconium acetate was rinsed off with methanol. Pretreatment with zirconium acetate seemed to improve uniformity of subsequent coats.

A pyrolysis step must be performed at 450°C after each coat. At 450°C, the thallium acetate decomposes and forms Tl_2O_3. The pyrolysis step is important for two reasons. If the film is initially fired above this temperature, a green flame emanates from the film indicating thallium acetate is decomposing and leaving the system. Thallium acetate contains thallium in the +1 oxidation state; however in all thallium-containing superconductors, thallium primarily occurs in the +3 oxidation state. Slightly above 450°C, Tl_2O_3 is initially formed but converts to the volatile Tl_2O compound with time. Below 400-450°C thallium acetate is not completely converted to Tl_2O_3.

After building up a thick film from repeated dipping and pyrolysis, unencapsulated films were fired in an oxidizing atmosphere. Sintering temperatures ranged from 550°C to 800°C with soak times between 2 minutes to 90 minutes.

Figures 2 through 5 show the effect of sintering temperature and time on the phase formation of the thallium superconductor. Below 600°C, no superconductor phase apparently forms. At 600°C for a 30 minute soak, a small amount of superconducting phase seems to form. Similar peaks appear for films which have been sintered at 750°C for 15 minutes. Many of the x-ray diffraction peaks of $Ca_2Cu_3O_x$ in Figure 6 are evident in Figures 2 through 6 suggesting incomplete reaction of precursors with thallium. As can be seen in Figure 3 and 4, changing the soak time when the film is fired at 600°C shows the possible superconductor peaks occur only when sintered for 30 minutes. It is possible longer soak times may degrade the superconducting phase due to thallium loss.

The films discussed above were dipped five times. Thicker films were produced after ten dip coats. These films appear to contain a significantly greater amount of thallium superconductor phase as evident in Figure 7. The high-temperature superconductor formed under these conditions is the $Tl_2Ba_2CaCu_2O_8$ phase which exhibits an optimum transition temperature of ~110K. A resistance versus temperature transition was attempted for this film but the film yielded a simple metallic resistance curve. This was probably due to electrical contacts diffusing through the film and touching the silver substrate.

Future work will examine the dependence of the superconducting phase on film thickness and stoichiometry. Also, firing the film at 750°C will be studied more closely.

Dielectrophoresis

Dielectrophoresis Background

A major impetus in the research of high temperature superconductors is to develop superconducting films and wires for applications ranging from microwave resonators, magnetic technology (for solenoids, motors, and magnetic shields), and electrical conduction lines. Although a large number of investigations have the examined physical properties and fabrication methods of superconducting films and wires there are only few methods with the potential for large scale production. A number of methods such as laser ablation and melt texturing have produced films with excellent homogeneity, transition temperatures, and critical currents densities for a variety of superconducting compounds. However because these techniques are costly and somewhat difficult to apply to long-length wire fabrication, they will probably not be used in most superconductor manufacturing methods.

An extremely simple and low cost coating method which has been well studied in many disciplines is electrophoresis. In this method particles which become charged in solution deposit on the anode or cathode depending on the surface charge. Many studies have applied electrophoresis to superconducting coatings, yet strongly oriented films have not been produced by simple electrophoretic deposition.[3-6] Only if the material is doped with rare-earth ions and subjected to high magnetic fields, on the order of 8 tesla, will electrophoresis produce preferred orientation in films.[7]

One technique which has not been investigated to date is dielectrophoretic deposition of superconducting films. In this method, a slurry of superconducting powder and a low conductivity liquid is subjected to a high, nonuniform electric field.[8-14] Under these conditions the superconducting grains in the slurry can develop a dipole and migrate to the region with the greatest field intensity. If a diverging field was created around a wire electrode, e.g. a wire electrode in the center of cylindrical, counter-electrode, the suspension of superconducting particles will migrate

to and deposit on the wire electrode. The method of deposition is similar to electrophoretic deposition in that suspended particles migrate to an electrode under the presence of an electric field. Yet, more restrictive conditions of high, nonuniform electric field allow the weak dielectrophoretic mechanism to arise.

In most systems, dielectrophoresis is a mild effect compared to electrophoresis. Yet, the utility of the dielectrophoretic technique arises from anisotropy inherent in certain particles and the consequent orientation of the particles in a strong electric field. Quite often a dielectrophoretically deposited coating exhibits a strong preferred orientation. Since the axis with the highest permittivity is along the c-axis in a superconductor crystal,[15] it is quite feasible that a c-axis orientation perpendicular to the axis of the wire could be created in dielectrophoretic deposited superconductor coatings. If this method were developed it could have the potential to be a straightforward, low-cost, fabrication method of superconducting wires and conduction lines.

Before the research is presented it is worthwhile to compare and contrast dielectrophoresis with its well-known counterpart electrophoresis. As shown in Table 1, electrophoresis can occur in a uniform or nonuniform field and could be used to create coatings on wires, plates, or substrates of virtually any configuration. However, due to the necessary condition of a diverging electric field, dielectrophorectic coatings only occur on electrode configurations which give rise to a nonuniform electric field.

Dielectrophoretic Deposition Technique

In order to create homogeneous superconducting powders, an acetate solution process was used. Particulars of the acetate process are describe in another NASA contract.[16] In this method Bi, Pb-, Ca-, Sr-, and Cu-acetate precursors are batched and mixed in solution. The acetate solution was dried and followed by pyrolysis. Four calcinations at 845°C for 12 hours with intermediate grindings produced the Bi-2223 phase. Since aggregated or agglomerated particles usually do not create dielectrophoretic depositions due to the random orientation of the attached particles, it was necessary to disperse single crystals in a liquid. To obtain single crystals, the powder was ground in a mortar and pestle and passed

through 400 mesh. Approximately 0.6 grams were added to n-butanol a sonicated for 5 minutes. The suspension was left undisturbed for 10 hours. After allowing the more massive particles to settle, the suspension was decanted and dried. The scanning electron photomicrographs of Bi-Pb-Ca-Sr-Cu-O powders displayed in Figure 8, shows particles which settled to the bottom of the were larger and aggregated compared to the particles which were in the suspension. A large percentage of fines in the suspension had a particle size below 1 micron. These dried fine particles were used to study dielectrophoretic deposition.

A number of solutions were examined to assess the potential as the suspending fluid when an electric field is applied. Most of liquids examined, i.e. toluene, trichloroethylene, acetone, alpha-terpineol, distilled/deionized water, and n-butanol and other alcohols, were too conductive to be utilized for dielectrophoresis without further purification. Also when electrophoretic or dielectrophoretic deposition was performed with various oils, particles would not adhere to the substrate. The best candidate for dielectrophoresis applications was the chlorofluorocarbon 1,1,2-trichloro-trifluoroethane. The liquid was highly resistive, hygroscopic, and created good particle/substrate adherence.

A diagram of the electrodes is shown in Figure 9. The outer electrode was 1.5 cm in diameter and had a length of 3 cm. The central silver wire electrode had a uniform diameter of 230 microns. To suspend the powder in the 30 ml of chlorofluorocarbon liquid, a small drop of Triton X-100 was added to approximately 0.15 grams fine powder followed by sonication for 5 minutes.

A voltage of 5,000 V was applied to the system producing a current less than 1 mA. Deposition was performed for 5 minutes. After depositing the particles on the wire, the wire was removed for examination with a scanning electron microscope. The wire was replaced with another silver wire of the same diameter. Again the same voltage was applied and a deposition occurred. Then the wire was cleaned, replaced, and subjected to the same conditions but with the electrodes of opposite polarity. Even with opposite polarity deposition occurred. Finally, both the cylindrical counter electrode and the inner wire electrode were replaced with two 0.25 cm by 4 cm parallel sheets of silver foil. Voltages from 500 to 6,000 V were applied. With parallel plate electrodes, no deposition occurred at any voltage.

The above observations strongly suggest that the films were dielectrophoretically and not electrophoretically deposited. With the cylinder and wire electrode configuration, deposition occurred on the wire regardless of polarity. However, no deposition occurred in the parallel plate electrode configuration. This is to be expected since the relatively uniform field created by the parallel plates will not give rise to dielectrophetic deposition.

Electrophoretically deposited films were developed to compare the results to dielectrophoretically deposited films. The suspending liquid for electrophoresis was n-butanol. Coarse, aggregated powders which settled after 10 hours in n-butanol were used as particles for deposition. Both the cylinder/wire and parallel plate electrodes were used to study electrophoretically deposited films. A voltage of 500 V was applied with a resulting current of approximately 2.5 mA. Under both electrode systems, particles migrated and deposited on the positive electrode. After 5 minutes of deposition, the electrodes were removed.

Figure 10 shows bare the silver wire and coated silver wire in the dielectrophoretic deposition. A coating of approximately 8 microns resulted from dielectrophoresis. In comparison the electrophoretic coating on silver foil is displayed in Figure 11. There seems to be no apparent orientation of the electrophoretically deposited film; however, the dielectrophoretically deposited films seem to show slight orientation. To determine the extent of orientation and phases produced by this technique, a Debye-Scherrer camera could be used; however, the instrument is not immediately available for use at Clemson University. Instead, the phases present in an electrophoretically deposited film sintered at 845°C for 12 hours was studied. The x-ray diffraction profile in Figure 12 shows the sintered film to be composed primarily of the Bi-2223 phase. Therefore, it seems quite promising that thin films of Bi-2223 can be also produced on silver wire with some degree of orientation.

This initial study of suggests dielectrophoresis is a novel technique with the possibility of producing oriented superconducting films. In addition, the technique could be used to orient ferroelectric films. Future research will examine many factors such as optimization of pH conditions, wire diameter, and particle size with their effect on deposition rate, orientation and solution stability.

Aqueous Processing of $YBa_2Cu_3O_{7-\delta}$

It is well-known that $YBa_2Cu_3O_{7-\delta}$ readily reacts with water to produce a nonsuperconducting article in a short time. However, it would be desirable to develop a method of milling 123 powders in water prior to the ceramic forming process. This would eliminate more costly organic solvents used for milling while reducing safety hazards.

The 123 phase readily undergoes decomposition via the reaction mechanism:[17,18]

$$2YBa_2Cu_3O_{7-x} + 3H_2O \rightarrow Y_2BaCuO_5 + 3Ba(OH)_2 + 5CuO + (0.5-x)O_2$$

$Ba(OH)_2$ is somewhat soluble in water and increases the alkalinity of water.[19] During this reaction the formal valence of Cu changes from +2.3 to +2. Since high-temperature superconductors are extremely sensitive to the valence of copper, a small amount barium leached into solution can destroy the superconductivity. If dissolved CO_2 is present in the water in the form of carbonic acid $Ba(OH)_2$ further reacts to form $BaCO_3$ by the following reaction:

$$Ba(OH)_2 + CO_2 \rightarrow BaCO_3 + H_2O.$$

The reaction products $Ba(OH)_2$ and $BaCO_3$ are indicated by white crystals on the ceramic or powder surface.

To reduce these reactions in water, silane additions to water were examined. Silanes are compounds with the general formula Si_nH_{2n+2} and are analogous to alkanes. Often, these are coupled with organic functional groups. These compounds are known to readily react with many oxide surfaces to create hydrophobic layers. When placed in an aqueous system, silanes effectively compete with water molecules for surface bonding states and form bridging siloxane bonds, $-O-SiR_2$, to the oxygen on the particle surface. Studies have shown large amounts of silica do not appreciably deteriorate superconducting properties.[20,21,22] Because of the potential of silanes reducing water/superconductor contact while not destroying superconductivity, a preliminary examination was undertaken to examine the effectiveness of silanes for aqueous milling of 123 powders.

Superconducting powders were fabricated by a process outlined in a previous report.[23] However instead of a final milling in trichloroethylene prior to forming, ceramic powders were milled in either 1,1,2-trichlorotrifluoroethane or water or water mixed with silanes.*

Since formation of $Ba(OH)_2$ in an aqueous system increases the alkalinity, the pH of the water was measured during ball-milling. Milling was performed in a nalgene bottle with zirconia media. Several batches of 75 grams of 123 powder and150 milliliters of water or a water/silane solution were examined for silane effects and reproducibility. Two and five weight percent (of the the total solvent weight) silane concentration were added to water in the mill. Superconducting powder was added immediately after silane additions. Also, in one 2 percent batch, silane was added to water and allowed to sit for 36 hours before the powder was added. After this time, the solution appeared slightly hazy. Then seventy five grams of 123 powder were added to the solution and milled.

Initial pH values of distilled water were approximately 5.5; silane additions produced no detectable effect on the initial pH. This is a typical value for water which has absorbed CO_2. Yet within a few minutes of milling, water basicity increased to 12. This is indicative of a rapid reaction of barium with water. After five minutes, pH stabilized and remained constant during the remaining milling. Alkalinity was also seen to increase within a few minutes with silane additions, yet pH increased only to 9.0 and stabilized. Milling in two and five percent silane yielded similar and reproducible pH curves. However, when silane was allowed to age in solution before adding powder, pH values slowly climbed to 11 when milled.

After grinding, the suspension was placed in a dryer for 16 hours. A thick layer of white crystals and blue-green crystals, indicating decomposition of 123 to $Ba(OH)_2$ and Cu_2O was evident in the superconducting powder milled in water. A similar layer of crystals was noted in the solution which was allowed to sit for thirty six hours before grinding. However, milling in the water/silane solutions, with powder immediately added, showed only a small amount of these decomposition products.

---

*The silane solution used was Dow Corning Z-6070. The solution contains methyl alcohol, dimethyldimethoxysilane, and methyltrimethoxysilane.

The smaller pH change and small amount of white crystals after drying suggests silanes markedly reduced decomposition of 123 in water. However if the silane was allowed to sit for an amount of time before powder was added, silane additions were not as effective. This could be due to hydrolysis followed by condensation and polycondensation of silanes to form complex siloxane structures in water.[24] This occurrence is often manifest by a hazy solution caused by micelle formation in water. Polycondensation can reduce the effectiveness of silane additions since siloxane bonds would have to be broken in order to react with the particle surface.

Dried powders were mixed in a mortar and pestle and pressed to form pellets. Although particle size measurements have not yet been performed on these powders, it was quite evident that silane treatments produced much finer grains than milling in an organic solvent. The effect of aqueous milling of ferrites in silanes was also noted in a German patent.[25] The fine grain size was attributed to the reduction of agglomeration by the silane layer.

The green bodies were sintered at 900°C for 5 hours and annealed at 450°C for 12 hours. After firing, pellets were cooled to liquid nitrogen temperature and checked for the Meissner effect. Pellets made from powder milled in water or the aged silane/water mixture did not levitate a 3 gram Sm-Co magnet. However, grinding in the organic solvent or silane/water solutions did lift the magnet off the surface. Apparently, silanes did effectively check the release of Ba^{2+}in water.

Resistance transition curves were plotted for the ceramics. Figure 14 shows the superconducting transition is severely degraded for powders milled in water compared to milling in an organic. However, Figure 15 shows silanes also seriously degraded the resistance transition. At first, this was considered surprising since silanes appeared to limit the superconductor decomposition (suggested by lower pH values, less decomposition products evident upon drying, and the Meissner effect) yet, upon reflection, this may be expected. Silanes reduce the surface reaction and protect the particle core in an aqueous system. Numerous studies have investigated the effects of carbon on 123.[26,27,28,29] Many of these studies have found CO_2 reacts with 123 upon sintering to form $BaCO_3$ or the barium oxycarbonate $BaCO_{4.8}$. These reaction products reside at the grain boundary without appreciable diffusion of carbon into the grain. Since

silanes coat the particle surface, carbon can be expected to reside at the grain boundaries. Therefore a ceramic pellet can exhibit a strong Meissner effect while exhibiting a poor resistive transition due to the presence of intergranular phases.

A future study will examine the effect of sintering temperature on the resistive transition. If the superconducting pellets are fired above 930°-950°C, it has been found that barium carbonate residing at the grain boundary starts to decompose with carbon leaving the system in the form of CO_2.[30,31] Altering the firing schedule coupled with decreased concentrations of silanes may improve the resistive transition in aqueous milled $YBa_2Cu_3O_{7-\delta}$. Also, chrome complexes, specifically Quilons and Volans from DuPont, will be investigated. These produce hydrophobic coatings on oxide surfaces similar to silanes. Results of these studies will be compared to silanes.

References

1. G. Haertling, "Development of High T_c (>110K) Bi, Tl, and Y-Based Materials as Superconducting Circuit Elements. Part II Development of Tl-Based Materials," NASA Semi-Annual Report, Contract No. NAG-1-1108 October 1991.

2. G. Kordas, "Sol-Gel Processing of Ceramic Superconductors," *J. Non. Crystal. Solids* **121**, 436-442 (1990).

3. N. Koura, H. Shoji, and A. Morita, "Prepation of Various Shape Superconducting Ceramics with Various Substrates by Electrophoretic Deposition Method," *Mol. Liq. Cryst.* **184**, 243-247 (1990).

4. H. Nojima, M. Nagata, H. Shintaku, and M. Koba, "Fabrication of Y-Ba-Cu-O Superconducting Films on Cu Substrates by an Electrophoretic Deposition Technique," *Japan. J. Appl. Physics* **29**, L1655-L1658 (1990).

5. R. Eggenhoffner, "Cryoelectrophoresis of Superconducting $YBa_2Cu_3O_{7-x}$ in Liquid Nitrogen," *Cryogenics* **31**, 756-759 (1991).

6. F. Schmidt, "Formation of Superconducting Articles by Electrodeposition," European Patent Application No. 8,9302,285, Oct. 1, 1990.

7. M. Hein, E. Mahner, G. Muller, H. Piel, L. Ponto, M. Becks, U. Klein, and M. Peineger, "Electrophoretic Deposition of Highly Textured Thick Films," *Physica C* **162-164**, 111-112 (1989).

8. H. A. Pohl, "Some Effects of Nonuniform Fields on Dielectrics," *J. Appl. Physics* **29**, 1182-1188 (1958).

9. H. A. Pohl, "The Motion and Precipitation of Suspensoids in Divergent Electric Fields," *J. Appl. Physics* **22**, 869-871 (1951).

10. L. Benguigui and I. J. Lin, "More About the Dielectrophoretic Force," *J. Appl. Phys.* **53**, 1141-1143 (1982).

11. T. B. Jones, "Dielectrophoretic Force in Axisymmetric Fields," *J. Electrostatics* **18**, 55-62 (1986).

12. L. Gherardi, E. R. Mognaschi, and A. Savini, "Dielectrophoretic Motion of a Lossy Dielectric Sphere in a Liquid of Non-Zero Conductivity," *IEEE Trans. Electr. Insul.* **EI-20**, 385-388 (1985).

13. N. C. Lockhart, "Dielectrophoresis in Clay Suspensions," *Powder Technology* **35**, 17-22 (1983).

14. E. R. Nognaschi and A. Savini, "Dielectrophoresis of Lossy Dielectrics," *IEEE Trans. Industry Appl.* **IA-21**, 926-929 (1985).

15. J. Kircher, M. K. Kelly, S. Rashdeev, M. Alouani, D. Fuchs, and M. Cardona, "Anisotropy and Oxygen-Stoichiometry Dependence of the Dielectric Tensor of $YBa_2Cu_3O_{7-\delta}$ ($0<\delta<1$)," *Phys. Rev. B* **44**, 217-224 (1991).

16. L. McIntyre and G. Haertling, "Superconductivity Devices: Commercial Use of Space, Part II," NASA Report Contract No. NAG-1-1301, May 5, 1992.

17. N. P. Bansal and A. L. Sandkul, "Chemical Durability of High-Temperature Superconductor $YBa_2Cu_3O_{7-x}$ in Aqueous Environments," *Appl. Phys. Lett.* **51**, 532-534 (1987).

18. M. F. Yan, T. L. Burns, H. M. O'Bryan, P. K. Gallagher, R. C. Sherwood, and S. Jin, "Water Interaction with the Superconducting $YBa_2Cu_3O_7$ Phase," *Appl. Phys. Lett.* **51**, 532-534 (1987).

19. N. P. Bansal, "Chemical Stability of High Temperature Superconductors," NASA Tech. Memorandum 10539, February 1992.

20. J. Marfaing, X. Y. Song, A. Bettah, Y. Wang, C. Boulesteix, P. Odier, and J. P. Sorbier, "Structural Characterization of YBaCuO Superconducting Screen-Printed Films on Silicon Dioxide and Nitride," *Mater. Sci. and Eng. B (Solid State Materials for Advanced Technology)* **B14,** 235-240 (1992).

21. A. R. Chourasia and D. R. Chopra, "A study of Y-Ba-Cu-O/Si Interfaces by X-Ray Photoelectron Spectroscopy," *J. Vac. Sci. Technol. A* **10,** 115-121 (1992).

22. C. X. Qiu and I. Shi, "Some Properties of Bulk Y-Ba-Cu-O Compounds Containing SiO_2," *J. Appl. Phys.* **64,** 2234-2236 (1988).

23. C.-S. Hsi and G. Haertling, "Superconductivity Devices: Commercial Use of Space, Part I," NASA Report Contract No. NAG-1-1301, May 5, 1992.

24. E. P. Plueddemann, *Silane Coupling Agents*, Plenum Press, NY 1982.

25. G. Zill, "Verfahren zur Herstellung von Hartferriten," E. German Patent 292,760 Aug. 8, 1991.

26. U. Balachandran, C. Zhang, D. Xu, Y. Gao, K. L. Markle, J. M. Bundy, R. B. Poeppel, G. Selvaduray, and J. O. Masen, "Degradation of Properties of $YBa_2Cu_3O_x$ Superconductors Sintered in CO_2 Containing Atmospheres," in *AIP Proceedings 219: Superconductivity and Its Applications*, ed. Y.-H. Kao, P. Coppens, and H.-S. Kwok 439-445 (1990).

27. L. Zhang, J. Chen, H. M. Chan, and M. P. Harmer, "Formation of Grain-Boundary Carbon-Containing Phase During Annealing and $YBa_2Cu_3O_{6+x}$," *J. Am. Ceram. Soc.* **72,** 1997-2000 (1989).

28. S. Wise, *$YBa_2Cu_3O_{7-x}$ and $Bi_{0.8}Pb_{0.2}SrCaCu_2O_x$ Superconductive Fibers by the Piggyback Process*, Ph.D Dissertation, Clemson University May 1992.

29. R. S. Roth, C. J. Rawn, and J. O. Anderson, "Phase Equilibria in the System Ba-Y-Cu-CO_2 in Air," in *Research Update 1988: Ceramic Superconductors II.* ed. M. F. Yan. Am. Ceram. Soc., Westerville, OH 1988.

30. P. K. Gallagher, G. S. Grader, and H. M. O'Bryan, "Some Effects of CO_2, CO, and H_2O Upon the Properties of $YBa_2Cu_3O_7$," *Mat. Res. Bull.* **23**, 1491-1494 (1988).

31. W.-K. Lee and A. S. Nowick, "Degradation of High-T_c Superconductors by Annealing in Dry and Moist Atmospheres," *J. Mater. Res.* **5**, 1855-1861 (1990).

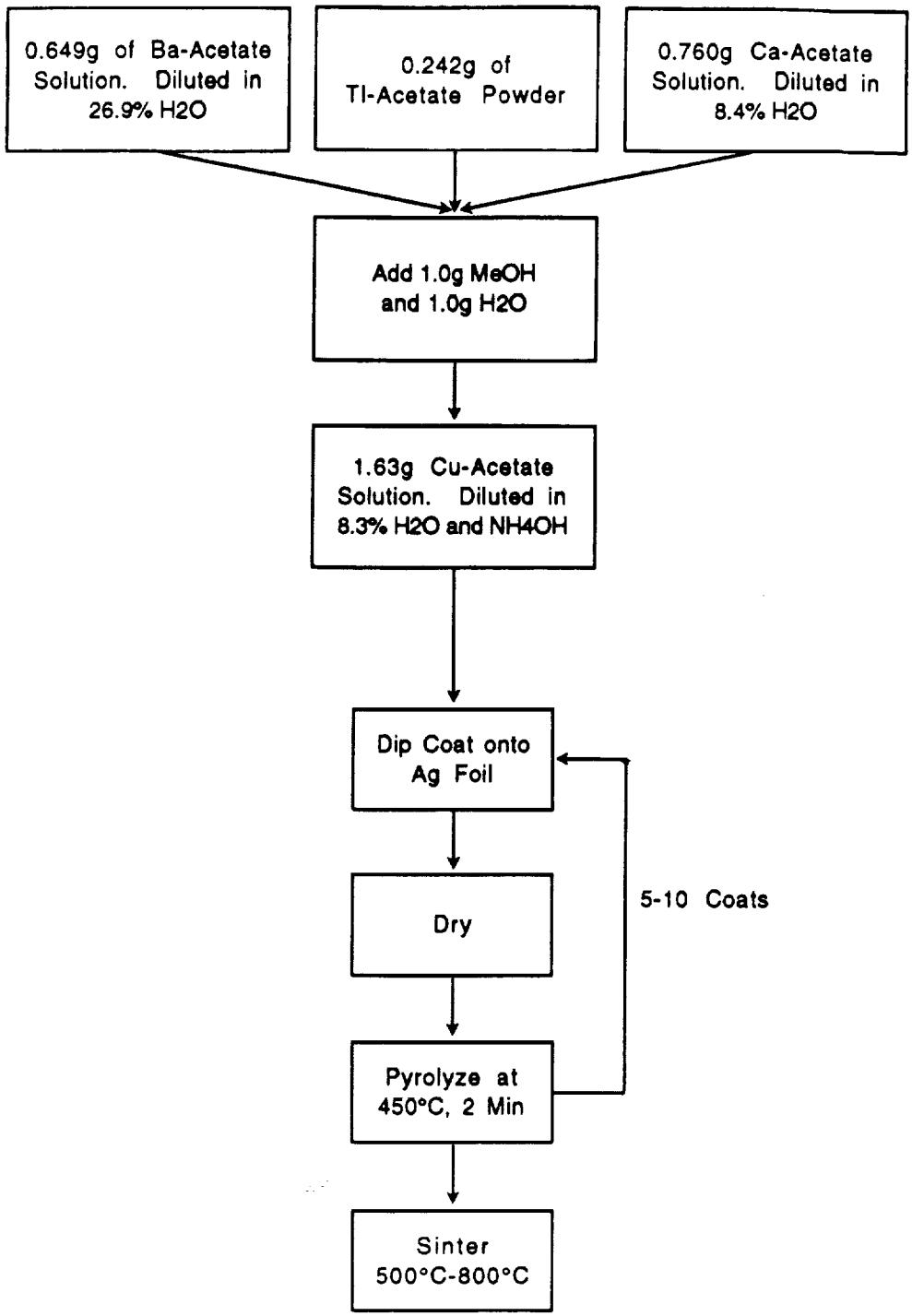

Figure 1

A Schematic Diagram of the Acetate Dip-Coat Technique Used in This Investigation

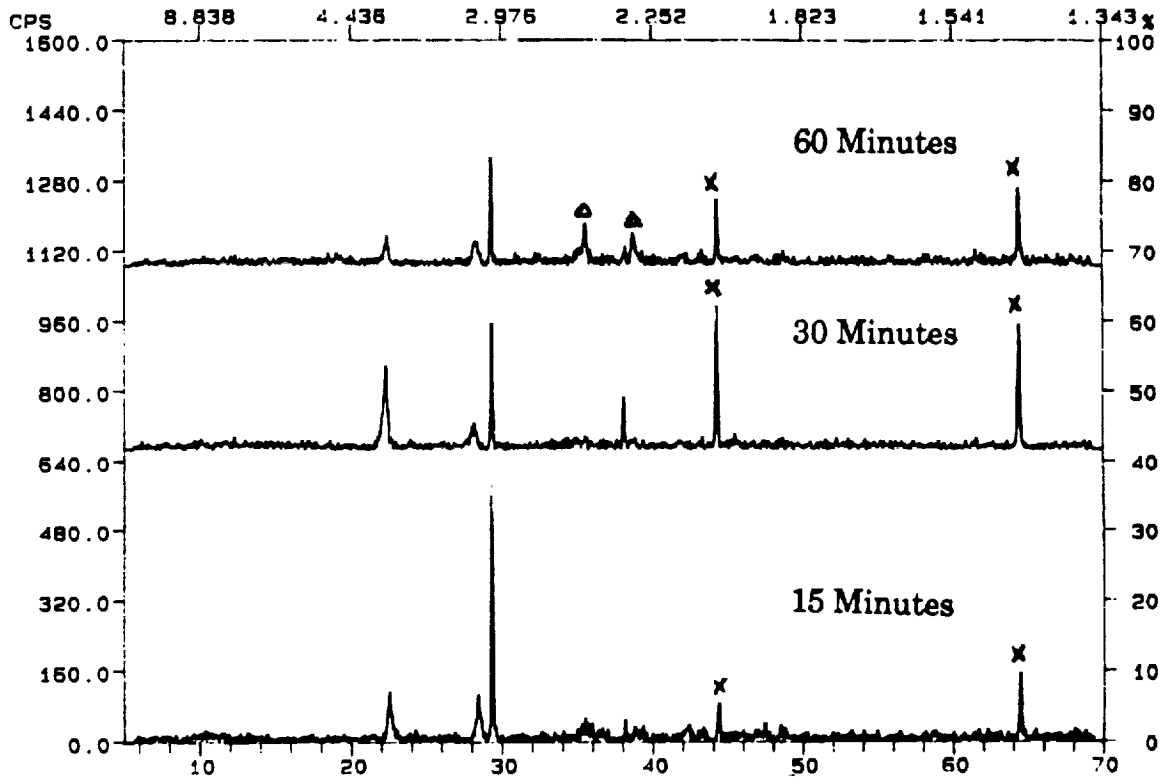

Figure 2

X-Ray Diffraction Profiles of Tl, Ba, Ca, Sr, and Cu Acetate Thick Films Fired at 500°C for Various Soak Times

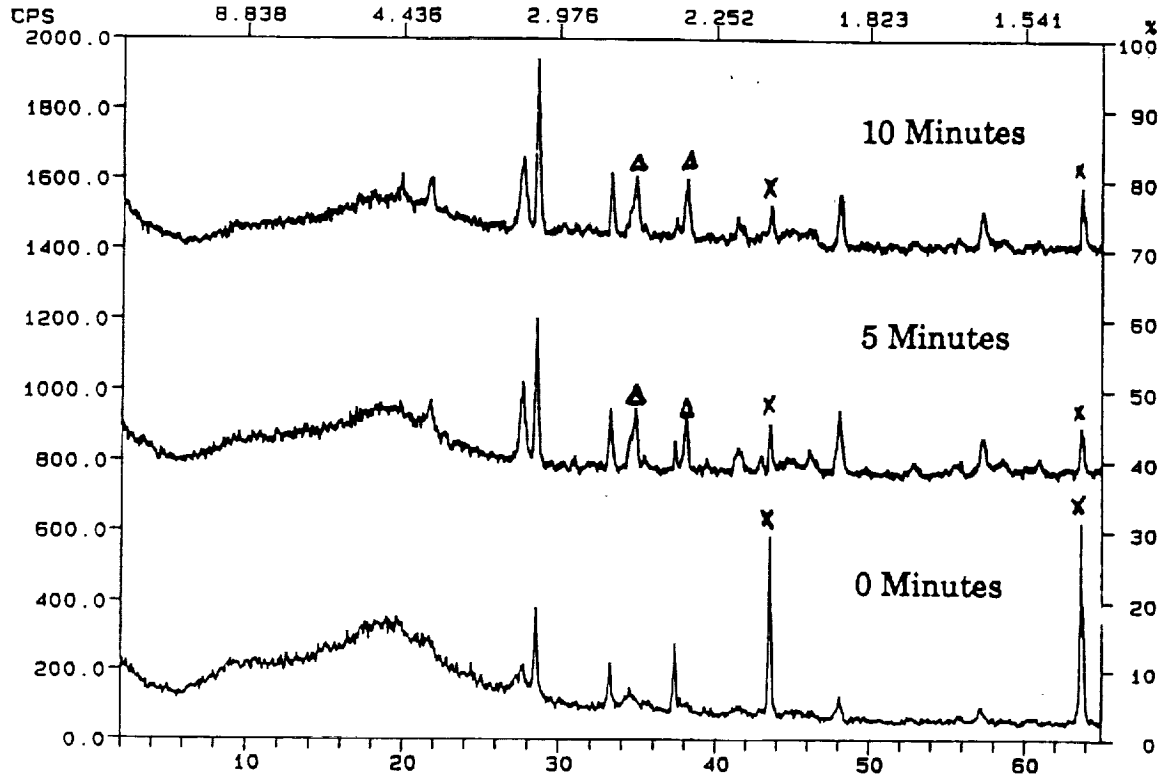

X Sample Holder

Δ $Ca_2Cu_3O_x$

Figure 3

X-Ray Diffraction Profiles of Tl, Ba, Ca, Sr, and Cu Acetate Thick Films Fired at 600°C for Soak Times Ranging from 0 to 10 Minutes

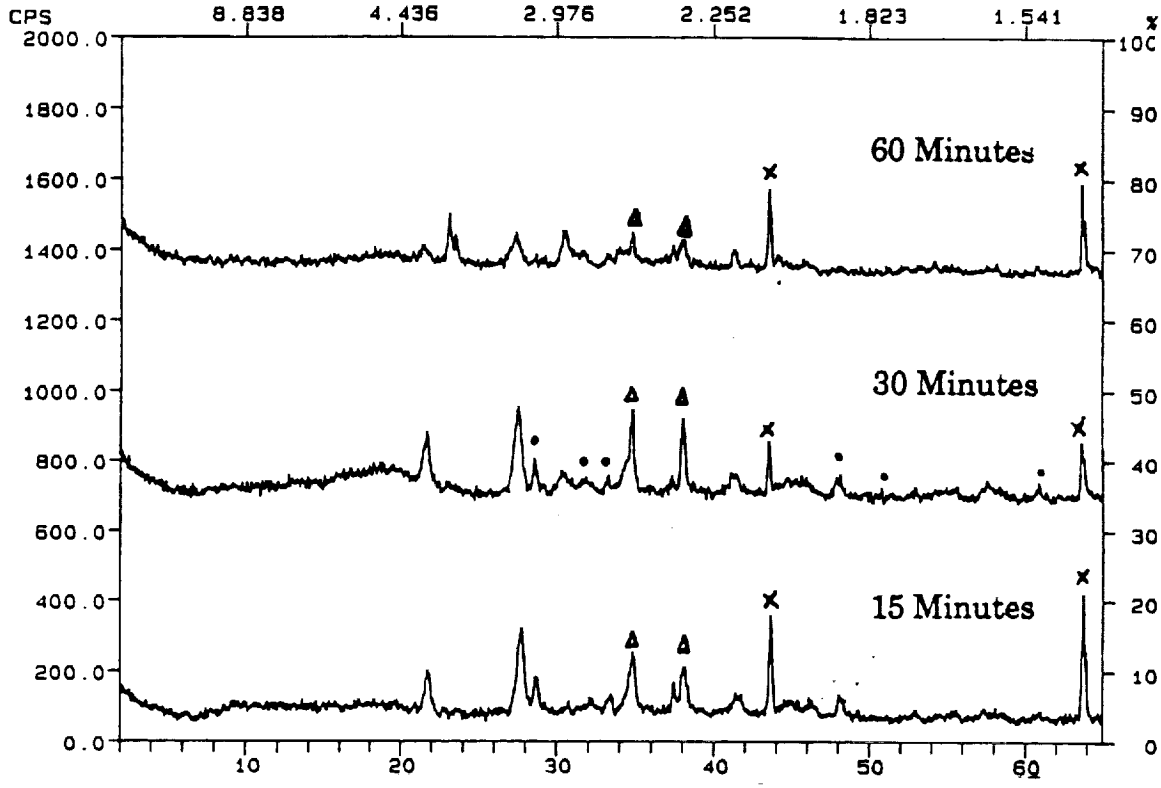

• Tl-2212 Superconducting Phase

X Sample Holder

Δ $Ca_2Cu_3O_x$

Figure 4

X-Ray Diffraction Profiles of Tl, Ba, Ca, Sr, and Cu Acetate Thick Films Fired at 600°C for Various Soak Times from 15 to 60 Minutes

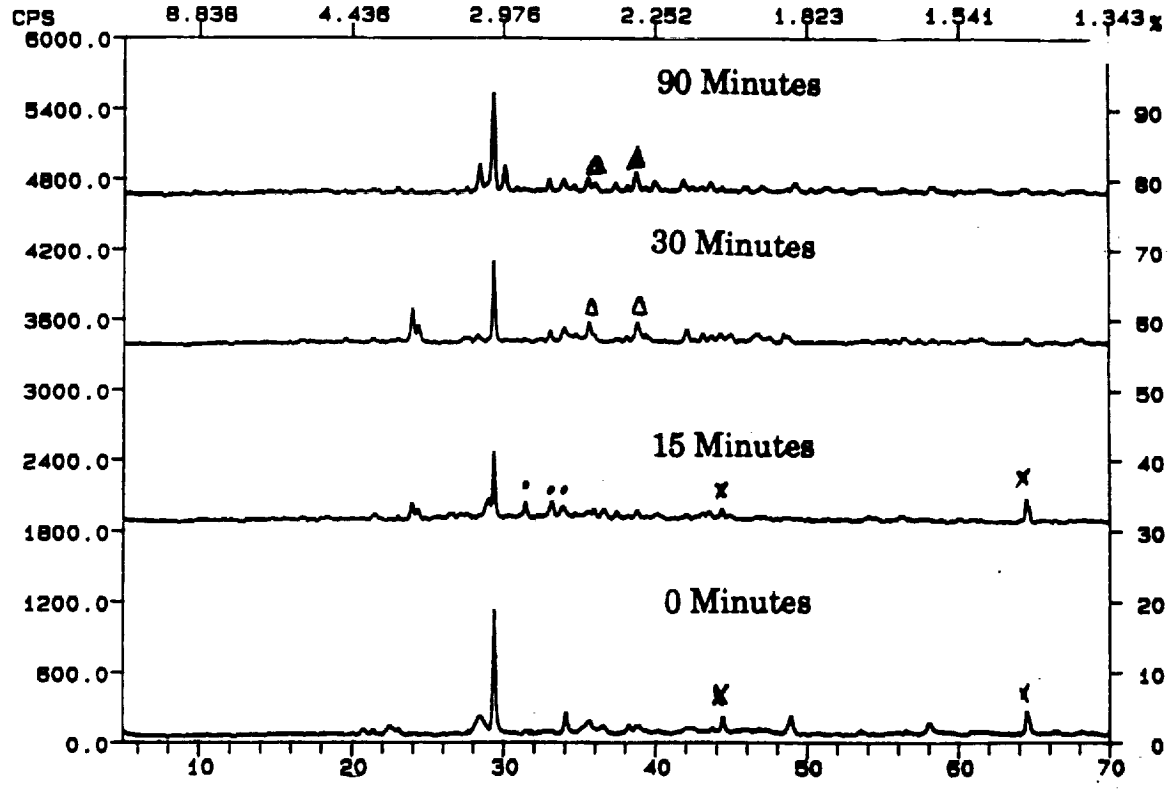

• Tl-2212 Superconducting Phase

x Sample Holder

Δ $Ca_2Cu_3O_x$

Figure 5

X-Ray Diffraction Profiles of Tl, Ba, Ca, Sr, and Cu Acetate Thick Films Fired at 750°C for Various Soak Times

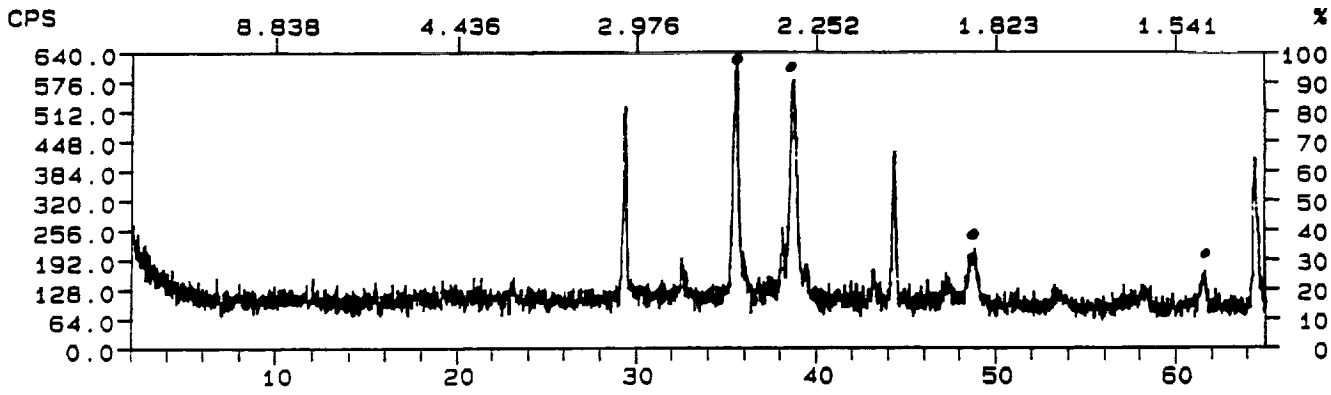

• $Ca_2Cu_3O_x$

Figure 6

X-Ray Diffraction Profile of $Ca_2Cu_3O_x$ Thick Film Derived from Acetate Precursors Fired at 600°C for 30 minutes

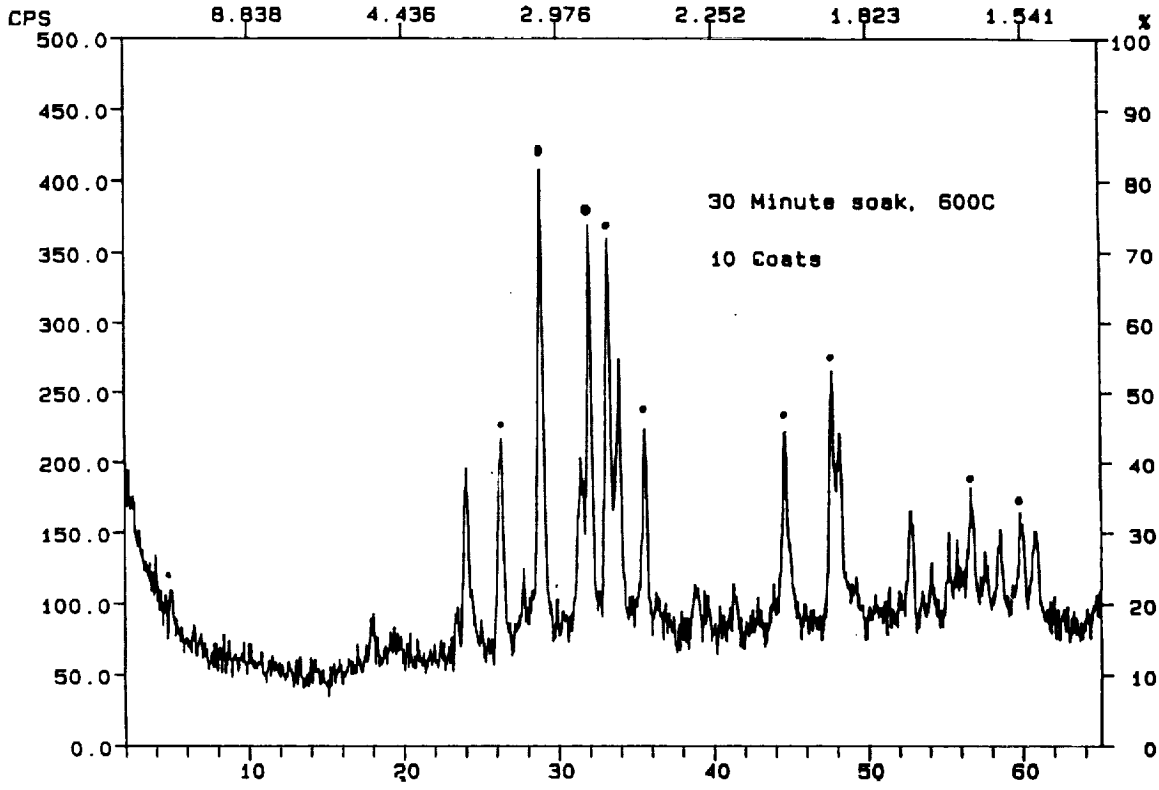

• Tl-2212 Superconducting Phase

Figure 7

X-Ray Diffraction Profiles of a Ten Coat Tl, Ba, Ca, Sr, and Cu Acetate Thick Film Fired at 600°C for 30 Minutes

a

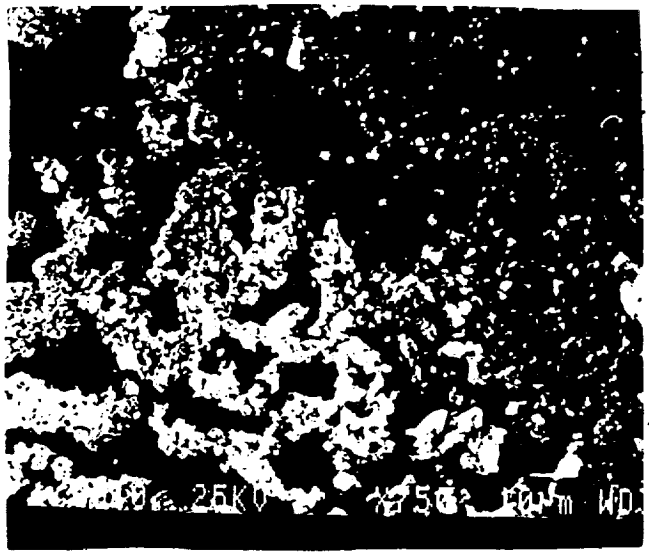

b

Figure 8

SEM Photomicrograph of Bi-Pb-Ca-Sr-Cu-O Powders
a) Particles which had settled after 10 hours in n-butanol
b) Particles which were in suspension after 10 hours in n-butanol

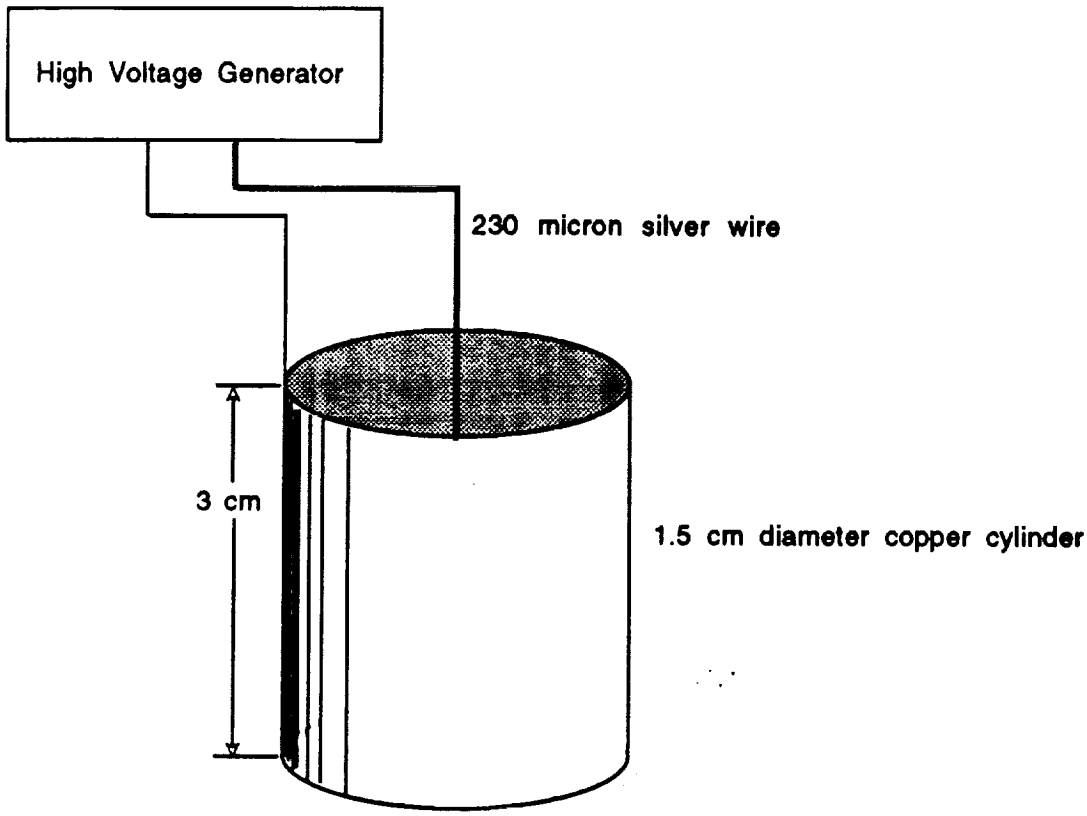

Figure 9

Schematic Diagram of the Dielectrophoretic Apparatus

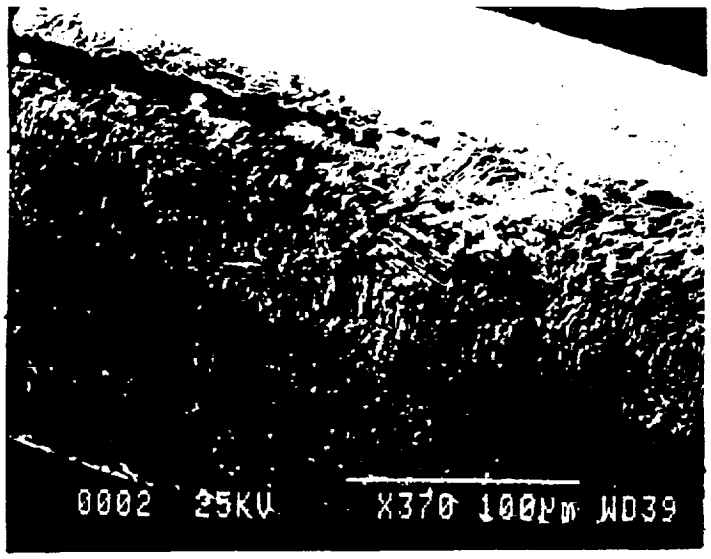

a

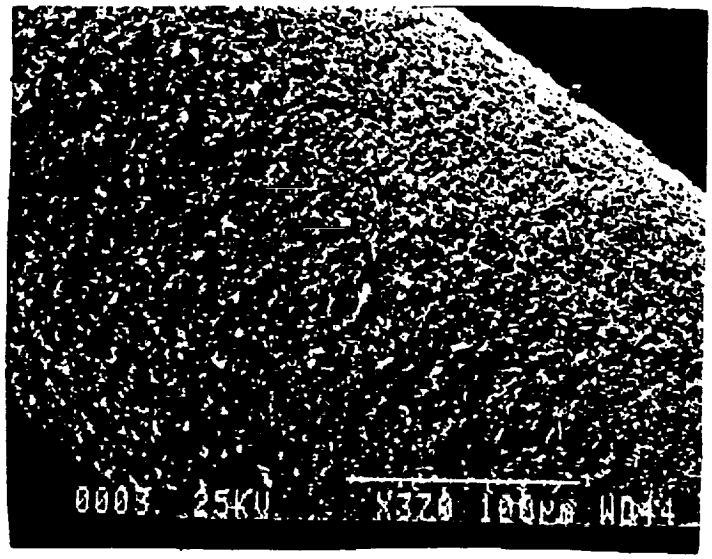

b

Figure 10

SEM Photomicrographs
a) Bare Silver Wire Before Dielectrophoretic Deposition
b) An 8 Micron Dielectrophoretic Coating on Silver Wire.
Deposition Conditions: 1.5 cm Diameter Cylindrical Counter Electrode, Applied Voltage was 5000V for 5 Minutes in 1,1,2-Trifluoro-Trichloroethane.

a

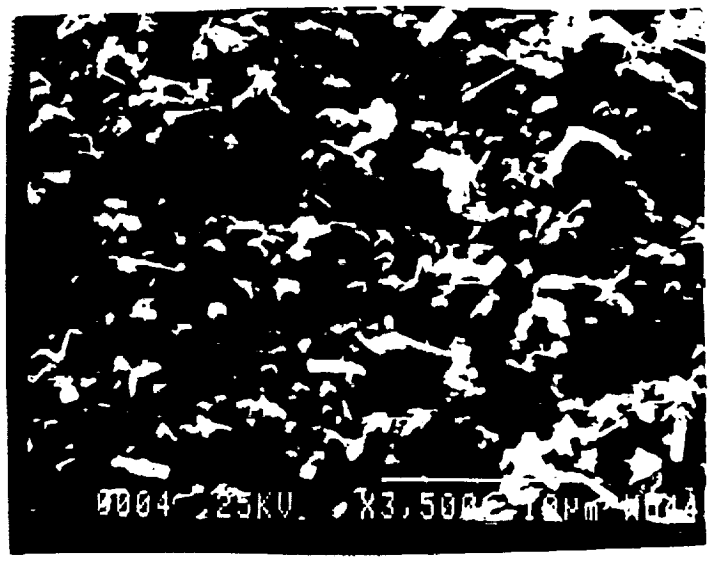

b

Figure 11

SEM Photomicrographs
a) Electrophoretic Deposition on Silver Foil Prior to Sintering
b) Dielectrophoretic Depostion on Silver Wire

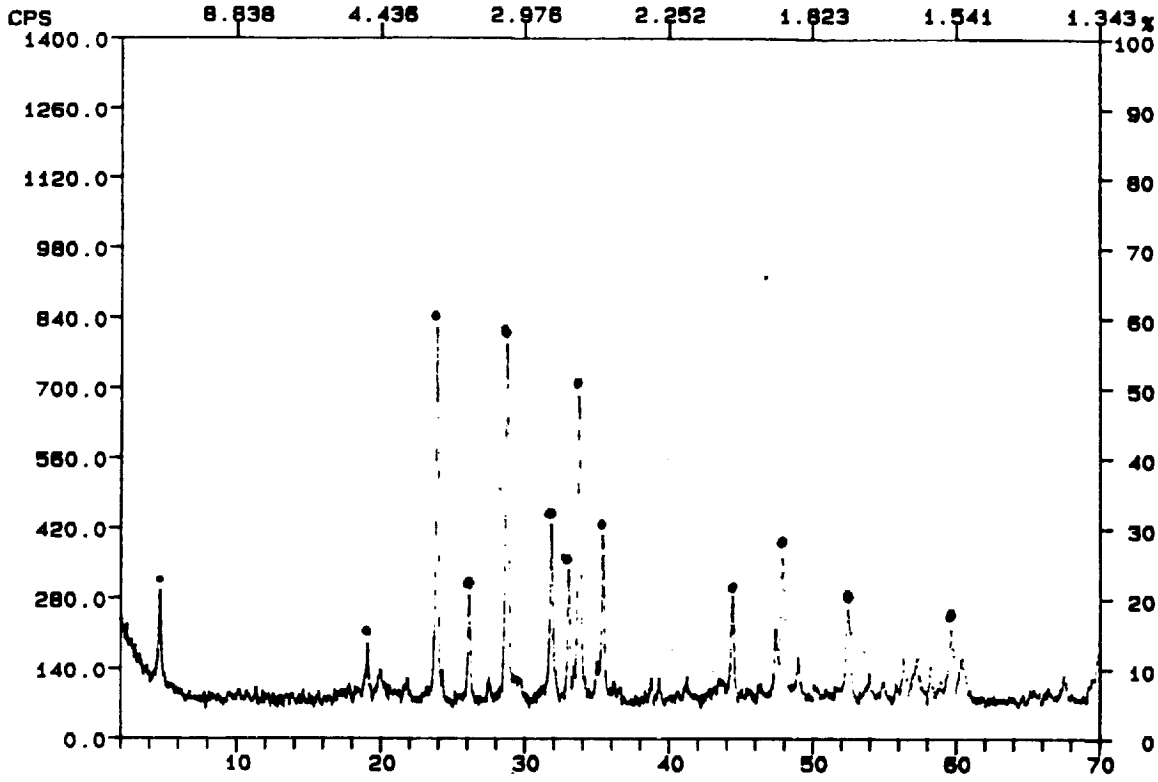

• Bi-2223 Superconducting Phase

Figure 12

X-Ray Diffraction Profile of a Sintered Electrophoretically Deposited Thick Film. Sintering Conditions: 845°C for 12 Hours.

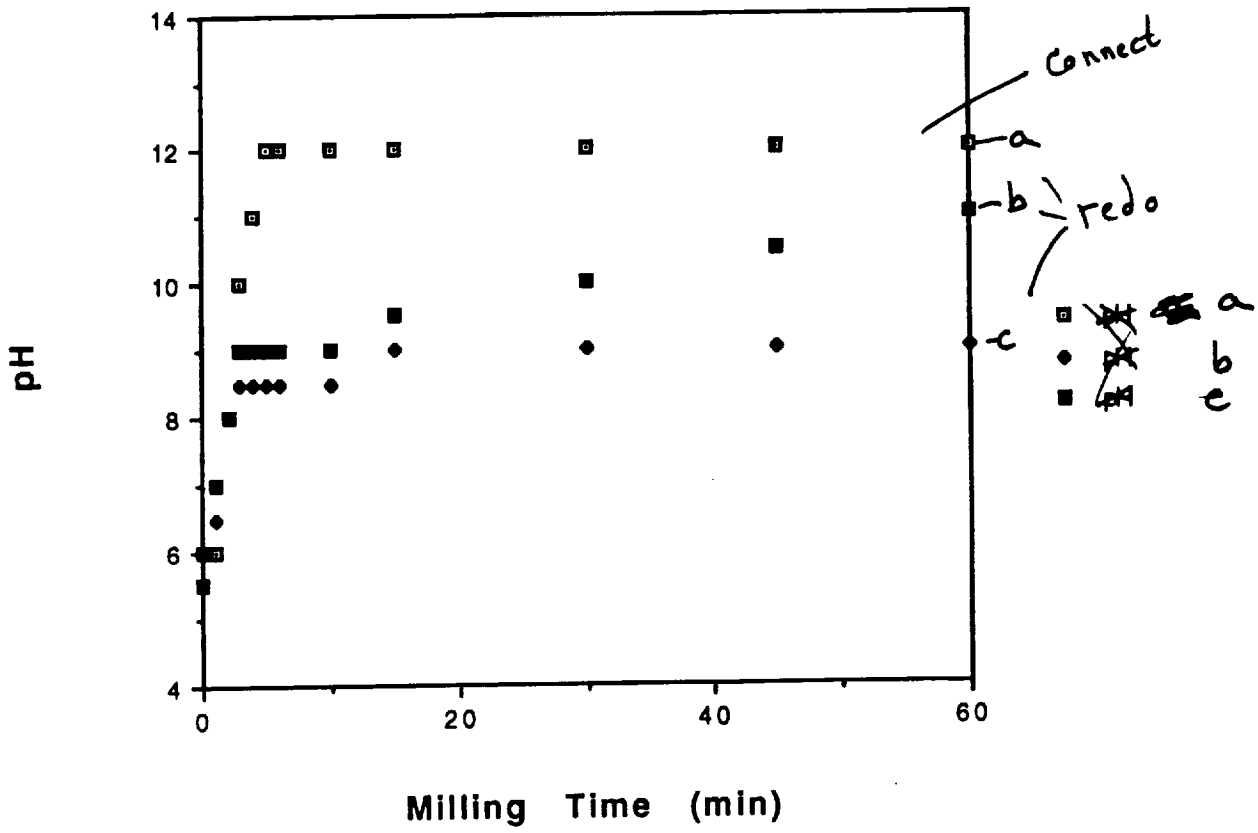

Figure 13

The Effect of $YBa_2Cu_3O_{7-\delta}$ Aqueous Milling on pH

a) no silane additions

b) 2 and 5 weight percent silane additions to water, then immediately milled with 123 powder

(both concentrations produced similar changes on pH)

c) 2 weight percent silane added to water, then aged for 36 hours before the addition of 123 powder.

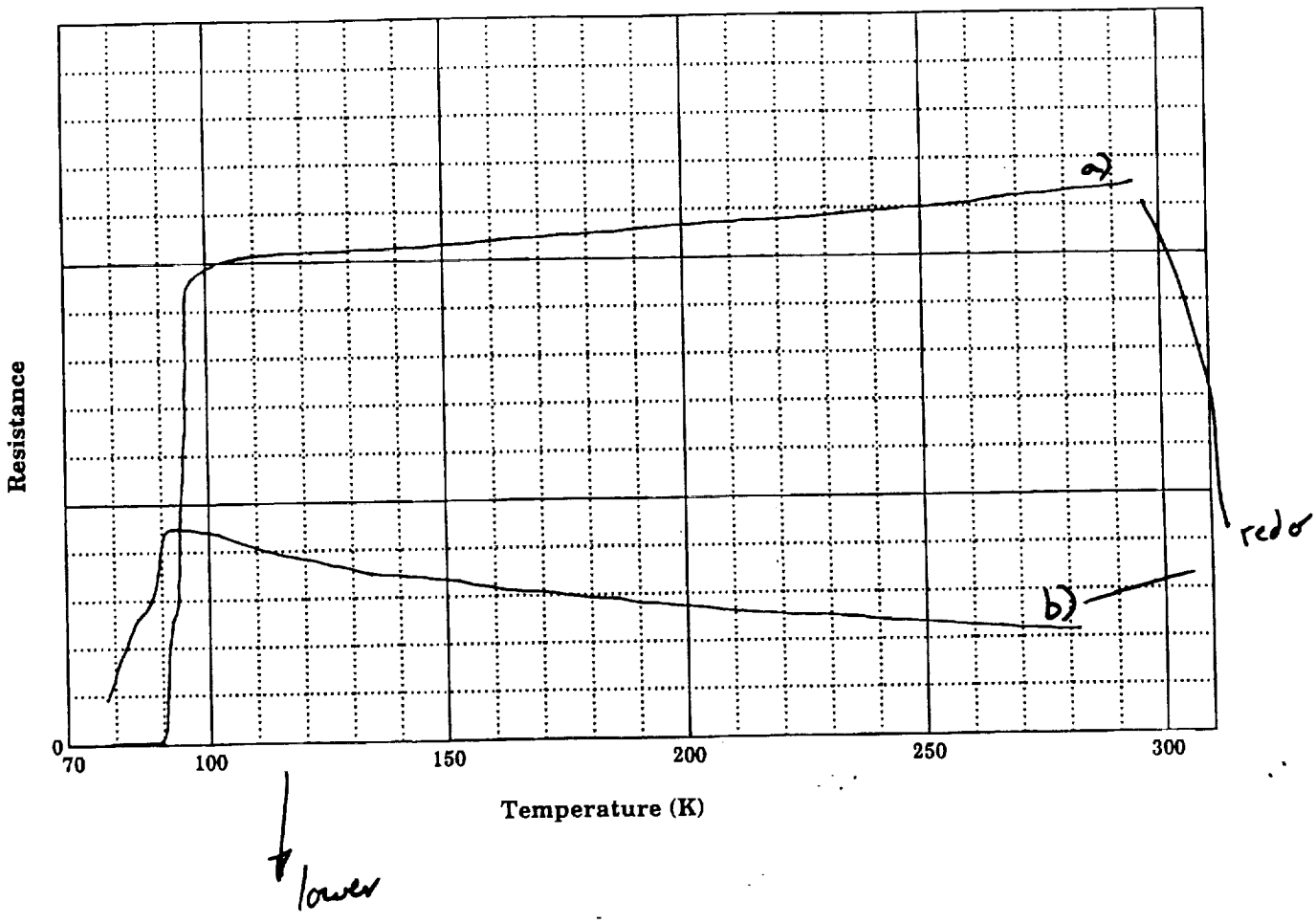

Figure 14

Superconducting Transition Resistance Curves of Ceramic $YBa_2Cu_3O_{7-\delta}$ Pellets

a) powder milled in 1,1,2 trichlorotriflouroethane

b) powder milled in water

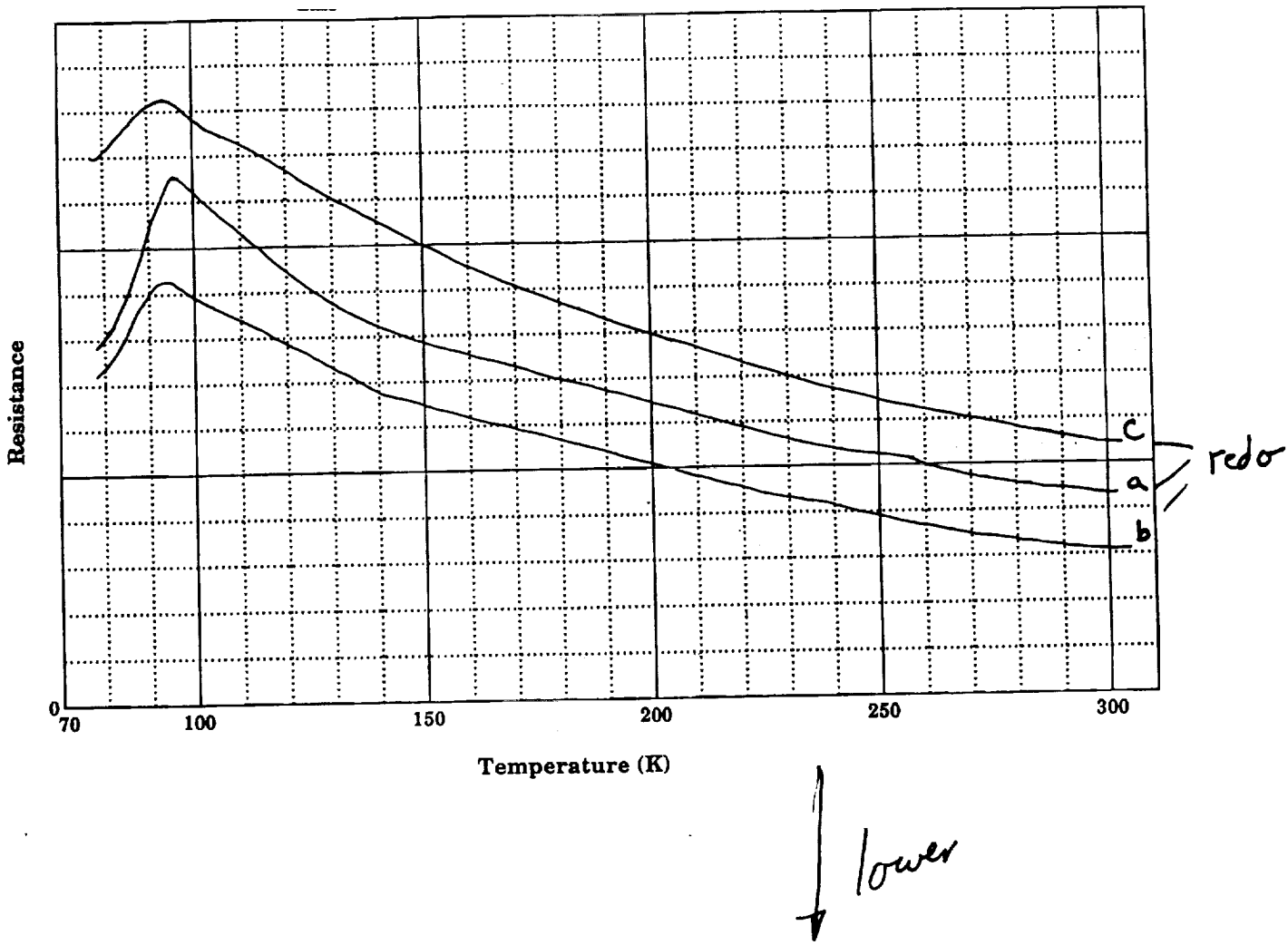

Figure 15

Superconducting Transition Resistance Curves of Ceramic $YBa_2Cu_3O_{7-\delta}$ Pellets

a) powder milled in 2 weight percent silane in water solution
--powder added immediately to solution

b) powder milled in 5 weight percent silane in water solution
--powder added immediately to solution

c) powder milled in 2 weight percent silane in water
--aged for 36 hours

Table 1

A Comparison of Dielectrophoresis and Electrophoresis

Dielectrophoresis

Dielectrophoresis arises from the tendency of matter to become polarized and move into regions of highest field strength. Some of the characteristics of dielectrophoresis are summarized below.

1. Produces motion of the particles in which the direction if motion is independent of the direction of the field, i.e., either dc or ac voltages can be employed.
2. Should be observable most readily in relatively coarse suspensions.
3. Requires highly divergent fields. No motion should be observed in the nondivergent field between centers of parallel plates, for example.
4. Requires relatively high field strengths.
5. Would be most apparent in fluids of low viscosity.
6. Will deposit weights of the particles in direct proportion to the voltage applied in equal times of deposition.
7. Is in general a weak effect easily observable only in strong fields and with coarse particles.

Electrophoresis

Electrophoresis arises from the electrostatic attraction of charged electrodes for charged particles. The direct action of an electric field on charged particles produces a different set of phenomena when compared to dielectrophoresis.

1. Produces motion of the particles in which the direction of the motion is dependent on the direction of the field. Reversal of the field reverses the direction of travel.
2. The phenomenon is observable with particles of any molecular size.
3. Operates in either divergent or uniform fields.
4. Requires relatively low voltages.
5. Requires relatively small charges per unit volume of the particles.